UNIVERSITY OF OKLAHOMA

GRADUATE COLLEGE

EXPERIMENTAL AND MODELING STUDIES ON HOLE CLEANING OF HORIZONTAL WELLS WITH FIBROUS FLUIDS

A DISSERTATION

SUBMITTED TO THE GRADUATE FACULTY

in partial fulfillment of the requirements for the

Degree of

DOCTOR OF PHILOSOPHY

By

Michael Mendez Restrepo
Norman, Oklahoma
2025

Downloaded from SHAREOK. Persistent Handle URL: https://hdl.handle.net/11244/341683

EXPERIMENTAL AND MODELING STUDIES ON HOLE CLEANING OF

HORIZONTAL WELLS WITH FIBROUS FLUIDS

A DISSERTATION APPROVED FOR THE
MEWBOURNE SCHOOL OF PETROLEUM AND GEOLOGICAL
ENGINEERING

BY THE COMMITTEE CONSISTING OF

Dr. Hamid Karami, Chair

Dr. Ramadan Ahmed, Co-Chair

Dr. Catalin Teodoriu

Dr. Andrés González

© Copyright by Michael Mendez 2025
All Rights Reserved.

TABLE OF CONTENTS

TABLE OF CONTENTS iv
LIST OF TABLES vii
LIST OF FIGURES viii
ACKNOWLEDGEMENTS xi
ABSTRACT xii
CHAPTER 1 1
Introduction 1
1.1 Statement of the problem 3
1.2 Motivation and Significance 3
1.3 Objectives 4
1.4 Hypothesis 5
1.5 Research Methodology 6
1.6 Dissertation Outline 7
CHAPTER 2 9
Literature Review 9
2.1 Effects of Viscosity 10
Coiled Tubing Operations 10
Drilling Operations 11
Flow Regime 12
Non-Newtonian Behavior 13
Hydrodynamic Forces 15
2.2 Effects of Pipe Rotation 16
Synergetic Effects and Other Influential Factors 18
Hydraulic Impact of Pipe Rotation 20
2.3 Effects of Fiber 21
Hole Cleaning Enhancement Mechanisms 22
Fiber Drag and Turbulent Suppression 24
Impact on Incipient Motion of Particles 25
2.4 Modelling Studies 26
Empirical and Semi-Empirical Models 26
Mechanistic Models 27
CFD Models 28
Machine Learning Models 29
Descriptive Data Analytics 29
AI Techniques 30
2.5 Industry Hole Cleaning Practices 31
CHAPTER 3 35
Experimental Studies 35
3.1 Testing Methodology 35
3.2 Test Variables and Scope 35

3.3 Experimental Setup 36
3.4 Test Fluids and Materials 40
3.5 Testing Procedure 44
CHAPTER 4 47
Experimental Results and Discussions 47
4.1 Effects of Fibers 47
4.1.1 Hole Cleaning 48
4.1.2 Hydraulics 54
4.1.2.1 Tests without Solid Beds 55
4.1.2.2 Tests with a Stationary Bed 57
4.2 Effect of Bed Irregularities on Hydraulics 59
4.3 Effect of Pipe Rotation 65
CHAPTER 5 72
Machine Learning Study 72
5.1 Theoretical Background 72
5.1.1 Linear Regression 73
5.1.2 Multivariate Adaptive Regression Spline (MARS) 73
5.1.3 Principal Component Analysis (PCA) 74
5.1.4 Decision Trees 74
5.1.5 Deep Learning (DL) 74
5.1.6 Mechanistic Model 75
5.2 Modelling 75
5.2.1 Data Characterization 75
5.2.2 Data Preparation 77
5.2.3 Dimensional Model Evaluation 82
5.3 Results and Discussion 84
5.3.1 Finalized Dataset 84
5.3.2 Model Predictions 85
5.4 Sensitivity Analysis 87
5.5 Comparison of ML and Mechanistic Modeling 88
CHAPTER 6 91
Conclusions and Recommendations 91
6.1 Conclusions 91
6.2 Recommendations 93
NOMENCLATURE 95
Symbols 95
Greek Letters 95
Acronyms 96
REFERENCES 98
Appendix A 108
Geometric Calculation 108

Appendix B 111
Hydraulic Models 111
B.1 Traditional (Original) Hydraulic Model 111
B.2 New Hydraulic Model 112
Appendix C 117
Bed Profiles 117
Appendix D 120
Dimensionless Variables 120

LIST OF TABLES

Table 3. 1. Rheological parameters of XG/PAC fluids (Mendez et al., 2023) 44

Table 4. 1. Test Matrix - No Pipe Rotation (Mendez et al., 2023) 49

Table 4. 2. Model validation for thick fluid without fiber (Mendez et al., 2023) 58

Table 4. 3. Model validation for thick fluid with long fiber (Mendez et al., 2023) 58

Table 4. 4. Model validation for thin fluid without fiber (Mendez et al., 2023) 58

Table 4. 5. Model validation for thin fluid with long fiber (Mendez et al., 2023) 59

Table 4. 6. Model validation for thin fluid without fiber repeat (Mendez et al., 2023) . 59

Table 4. 7. Model validation for thin fluid with short fiber (Mendez et al., 2023) 59

Table 4. 8. Test Matrix - Pipe Rotation (Garcia et al., 2024) 66

Table 5. 1. Data summary of some of the input parameters (Mendez et al., 2023)..... 77

Table 5. 2. Analysis of Variance (Mendez et al., 2023) 81

Table 5. 3. Percentage of variance of principal component regression 83

Table 5. 4. Dataset summary 84

Table 5. 5. Fitting parameters of ML models (Mendez et al., 2023)..... 87

Table 5. 6. Dataset used for ML and mechanistic model comparison..... 89

Table B. 1. Empirical coefficients values used in Eqn. (B.7)..... 113

Table B. 2. Empirical coefficient used in Eqn. (B.15) (Rojas et al. 2017)..... 115

Table B. 3. Empirical coefficients used in Eqns. (B.12) and (B.13) 116

LIST OF FIGURES

Figure 2. 1. Drill pipe rotation and wobbling motion (Garcia et al. 2023)..... 17

Figure 2. 2. Inclined wellbore with cutting beds and dunes (Zhang et al., 2015) 19

Figure 2. 3. a) Drill pipe rotation in eccentric annulus; and b) local velocity profile near cutting bed (Garcia et al., 2024) 23

Figure 3. 1. Schematic of the experimental setup (Mendez et al., 2023) 37

Figure 3. 2. A photo of the flow loop 38

Figure 3. 3. Annular test section..... 39

Figure 3. 4. Pipe rotation system 40

Figure 3. 5. Particle size distribution of sand (Garcia et al., 2024) 41

Figure 3. 6. Rheology of test fluids measured using a rotational viscometer with and without fiber: a) thick fluid (long fiber); b) thin fluid (long fiber); and c) thin fluid (short fiber) (Mendez et al., 2023) 42

Figure 3. 7. Pressure loss versus flow rate in pipe viscometer for different fluids: a) thick fluid; and b) thin fluid (Mendez et al., 2023) 43

Figure 3. 8. Main test parameters during the erosion process: a) flowrate; and b) annular pressure loss (Mendez et al., 2023) 46

Figure 4. 1. Dimensionless bed height vs. flow rate (Mendez et al., 2023) 50

Figure 4. 2. Bed coverage at different flow rates with and without fiber (Mendez et al., 2023)..... 52

Figure 4. 3. Measured and predicted ΔP for hydraulic tests with thick fluid: a) without fiber; and b) with long fiber (Mendez et al., 2023) 56
Figure 4. 4. Measured and predicted ΔP for hydraulic tests with thin fluid: a) without fiber; and b) with long fiber (Mendez et al., 2023) 57
Figure 4. 5. Comparison of original and new model predictions with measurements: a) thick fluid, b) thick fluid with fiber, c) thin fluid, and d) thin fluid with fiber..... 60
Figure 4. 6. Bed Height profile thin fluid no fiber at 75 GPM (Mendez et al., 2023).... 62
Figure 4. 7. Bed height profile thick fluid with fiber at 195 GPM (Mendez et al., 2023) 62
Figure 4. 8. Model prediction error vs. CV (Mendez et al., 2023) 63
Figure 4. 9. CV versus normalized bed shear stress (Mendez et al., 2023)..... 65
Figure 4. 10. Dimensionless bed height vs. flow rate (Thin and Thick fluid, no fiber) (Garcia et al., 2024) 67
Figure 4. 11. Dimensionless bed height vs. flow rate (Thin fluid) (Garcia et al., 2024) 69
Figure 4. 12. Dimensionless bed height vs. flow rate (Thick fluid) (Garcia et al., 2024) 71
Figure 5. 1. Cross-correlation plot between all the tested variables (Mendez et al., 2023) 78
Figure 5. 2. Comparison of Measured vs. Predicted training data with BDT Model..... 79
Figure 5. 3. BDT (left) and RF (right) charts for the most influential parameters in hole cleaning prediction (Mendez et al., 2023) 80

Figure 5. 4. PCA for the first two principal components and their relations with analyzed variables (Mendez et al., 2023)..... 82
Figure 5. 5. Observed vs Predicted training data, after outlier removal and addition of dimensionless variables (Mendez et al., 2023)..... 83
Figure 5. 6. Predictions of ML models for the Test Dataset (Mendez et al., 2023) 86
Figure 5. 7. Sensitivity analysis using BDT model. Flow Rate (Top left), Pipe Rotation (Top right), n (Bottom left), K (Bottom Right). (Mendez et al., 2023)..... 88
Figure 5. 8. Comparison of the predictions of mechanistic (left) and BDT (Right) models (Mendez et al., 2023)..... 90
Figure A. 1. Standard geometry configuration for eccentric annulus (Elgaddafi et al., 2021)..... 108
Figure B. 1. Block diagram showing the numerical procedure for determining the bed shear stress..... 116
Figure C. 1. Bed Height profile of thick fluid no fiber at 35, 115 and 195 GPM 117
Figure C. 2. Bed Height profile of thick fluid with long fiber at 35, 115 and 195 GPM 117
Figure C. 3. Bed height profile of thin fluid no fiber at 35, 115 and 195 GPM 118
Figure C. 4. Bed height profile of thin fluid with short fiber at 35, 115 and 195 GPM118
Figure C. 5. Bed height profile of thin fluid no fiber repeat at 35, 115 and 195 GPM 119
Figure C. 6. Bed height profile of thin fluid with short fiber at 35, 115 and 195 GPM119

ACKNOWLEDGEMENTS

I would like to express my deepest gratitude to my advisors, Dr. Ramadan Ahmed and Dr. Hamid Karami, for their unwavering support, guidance, and encouragement from the very beginning of this journey. Their mentorship and the opportunity to work on this project as their student have been truly invaluable.

I am also grateful to my committee members, Dr. Andrés Gonzáles and Dr. Catalin Teodoriu, for their insightful feedback and support throughout the dissertation process.

A special thanks goes to Jeff McCaskill for his invaluable help and training during the construction of the experimental facility. His expertise and willingness to assist were essential to the success of this work.

Finally, I would like to thank my family and friends for their continuous support, understanding, and encouragement throughout this entire endeavor. I would also like to express my appreciation to Yuliana Zapata, whose help with editing and formatting greatly improved the quality of this dissertation

ABSTRACT

The drilling of horizontal and highly deviated wells has become essential for maximizing reservoir contact and improving hydrocarbon recovery. However, effective hole cleaning remains one of the most critical challenges due to limited hydrodynamic assistance, leading to cuttings bed formation and associated problems such as increased torque, drag, stuck pipe, and non-productive time. Conventional drilling fluids often fail to maintain adequate solids transport under these conditions. Recent studies suggest that fibrous fluids can enhance suspension and transport characteristics, but their mechanisms and modeling remain poorly understood.

This research evaluates the effectiveness of fibrous fluids in improving hole cleaning in horizontal wells using experimental and modeling approaches. A customized horizontal flow loop was developed to replicate wellbore conditions. Polymer-based drilling fluids were tested by measuring equilibrium bed height and pressure loss under varying flow rates, pipe rotation speeds, and fiber concentrations. Results demonstrated that the addition of long synthetic fibers significantly enhanced cuttings transport efficiency, particularly in low-viscosity fluids at high flow rates. Short fibers, however, provided minimal benefits. Pipe rotation exhibited a strong synergistic effect with fibrous fluids by promoting disturbance and resuspension of settled cuttings beds. The resuspension improved transport efficiency, especially under laminar flow regimes where turbulence is absent.

A recent mechanistic model was applied to predict hydraulic performance in eccentric annuli with partial obstruction. The predictions were validated against experimental data, showing superior accuracy over traditional models under laminar conditions. Furthermore, a machine learning model was developed based on a comprehensive dataset on hole cleanings. Model evaluations demonstrated higher predictive accuracy of the machine learning model for equilibrium bed height across diverse operational scenarios. This study provides new insights into the mechanisms of fibrous fluids in enhancing hole-cleaning efficiency. It introduces validated predictive tools to optimize wellbore cleaning strategies in horizontal drilling operations.

CHAPTER 1

Introduction

The drilling of horizontal and highly deviated wells has become increasingly prevalent in the oil and gas sector. Horizontal wells maximize reservoir contact, improve hydrocarbon recovery, and reduce surface footprint. One of the most persistent and challenging issues in horizontal drilling is effective hole cleaning, or the process of removing rock cuttings generated during drilling operations from the wellbore. Inadequate removal of these cuttings can lead to a variety of operational problems, including excessive torque and drag, increased fluid loss and stuck pipe incidents, poor logging conditions, and wellbore collapse. These complications result in substantial non-productive time (NPT) and increased operational costs.

Unlike vertical wells, where hydrodynamic drag aids in cuttings transport, gravitational settling of particles predominates in horizontal wells, rendering traditional cleaning strategies such as increasing viscosity or flow rate less effective. Conventional drilling fluids often fail to provide sufficient solids transport, particularly in the absence of pipe rotation or turbulent flow. Additionally, the presence of stagnant flow zones in eccentric annular geometries and the development of non-uniform cuttings beds introduce further complexities that exceed the predictive capabilities of existing hydraulic models.

In recent years, the use of fibrous drilling fluids, enhanced with small amounts of synthetic fibers, has emerged as a promising approach to improve solids transport and

suspension characteristics. When fully dispersed in the fluid, fibers interact to form a network-like structure that increases the drag force acting on settling particles, thereby reducing their settling velocity and improving transport efficiency. Although preliminary studies indicate that fibrous fluids enhance hole cleaning, their behavior remains poorly understood, and particularly in horizontal wells. The effects of fiber type, length, and concentration on fluid rheology and hydraulic performance have yet to be systematically investigated.

Existing models for predicting pressure gradients and cuttings bed behavior often assume concentric flow and uniform bed conditions. These assumptions are inadequate for inclined and horizontal wells, where wellbore geometry becomes eccentric and fiber-modified fluid systems are required. To address this limitation, accurate modeling tools must be developed to incorporate the effects of fibers, annular eccentricity, and bed irregularities under laminar and transitional flow regimes. This dissertation aims to experimentally evaluate the impact of fibrous fluids on hole-cleaning efficiency in a horizontal configuration. Through a combination of laboratory testing and advanced modeling, including mechanistic and machine learning approaches, this research seeks to enhance the understanding and design of effective wellbore cleaning strategies using fiber-enhanced fluids.

1.1 Statement of the problem

Effective hole cleaning in horizontal and highly deviated wells remains a critical operational challenge due to the limited contribution of hydrodynamic drag in suspending and transporting cuttings within the wellbore. Conventional drilling fluids often exhibit insufficient cuttings-carrying capacity, leading to the accumulation of cuttings beds. This accumulation contributes to elevated bottom-hole pressure and equivalent circulating density (ECD), excessive fluid loss, and an increased risk of differential sticking. Additionally, it exacerbates mechanical drag and torque on the drillstring, ultimately raising the likelihood of operational failures. While pipe rotation can enhance hole-cleaning efficiency, its benefits are constrained by associated ECD increases and its impracticality in coiled tubing operations. Recent studies have proposed fibrous fluid formulations as a potential solution, offering improved suspension and transport characteristics. However, their underlying mechanisms, impact on rheological behavior, and interactions with cuttings beds remain inadequately understood and are not accurately captured by existing predictive models.

1.2 Motivation and Significance

Hole cleaning remains one of the most critical challenges in drilling horizontal and highly deviated wells. Inadequate removal of cuttings can cause severe operational problems, including excessive fluid loss, lost circulation, stuck pipe incidents, high torque and drag, wellbore instability, and poor logging conditions. These issues not only increase

non-productive time (NPT) but also result in significant financial losses and operational risks. Conventional drilling fluids and traditional cleaning strategies, such as increasing fluid viscosity or flow rate, are often ineffective under laminar and transitional flow regimes and eccentric annular geometry typical of horizontal and inclined sections. Furthermore, their limitations become more pronounced when pipe rotation is restricted, such as in coiled tubing applications.

The introduction of fibrous drilling fluids offers a promising alternative by improving solids suspension and transport without drastically increasing viscosity or frictional pressure loss. However, despite their potential, the mechanisms governing fiber-fluid-particle interactions, as well as their influence on fluid rheology and hydraulic performance, remain poorly understood. Moreover, current predictive models fail to account for the complexities of flow in eccentric annuli, irregular cuttings bed formation, and the characteristics of fibrous fluids.

This research is significant because it systematically evaluates the performance of fibrous fluids under controlled conditions and introduces advanced modeling techniques, including machine learning approach, to improve the accuracy of hole-cleaning predictions and optimize drilling practices.

1.3 Objectives

The main objective of this study is to evaluate the effectiveness of fibrous fluids in enhancing hole-cleaning efficiency in horizontal wells through experimental testing

and advanced modeling, including mechanistic and machine learning approaches, to improve prediction accuracy of hydraulic and cutting transport performance and optimize wellbore cleaning strategies under complex operational conditions. The detailed objectives of this study include:

- Investigating the role of fiber characteristics (length and concentration) in improving hole cleaning performance of polymer-based drilling fluids through controlled laboratory experiments.
- Assessing the effects of pipe rotation and bed irregularities on cuttings transport and hydraulic performance in horizontal wells.
- Validating mechanistic models capable of accurately predicting pressure loss and equilibrium bed height in eccentric annuli with partial obstruction.
- Evaluating and comparing the predictive capabilities of machine learning models against mechanistic modeling approaches for predicting hole cleaning performance metrics.

1.4 Hypothesis

This work is guided by the a few primary hypotheses. Firstly, it is believed that synthetic fibers improve hole cleaning efficiency of polymer-based drilling fluids in horizontal wells by enhancing particle suspension capacity of the fluid and reducing the formation of cuttings bed height. This improvement is expected to be more pronounced with long fibers compared to short fibers. This is due to the greater ability of long fibers

to form a stable network structure that generates additional fiber-induced drag forces when rock cuttings settle in the drilling fluid. The effect is further enhanced when combined with pipe rotation, which contributes mechanical agitation that improves cuttings mobilization and fluid-particle interactions.

Traditional hydraulic models fail to accurately predict pressure gradient and equilibrium bed thickness in eccentric annuli containing fibrous fluids and irregular solids beds. These models often assume uniform bed geometry and concentric flow. They are insufficient under complex flow conditions involving non-Newtonian fluids, fiber interactions, and mechanical disturbances such as pipe rotation. A mechanistic model that incorporates eccentric geometry, bed height variability, and fiber effects, could provide improved accuracy in predicting pressure losses and hole-cleaning.

When trained with sufficient data and optimized using appropriate hyperparameters, machine learning models can outperform mechanistic models in predicting key performance metrics such as pressure gradient and equilibrium bed height. Their superior performance stems from the ability to capture complex, nonlinear relationships within experimental and field datasets involving diverse fluid formulations, geometries, and operational conditions.

1.5 Research Methodology

The research methodology integrates both experimental and modeling approaches. Experimental investigations were carried out using a 48-ft horizontal annular

test section constructed with a transparent acrylic tube to enable visualization of cuttings bed thickness and profile. Tests were performed under varying fiber types, concentrations, flow rates, and pipe rotation speeds to assess hole-cleaning performance based on equilibrium bed height and frictional pressure loss. The rheological properties of the drilling fluids were measured using both rotational and pipe viscometers to ensure accurate characterization.

On the modeling side, a machine learning model was developed using an extensive dataset comprising experimental measurements from this study and published literature. The model was trained to predict equilibrium bed height under diverse operating conditions. Additionally, a mechanistic model that accounts for annular eccentricity and flow regime effects was incorporated for comparative analysis. Predictions from the machine learning approach were evaluated against experimental data and mechanistic model outputs using statistical performance metrics to validate accuracy and robustness.

1.6 Dissertation Outline

In this dissertation, **Chapter 1** introduces the study by presenting the context of horizontal drilling challenges, outlining the problem, and defining the objectives, hypothesis, and methodology. **Chapter 2** reviews relevant literature, including prior work on the effects of viscosity, pipe rotation, fiber-enhanced fluids, and various modeling techniques. **Chapter 3** details the experimental facility design, describing the flow loop

setup, instrumentation, test fluids, experimental procedures, data acquisition system, and the test matrix used to evaluate hole cleaning under various conditions. **Chapter 4** presents the experimental results, emphasizing the effects of fiber addition and pipe rotation on pressure loss, bed height variability, and the performance of predictive hydraulic models. **Chapter 5** discusses the modeling efforts, including the validation of a mechanistic model for eccentric annuli and partially blocked flow, as well as the application of machine learning techniques such as regression, PCA, and deep learning to estimate pressure loss and bed behavior. Finally, **Chapter 6** summarizes the key findings, provides recommendations for field implementation and model improvement, and outlines directions for future research.

CHAPTER 2

Literature Review

This chapter presents a comprehensive review of technical and scientific publications focused on understanding and improving hole-cleaning operations. The review systematically examines key parameters that influence cutting transport efficiency. It begins with the effect of viscosity, a fundamental drilling fluid property that controls suspension and transport of cuttings. Maintaining optimal viscosity is essential to prevent deposition and ensure effective removal, particularly in highly deviated and horizontal wells. The role of pipe rotation in hole cleaning is then explored. Pipe rotation enhances turbulence and disrupts the cuttings bed, reducing deposition in deviated and horizontal sections where the absence of a strong vertical hydrodynamic drag component exacerbates settling. Increased agitation facilitates continuous cuttings transport, thereby improving cleaning efficiency. The review also addresses the contribution of fibers to hole cleaning, particularly in high-angle wells. Fibers improve the fluid's carrying capacity by mitigating particle settling and increasing suspension stability. Finally, various modeling approaches are discussed, including empirical, semi-empirical, mechanistic, and machine-learning models, which provide predictive capabilities for optimizing hole-cleaning performance.

2.1 Effects of Viscosity

Viscosity significantly influences hole cleaning efficiency in coiled tubing and drilling operations by affecting cuttings transport and frictional pressure losses. In the absence of pipe rotation, flow rate and fluid viscosity become the primary parameters controlling cutting removal in coiled tubing operations. Higher viscosity enhances the suspension of cuttings at low flow rates but may induce laminar flow, reducing transport efficiency, particularly in highly deviated and horizontal wells. In contrast, lower-viscosity fluids, such as water, transition to turbulent flow at lower flow rates, improving cuttings removal. Furthermore, drilling fluids exhibit non-Newtonian behavior, with their rheological parameters determining the flow regime. Also, gravitational forces dominate in horizontal configurations, leading to cutting bed formation. Achieving an optimal balance between viscosity and flow rate is crucial for maintaining efficient hole cleaning while preventing fluid loss, lost circulation, and differential sticking, and excessive torque and drag, and other drilling problems associated with poor hole cleaning.

Coiled Tubing Operations

Numerous studies (Li & Walker, 2001; Li et al., 2002; Li et al., 2005; Pandya et al., 2019; 2020; Naik, 2015) on hole cleaning in coiled tubing operations have focused on two objectives: minimizing cutting bed height and reducing frictional pressure losses. Unlike conventional drilling, coiled tubing cleanout operations lack pipe rotation, eliminating the mechanical agitation that typically enhances cuttings transport. Consequently, flow rate and fluid viscosity become the dominant parameters influencing

cutting removal efficiency while simultaneously allowing effective pressure loss management. Optimizing hole cleaning under these conditions requires a thorough understanding of equipment constraints, including surface pumping pressure and flow rate limitations. The effectiveness of cuttings transport is further constrained by the maximum bottom hole pressure that the formation can sustain without fracturing, commonly referred to as the formation fracture pressure. The bottom hole pressure is a function of two primary components: the hydrostatic pressure exerted by the fluid in the annulus and the frictional pressure losses occurring within the annular space. Therefore, the upper limit for flow rate in coiled tubing operations is dictated by both the surface pump's capacity, encompassing pressure and flow rate restrictions, and the pressure losses within the annulus. Achieving optimal hole cleaning requires a balance between maximizing flow rate for efficient cuttings transport while preventing extreme fluid loss and formation fracturing due to excessive pressure (Ahmed & Takach, 2009).

Drilling Operations

In drilling operations, in addition to the formation fracture pressure, the use of mud motors imposes additional constraints on pressure management. Mud motors operate by utilizing the hydraulic power of drilling fluids, which results in a significant pressure drop within the drill string, consequently leading to an increase in standpipe pressure (SPP). This pressure increase must be carefully managed to prevent excessive mechanical fatigue in coiled tubing, which can compromise operational efficiency and tool longevity. For instance, Leising & Newman (1993) reported that a standard 2-7/8-inch positive

displacement downhole motor commonly used in coiled tubing drilling operates within a typical flow rate range of 84–126 gallons per minute (gpm). To mitigate the risk of coiled tubing fatigue at elevated pressures, drilling operations generally cap SPP within the range of 3800–4000 psi. However, effective hole cleaning in horizontal wellbores presents additional challenges. For a 2-inch coiled tubing deployed in a 4.75-inch horizontal wellbore, achieving optimal hole cleaning requires a critical flow rate of approximately 134 gpm, corresponding to an annular velocity of 180 feet per minute. If SPP limitations restrict the operational flow rate to below 134 gpm, the necessary annular velocity for efficient cuttings transport cannot be attained, resulting in suboptimal hole-cleaning performance. Therefore, pressure management is crucial in coiled tubing drilling operations. A comprehensive evaluation of pipe and annular frictional pressure losses, pressure drop across downhole tools such as the drill motor and drill bit, and hydrostatic pressure variations between the annulus and the drill pipe is essential in coiled tubing operations. Proper pressure control enables accurate process optimization, facilitates the selection of appropriate downhole tools, and ensures the use of suitable coiled tubing sizes to achieve both operational efficiency and formation integrity.

Flow Regime

The flow regime in the annulus, which can be either laminar or turbulent, is primarily determined by the drilling fluid's viscosity and significantly influences overall flow behavior. Consequently, the prevailing flow regime is crucial in determining hole-cleaning efficiency. In drilling and completion operations, the flow characteristics of

different fluids vary considerably. Water typically flows under turbulent conditions within the annulus, whereas viscous fluids containing polymers may exhibit laminar flow, depending on polymer type and concentration. Brown, Bern, & Weaver (1989) observed that polymer-based fluids generally demonstrate superior cuttings removal efficiency compared to water in vertical wells. However, this performance advantage diminishes as inclination angle increases due to the reduction in the vertical component of hydrodynamic drag. In horizontal and highly deviated wellbores, water removes cuttings effectively as it flows turbulently, exhibiting a velocity profile that facilitates the removal of solids from cutting beds. Conversely, polymeric fluids often maintain laminar flow under similar conditions due to their increased viscosity, reducing their capacity to re-suspend deposited solids efficiently. This limitation is particularly evident in an eccentric annulus, where stagnant fluid zones form between the drill pipe and the wellbore or casing along the low side of the hole. These stagnant regions hinder cuttings removal, further diminishing hole-cleaning efficiency in highly deviated wells (Pandya et al. 2019;2020).

Non-Newtonian Behavior

Drilling muds are predominantly non-Newtonian fluids, meaning their viscosity varies with shear rate. As a result, their viscous behavior is described by a property known as apparent viscosity. The apparent viscosity of drilling fluids must be represented by appropriate rheological models that accurately describe their viscous behavior under varying shear rate conditions. Several analytical models are commonly employed to characterize drilling fluid rheology, including the Newtonian ($\tau = \mu\dot{\gamma}$), Bingham plastic

($\tau = \tau_y + \mu_p \dot{\gamma}$), and power-law ($\tau = K\dot{\gamma}^n$) models. Among these, the power-law model is widely utilized to represent the non-Newtonian flow behavior of polymer-based drilling and completion fluids. The two key parameters of the power-law model, the consistency index (K) and the flow behavior index (n), play a crucial role in influencing hole-cleaning efficiency. These parameters directly impact fluid viscosity and determine the prevailing flow regime, thereby affecting the resuspension and transport of cuttings within the annulus (Kerunwa et al., 2021; (Azouz et al., 1993; Kenny, Sunde, & Hemphill, 1996). Proper characterization and management of rheological behavior is essential for optimizing drilling fluid performance and ensuring effective hole cleaning.

Bingham plastic model is characterized flow behaviors of fluids by two key rheological parameters: plastic viscosity (μ_p) and yield stress (τ_y). The yield stress represents the fluid's gelling characteristics and indicates the minimum shear stress required to initiate flow. The presence of yield stress signifies that the fluid exhibits high viscosity at low shear rates, commonly referred to as low shear rate viscosity. This property plays a critical role in cuttings suspension and transport, particularly in deviated and horizontal wells. Zamora & Hanson (1990) conducted experimental investigations on hole cleaning across various well inclinations using different fluids, including water, polymer-based fluids, and oil-based drilling fluids. Their findings indicated that increasing low shear rate viscosity and gel strength improved cuttings transport efficiency under laminar flow conditions. However, in horizontal wellbores, turbulent flow was generally more effective for hole cleaning. Additionally, gel strength and other

rheological properties were identified as essential factors in enhancing hole-cleaning performance, particularly in horizontal drilling operations.

Hydrodynamic Forces

The fluid viscosity is one of the parameters that influences hydrodynamic drag and lift forces acting on the particles during hole cleaning. In highly inclined and horizontal orientations, the vertical component of fluid velocity becomes negligible, resulting in gravitational forces predominantly governing the motion of suspended particles. Consequently, when cuttings travel away from the drill bit, they tend to settle on the low side of the wellbore, forming stationary beds. The accumulation of the cutting and the deformation of stable beds reduce the effective flow area, thereby increasing the velocity of the fluid and the shear stress acting on the beds. Under such conditions, particles on the surface of the beds are directly exposed to the local fluid velocity and experience hydrodynamic forces, which influence their mobilization and transport.

The hydrodynamic forces exerted by the fluid on bed particles have been extensively analyzed, leading to the determination of a critical flow rate necessary to initiate particle movement and facilitate cuttings transport (Clark & Bickham, 1994; Masuda et al., 2000; Ahmed et al., 2001; 2003; 2004; Li & Luft, 2014). However, this critical flow rate is often insufficient to maintain cuttings in continuous suspension. Instead, a phenomenon known as "saltation" occurs, wherein particles are intermittently lifted by the fluid flow and subsequently redeposited into the cuttings bed. The cyclic

lifting and settling behavior complicate the cuttings removal process and reduces overall cleanout efficiency. As a result, optimizing flow conditions and fluid properties is essential to enhancing hole-cleaning performance in highly deviated and horizontal wells.

2.2 Effects of Pipe Rotation

Pipe rotation enhances hole-cleaning efficiency in horizontal and deviated wells by inducing hydrodynamic and mechanical effects that disrupt stagnant fluid zones, increase turbulence, agitate and disperse deposited cuttings, and consequently improve cuttings transport. The rotational motion generates a helical flow pattern, which, combined with axial movement, prevents cuttings bed formation and enhances the suspension of solid particles. In eccentric annuli, rotation induces a wobbling effect, further agitating deposited cuttings. The combined effects of drill pipe rotation, fluid rheology, and flow dynamics necessitates the optimization of operational parameters to balance enhanced cuttings removal with manageable pressure losses.

Extensive research has examined hole-cleaning performance during the drilling of horizontal and directional wells, emphasizing the critical role of pipe rotation in improving efficiency. This enhancement is attributed to the combined hydrodynamic and mechanical effects induced by pipe movement. Pipe rotation modifies annular flow characteristics, particularly in eccentric configurations where significant cuttings beds tend to accumulate along the wellbore. The rotational motion disrupts stagnant fluid

regions, increases turbulence, and promotes cuttings agitation, thereby improving their mobilization and transport and ultimately enhancing overall hole cleaning.

Furthermore, the rotation of the drill string generates a swirling or helical flow pattern within the wellbore, as reported by Ahmed & Miska (2008). When coupled with axial motion, this rotational effect agitates settled cuttings and maintains them in suspension, reducing the likelihood of cuttings bed formation. The impact of drill pipe rotation is especially pronounced in eccentric annuli, where the pipe contacts the borehole wall during rotation (Fig. 2.1a). Under these conditions, the pipe experiences periodic upward (Fig. 2.1b) and downward (Fig. 2.1c) movements resulting from the combined influence of buoyancy, gravity, friction, and centrifugal forces. These interactions produce a continuous climbing and falling motion, leading to a dynamic wobbling effect. The amplitude of this wobbling depends on factors such as eccentricity, bed characteristics (consolidated or unconsolidated), rotational speed, and the mechanical properties of the drill string (Garcia et al., 2024).

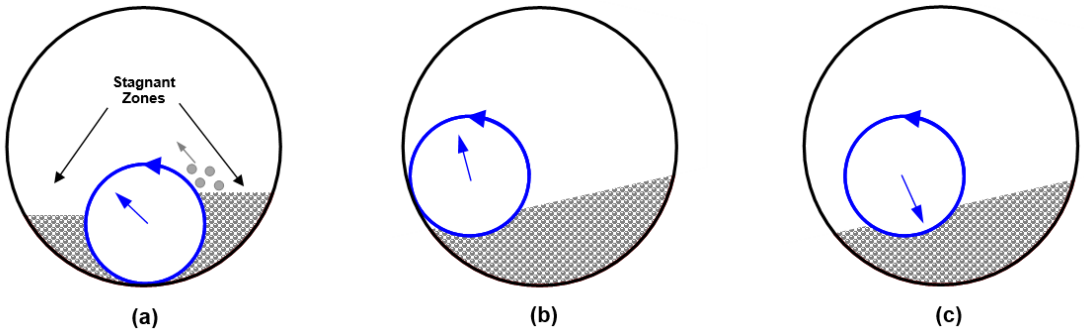


Figure 2. 1. Drill pipe rotation and wobbling motion (Garcia et al. 2023)

In controlled laboratory experiments, the extent of pipe wobbling is typically limited due to the constrained length of the test section. However, even minor wobbling is sufficient to generate a turbulent flow regime characterized by the presence of large-scale eddies. These eddies play a vital role in improving hole-cleaning efficiency by redistributing cuttings more uniformly throughout the drilling fluid, thereby reducing particle settling and minimizing the formation of stationary cutting beds. As a result, the combined effects of drill pipe mechanical actions and induced turbulence enhance cuttings transport, ultimately improving the overall efficiency of hole cleaning in horizontal and deviated wells.

The mechanical actions of the drill string play a crucial role in enhancing hole cleaning during drilling operations. The rotational and wobbling motions of the drill pipe, along with vibrations, work together to dislodge and disperse drilled cuttings (Fig. 1a). This disruption prevents the formation of stationery and compacted cutting beds that are challenging to clean. In eccentric annuli, where hydrodynamic effects are limited, the mechanical action of the pipe effectively disperses rock cuttings in the fluid, hindering settling and bed formation. There is a strong synergy between the flow hydrodynamic and mechanical actions of the drill string, leading to a significant improvement in the removal and transport of cuttings in deviated wells.

Synergetic Effects and Other Influential Factors

Sanchez et al. (1999) conducted an experimental study using a 100-ft wellbore simulator to evaluate the influence of drill pipe rotation on hole cleaning during

directional drilling. The experiment utilized a 4.5-inch drill pipe within an 8-inch diameter borehole and examined key variables, including rotary speed, hole inclination, mud rheology, cuttings size, and flow rate. The findings demonstrated a substantial improvement in hole-cleaning efficiency due to drill pipe rotation. However, the extent of this enhancement was influenced by factors such as mud rheology, cuttings size, inclination angle, and flow rate. The study revealed that low-viscosity drilling fluids exhibited superior hole-cleaning performance compared to high-viscosity muds in horizontal and highly deviated wells. One of the major challenges observed was the formation of unstable cuttings beds and dunes, which were significantly affected by the dynamic behavior of the drill pipe, including rotation, wobbling, and vibration. Figure 2.2 shows an inclined wellbore with cutting beds and dunes. The dynamic behavior of the drill pipe played a crucial role in cuttings mobilization and transport. Additionally, smaller cuttings were found to be more difficult to clean, as they exhibited a lower tendency to resuspend. However, increasing the rotary speed and utilizing high-viscosity muds improved the suspension and transport of smaller cuttings, thereby enhancing overall hole-cleaning efficiency.

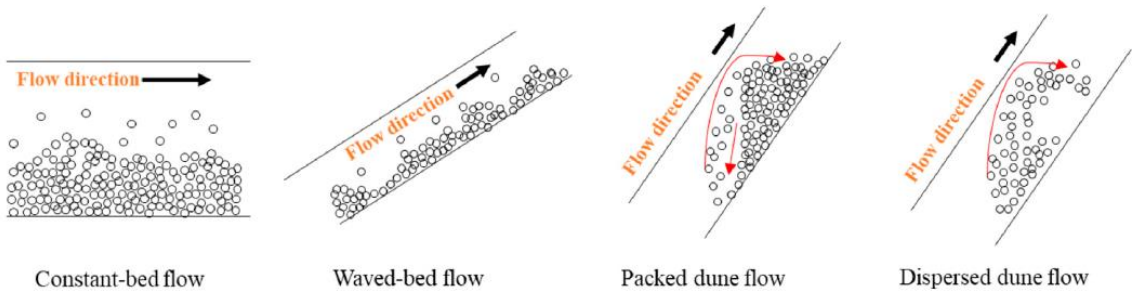


Figure 2. 2. Inclined wellbore with cutting beds and dunes (Zhang et al., 2015)

A similar study (Duan et al., 2008) examined the effect of pipe rotation on hole cleaning in highly deviated wellbores, specifically within a deviation range of 70° to 90°. The investigation was performed using a 100-ft-long flow loop with an annular test section measuring 8 inches in borehole diameter and 4.5 inches in drill pipe diameter. The study examined the influence of key parameters, including drill pipe rotation, flow rate, fluid rheology, and hole inclination, on cuttings transport efficiency. Three different cuttings sizes, ranging from 0.45 mm to 3.3 mm, were tested to assess the impact of particle size on hole cleaning performance. The findings revealed that smaller cuttings were more difficult to remove than larger ones, consistent with previous research (Ahmed et al., 2001). Additionally, results demonstrated that flow rate played a significant role in improving the transport of larger cuttings. However, for smaller cuttings, achieving effective hole cleaning required careful optimization of both drill pipe rotation and fluid rheology, as these factors were critical in maintaining particles in suspension and enhancing cuttings transport within the annulus.

Hydraulic Impact of Pipe Rotation

While drill pipe rotation enhances hole-cleaning efficiency, it also leads to increased frictional pressure losses within the annulus. Field measurements conducted by a number of studies (Delwiche et al. 1992; Isambourg et al. 1998; Charlez et al. 1998) have shown that pipe rotation can result in a significant rise in pressure loss, reaching up to 100% in some cases. The relationship between drill pipe rotation and frictional pressure losses is highly complex and is influenced by multiple factors, including fluid properties

such as rheology and density, the prevailing flow regime, the pipe-to-hole diameter ratio, and the degree of pipe eccentricity (Ahmed & Miska, 2008; Ahmed et al. 2010).

2.3 Effects of Fiber

Numerous studies (Ahmed & Takach, 2009; Ahmed et al., 2009; (George et al., 2014; Mahmoud et al., 2020) have been conducted to evaluate the cleaning efficiency of fibrous fluids in drilling applications. Ahmed et al. (2009) investigated fiber sweeps in polymer-based fluids under horizontal and highly deviated wellbore conditions. Their findings indicated that while fiber incorporation had minimal impact on fluid rheology, it enhanced cuttings transport efficiency in horizontal configurations. However, in inclined wellbores (68° from vertical), the improvement in hole cleaning was less pronounced.

George et al. (2011) analyzed the effect of fiber on drilling fluid rheology, reporting that fiber concentrations up to 0.08 wt% had negligible influence on viscosity under both ambient and elevated temperatures. However, in most cases, the introduction of fiber increased the non-Newtonian characteristics of the fluid. In a subsequent study, George et al. 2014 examined the impact of fiber on the hole-cleaning performance of synthetic-based fluids. Their results demonstrated that while pipe rotation improved cuttings transport efficiency at an inclination of 72°, no significant enhancement was observed at 90°. Notably, the introduction of fiber into the drilling fluid significantly increased cuttings removal efficiency in the presence of pipe rotation.

A recent study (Mahmoud et al., 2020) investigated the influence of polymer anionicity and fiber on the solids-carrying capacity of polymer-based fluids. Their study revealed that increased anionicity, due to higher negative charge density, enhanced the carrying capacity by intensifying electrostatic repulsion between suspended particles and polymer molecules. The addition of fiber at a concentration of 0.08 wt% further improved cuttings suspension with minimal impact on the base fluid's rheology. Fiber performance was found to be dependent on its stability within the fluid, while cuttings size played a critical role in determining the solids-carrying capacity of fibrous fluids.

Hole Cleaning Enhancement Mechanisms

The incorporation of fiber into drilling fluids significantly enhances hole-cleaning efficiency by reducing the settling velocity of solid particles. This improvement is attributed to the increased drag force generated by the formation of a fiber network within the fluid, which enhances particle suspension and transport (Xu & Aidun, 2004; Ahmed & Takach, 2009). In fibrous fluids, in addition to the conventional viscous drag force, an additional fiber-induced drag force is present (Elgaddafi et al., 2012). This force arises from the combined mechanical and hydrodynamic interactions between the fiber network and suspended particles, further contributing to improved cuttings transport and hole cleaning.

When a sufficient concentration of fiber is dispersed within the fluid, fiber particles establish multiple three-dimensional contacts with adjacent particles, forming a contact-based network structure (Fig. 2.3). This network effectively inhibits the settling

of solid particles by enhancing their suspension. Due to their nearly neutral buoyancy, fiber particles move upward with the fluid in vertical wells without segregation, facilitating the lifting of solid particles and minimizing slippage and sedimentation. The lifting effect is attributed to both the mechanical and hydrodynamic interactions of the fiber particles. As a solid particle settles, it interacts directly with the fiber network, which exerts a mechanical drag force, impeding its downward motion. Additionally, fiber particles hydrodynamically interfere with settling particles by disrupting their descent, further inhibiting sedimentation (Garcia et al., 2024).

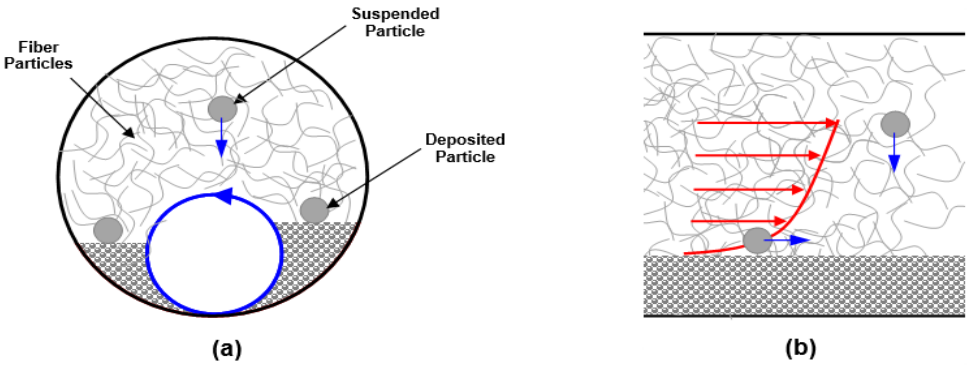


Figure 2. 3. a) Drill pipe rotation in eccentric annulus; and b) local velocity profile near cutting bed (Garcia et al., 2024)

In deviated and horizontal wellbores, some particles settle along the lower side of the wellbore, while others remain suspended within the fluid (Fig. 2.3a). Suspended particles are more readily transported, whereas deposited particles require substantial hydrodynamic forces to initiate motion through lifting or rolling mechanisms (Clark & Bickham, 1994; Ahmed et al., 2001). Therefore, an optimal drilling fluid for hole cleaning in deviated wells should effectively lift or roll settled particles while simultaneously

preventing the sedimentation of suspended particles. In the absence of fiber, highly viscous fluids can reduce the sedimentation of suspended particles; however, they are less effective in mobilizing deposited particles. This limitation arises from their viscous properties, which can reduce local fluid velocity (Fig. 2.3b) and diminish hydrodynamic forces acting on settled particles. In contrast, lower-viscosity fluids can generate higher local velocities near deposited particles, enhancing their mobilization. Overall, the effectiveness of cleaning fluids in deviated wells is governed by factors such as flow regime, fluid properties, wellbore geometry, and other flow parameters, which collectively influence cuttings transport and removal efficiency (Garcia et al., 2024).

Fiber Drag and Turbulent Suppression

Particle settling in drilling fluids can be mitigated by increasing viscous momentum transfer, which enhances the interaction between the moving fluid and deposited bed particles in horizontal and highly deviated wells. This mechanism facilitates the mobilization of settled particles by increasing the drag forces (hydrodynamic and fiber drag) exerted by the fluid, thereby promoting their transport. The introduction of more fiber into the fluid further influences this process by enhancing the fiber drag. Although fiber addition generally reduces turbulent intensity, its impact remains limited at low concentrations (less than 0.1% w/w). Under these conditions, the effect of enhanced momentum transfer due to fiber drag dominates over the fiber-induced suppression of turbulence, leading to improved hole cleaning performance.

The fiber network within the fluid increases the drag total force acting on suspended and deposited particles, aiding in their mobilization and preventing re-settling. Additionally, the interaction between fiber and solid particles contributes to a more uniform distribution of cuttings within the annulus, reducing the likelihood of localized accumulation and bed formation. The effectiveness of this mechanism is influenced by several parameters, including fiber type and concentration, fluid flow rate, wellbore inclination, and fluid viscosity. Proper optimization of fiber concentration and fluid properties is essential to maximize the benefits of viscous momentum transfer while minimizing any adverse effects on flow behavior such as suppression of turbulence (Garcia et al., 2024).

Impact on Incipient Motion of Particles

The initiation of lifting or rolling of deposited particles occurs when the net force or net moment acting on the particle becomes positive, as determined by a mechanical force balance. In drilling fluids, this process is governed by multiple interacting forces, including gravitational and buoyant forces, hydrodynamic forces such as drag and lift, and the plastic force associated with the fluid's yield stress, which resists particle motion (Ahmed et al., 2003). The interplay between these forces determines whether a particle remains stationary or becomes mobilized under fluid flow conditions.

In fibrous fluids, the presence of fiber significantly alters the force balance by introducing additional mechanical and hydrodynamic interactions. Fiber particles dispersed within the fluid establish a network through fiber entanglement and fiber-fiber

interactions, causing fiber motion to become collective rather than independent. As a result, deposited particles experience fiber-induced drag, which enhances their mobilization. The fiber drag reduces the critical fluid velocity required to initiate particle movement, improving hole cleaning efficiency at lower flow rates. The extent of fiber drag is influenced by fiber concentration, fiber length, and flow conditions, highlighting the importance of optimizing fiber properties to maximize cuttings transport in deviated and horizontal wellbores.

2.4 Modelling Studies

Various modeling approaches have been developed to evaluate and optimize the hole-cleaning process, contributing significantly to the understanding of the effects of different operational variables on cuttings transport efficiency (Rasi, 1994; Larsen et al., 1997; Ahmed et al., 2001; 2003; Duan et al., 2009; George et al., 2014; Naik, 2015; Elgaddafi & Ahmed, 2020). These models employ diverse methodologies, including empirical, semi-empirical, and mechanistic approaches, CFD techniques, and machine learning methodologies to analyze cuttings transport dynamics and predict hole-cleaning performance under varying conditions.

Empirical and Semi-Empirical Models

Empirical models (Rasi, 1994; Larsen et al., 1997; George et al., 2014; Naik, 2015) are primarily based on experimental data and provide correlations derived from observed trends in laboratory or field studies. Semi-empirical models integrate analytical

formulations with empirical correlations, offering improved predictive capability by incorporating theoretical and experimental insights. Empirical and semi-empirical models are often employed to estimate Critical Transport Velocity (CTV) and equilibrium cuttings bed height in highly deviated and horizontal wells, aiding in the optimization of wellbore cleanout strategies. These modeling approaches play a crucial role in optimizing drilling fluid properties, flow conditions, and operational parameters to enhance cuttings transport and minimize wellbore obstructions by providing quantitative assessments of hole-cleaning efficiency.

Mechanistic Models

Mechanistic models mathematically characterize the fundamental physical principles governing the hole-cleaning process. These models are generally categorized into two types: two-layer and three-layer models. Three-layer models provide a more comprehensive representation by accounting for the interactions between moving and stationary cuttings beds and suspended fluid layers (Cho et al., 2000; Ahmed et al., 2005). Their accuracy depends on incorporating precise hydraulic models to determine fluid velocity profiles and shear stress distribution at the solid bed interface.

Due to their complexity, mechanistic models are mathematically intensive and require extensive computational effort for development. They rely on several assumptions, including uniform particle size and shape and the flatness of cutting beds (Ahmed et al., 2001; 2003). While necessary for tractability, these simplifications may introduce discrepancies between model predictions and actual field conditions.

Furthermore, many early mechanistic models did not account for the effects of pipe eccentricity in horizontal and deviated wells, which can significantly influence flow dynamics and cuttings transport efficiency. As a result, the accuracy of such models is often limited in non-vertical well configurations, necessitating further refinement to improve predictive capabilities and applicability in complex drilling environments.

CFD Models

Recent advancements in numerical modeling have significantly enhanced the ability to simulate steady-state and transient solids transport in highly deviated and horizontal wellbores (Guo & Li, 2017; Akhshik et al., 2015). These simulations provide valuable insights into the complex fluid-particle interactions governing cuttings transport, enabling a more detailed assessment of operational parameters such as flow regime, fluid rheology, and pipe rotation. Numerical models utilize computational fluid dynamics (CFD) and discrete element methods (DEM) to predict particle movement, deposition, and resuspension under various flow conditions.

Despite improvements in computational capabilities, these simulations remain computationally intensive, often requiring several hours or even days to complete, particularly when accounting for multiphase flow interactions and non-Newtonian fluid behavior. The accuracy of numerical models is highly dependent on grid resolution, turbulence modeling, and boundary condition assumptions. Ongoing research continues to refine these models to improve efficiency, reduce computational costs, and enhance their predictive capabilities for optimizing hole-cleaning operations.

Machine Learning Models

Recent studies have applied machine learning (ML) techniques to model hole-cleaning processes, leveraging the availability of extensive field and laboratory datasets (Ozbayoglu et al., 2021; Khaled et al., 2021; Salaheldin., 2019). ML algorithms provide a data-driven approach to optimizing hyperparameters, identifying anomalies, and classifying patterns through statistical analysis. These methods offer enhanced predictive accuracy compared to conventional empirical models by capturing complex, nonlinear relationships within the data.

Machine learning techniques also facilitate real-time adjustments based on observed operational conditions, enabling dynamic decision-making during hole-cleaning processes. This adaptability enhances operational efficiency by allowing for rapid modifications to drilling parameters, reducing uncertainties, and improving cuttings transport performance. Additionally, ML-based models contribute to cost reduction by minimizing operational delays and optimizing fluid properties and flow conditions. The integration of ML into hole-cleaning modeling represents a significant advancement in predictive analytics, offering a more efficient and data-driven approach to wellbore cleaning optimization.

Descriptive Data Analytics

Descriptive data analytics has been employed to investigate the influence of key rheological parameters on hole-cleaning efficiency. Alkinani et al. (2019) analyzed drilling records from over 2,000 wells in southern Iraq to assess the effects of plastic

viscosity (PV), yield point (YP), and flow rate on cuttings transport. Using Pearson correlation and sensitivity analyses, they quantified the relationships between these variables. The study revealed that YP exhibited a stronger correlation with cleaning rate compared to PV, indicating that an increase in the YP/PV ratio could improve hole-cleaning performance. This finding suggests that optimizing the fluid's rheological properties can enhance cuttings transport efficiency under various operational conditions. Additionally, their analysis provided insights into predicting the necessary flow rate adjustments to achieve optimal hole cleaning. These results demonstrate the efficacy of descriptive data analytics in identifying critical parameters and improving wellbore cleaning strategies through data-driven decision-making.

AI Techniques

Salaheldin et al. (2019) employed artificial intelligence (AI) techniques to predict cuttings concentration in the wellbore, utilizing a dataset comprising 116 experimental measurements. Their analysis incorporated multiple operational and fluid parameters, including mud density, rheological properties, wellbore inclination, penetration rate, rotation speed, flow rate, pipe eccentricity, and temperature. Support vector machines (SVM) and artificial neural networks (ANN) were implemented to develop predictive models, achieving an average absolute error of less than 5% and a correlation coefficient exceeding 0.9. The AI-based approach demonstrated superior accuracy compared to conventional models reported in the literature. These findings highlight the effectiveness of AI techniques in capturing complex, nonlinear relationships governing cuttings

transport and wellbore hydraulics. By leveraging machine learning algorithms, the study provided an improved predictive framework for optimizing drilling parameters and enhancing hole-cleaning efficiency in various wellbore conditions.

A similar study (Ozbayoglu et al., 2021) applied artificial neural networks (ANNs) to model wellbore cleanout during drilling using laboratory-generated data. The model incorporated key parameters affecting hole cleaning, including wellbore and pipe diameters, rate of penetration (ROP), flow rate, drillpipe rotational speed, inclination, and the physical properties of both the fluid and cuttings. The ANN-based model demonstrated superior predictive performance compared to traditional mechanistic models, effectively capturing complex nonlinear relationships among the input variables. Additionally, a generalized ANN algorithm was employed to optimize drillpipe rotational speed and flow rate, aiming to minimize energy consumption while enhancing hole-cleaning efficiency. These results underscore the potential of AI-driven approaches for improving wellbore cleaning by providing data-driven optimization of drilling parameters and enhancing predictive accuracy in dynamic drilling environments.

2.5 Industry Hole Cleaning Practices

Oil-based mud (OBM) is the most commonly used drilling fluid in horizontal well operations. Compared to water-based muds (WBM), OBMs offer several operational advantages. They provide superior lubricity, which is essential for protecting the sensitive internal components of measurement-while-drilling (MWD) tools and rotary steerable systems. OBMs also reduce downhole torque, allowing for the extension of long

horizontal laterals. In addition, OBMs offer greater shale inhibition, which is critical in formations that are prone to hydration and swelling. This is largely due to their composition, typically with oil-to-water ratios ranging from 70:30 to 90:10 and calcium chloride brines in the water phase. This composition provides effective inhibition for reactive shales and minimizes the risk of wellbore instability and stuck pipe incidents.

Although OBMs dominate horizontal drilling, WBMs remain relevant in specific operational scenarios. They are often used when environmental constraints prevent the use of OBMs or when synthetic-based mud systems are cost-prohibitive. WBMs are also preferred in formations where high fluid losses are expected, as their lower cost makes them more viable for loss control operations. While the industry increasingly focuses on optimizing hole cleaning with OBMs, many of the same operational principles and additives can be adapted for WBMs. Despite a decline in their use for horizontal wells, WBMs remain indispensable in certain fields where OBM deployment is restricted or impractical.

Findings of this dissertation emphasize the importance of tailored fluid selection and operational parameters. Similarly, industry practices support the modeling of each horizontal well on a case-by-case basis. This helps define the optimum fluid properties and mechanical parameters to achieve efficient hole cleaning under specific conditions. One widely used practical indicator for evaluating a fluid's hole-cleaning capability is the 6-rpm reading from a Fann viscometer. A target range of 1.0 to 1.5 times the drill bit diameter (in inches) is recommended as a rule of thumb. While this guideline serves as a

useful benchmark, actual hole-cleaning performance is influenced by multiple interacting variables, including flow rate, pipe rotation, annular geometry, and bed irregularities.

Regarding flow rate, best practices suggest pumping at the highest feasible rate without exceeding the formation's fracture gradient or inducing excessive equivalent circulating density (ECD). Maximizing annular velocity is key to disturbing and transporting settled cuttings, especially in the horizontal section where gravitational assistance is minimal. Similarly, pipe rotation should be applied as aggressively as allowed by surface torque and tool integrity. During cleanout cycles, working the string up and down enhances the mechanical agitation of the cuttings bed. Tool joints can act as mechanical disruptors, further assisting in breaking up and mobilizing accumulated solids from the wellbore bottomhole into the flow stream.

Proper hole cleaning is also critical during completion operations, particularly in wells completed using the "plug-and-perf" method. After hydraulic fracturing, coiled tubing (CT) or jointed pipe operations are typically used to mill out bridge plugs. If not effectively removed, these milling operations generate debris, which can lead to bottom hole assembly (BHA) sticking or loss of well control. Efficient plug debris removal is essential for maintaining wellbore integrity and ensuring that post-frac production proceeds as planned.

The fluid system used during CT cleanout is intentionally simple, typically consisting of water, a friction reducer (FR), and a biocide. The primary objective is to achieve turbulent flow to lift and transport solids efficiently, while minimizing costs.

Numerous field trials have demonstrated that water-based systems can achieve sufficient flow turbulence for effective hole cleaning under the right conditions. The FR is used to reduce drag and circulating pressure, especially along the cased hole. The biocide mitigates the risk of bacterial contamination. If water and FR are insufficient to clean the wellbore, a xanthan gum sweep may be deployed to increase viscosity and enhance suspension. Common operating viscosities range between 80 and 100 funnel vis when using FR. If hydrogen sulfide (H_2S) is present in the reservoir fluid, H_2S scavengers are also added to the fluid to ensure personnel safety and equipment integrity.

These field practices confirm many of the experimental findings presented in this dissertation. Some specific findings include the effectiveness of low-viscosity fluids under turbulent conditions, the role of mechanical agitation (e.g., pipe rotation), and the importance of customized strategies for hole cleaning. As demonstrated in both laboratory and industry settings, optimizing hole-cleaning performance requires a holistic approach that integrates fluid properties, well geometry, and dynamic flow behavior.

CHAPTER 3

Experimental Studies

This chapter provides a detailed overview of the experimental design and methodology employed in this research. It outlines the test variables, describes the experimental facility, and specifies the measuring instruments utilized. Additionally, the chapter presents the characteristics of the test fluids and materials used throughout the investigation. The subsequent sections systematically detail the testing procedures to ensure reproducibility and accuracy in data collection and analysis.

3.1 Testing Methodology

The experimental methodology employed in this investigation involved the erosion of deposited cuttings beds at a constant flow rate until an equilibrium condition was achieved. Upon reaching equilibrium, the corresponding bed height was measured and recorded for the specified flow rate. The test was conducted stepwise across a range of flow rates, beginning with the lowest and progressively increasing to the highest rate capable of fully cleaning the test section.

3.2 Test Variables and Scope

Several factors influence equilibrium bed height measurements, including temperature, pressure, flow rate, fluid and solids properties, wellbore geometry, fiber type

and concentration, and hole inclination. In this investigation, specific test parameters, including temperature, pressure, wellbore geometry, solids properties, and hole inclination, were held constant to ensure controlled experimental conditions. The pressure was maintained below 50 psi to prevent potential damage to the test section, while all tests were conducted at an ambient temperature of 25 ± 2°C. Minor pressure variations below 50 psi are not expected to affect the measurements, as the rheological properties of drilling fluids remain largely insensitive to pressure changes within this range. The experimental variables adjusted during testing included flow rate, pipe rotation speeds, fiber type, and fiber concentration to evaluate their influence on equilibrium bed height.

In addition to hole-cleaning experiments, pipe viscometer tests were conducted to examine the effects of fiber on fluid rheology and hydraulics, providing further insight into the influence of fiber on flow behavior and cuttings transport efficiency.

3.3 Experimental Setup

The hole-cleaning experiments were conducted in a horizontal configuration using an annular test section. Additionally, a pipe viscometer section was installed in parallel with the annulus to analyze the rheological behavior and hydraulic characteristics of the test fluids. A simplified schematic of the test setup used for hydraulic and wellbore cleanout studies is presented in Fig. 3.1.

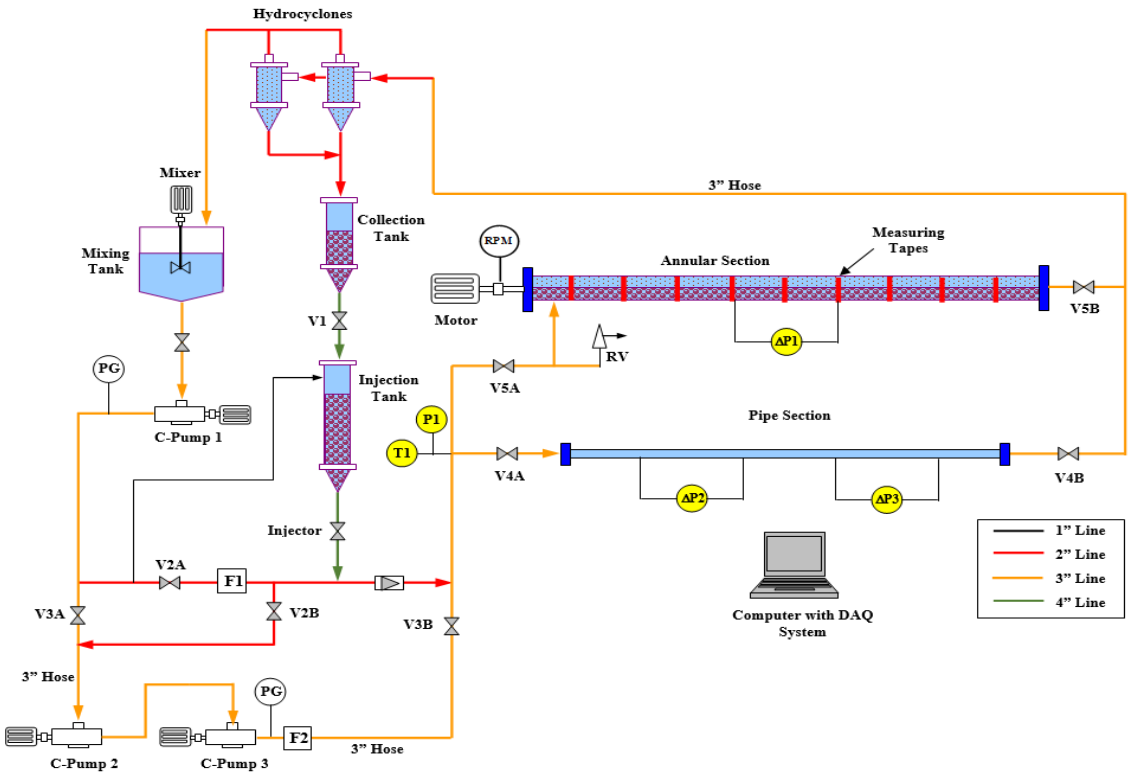


Figure 3. 1. Schematic of the experimental setup (Mendez et al., 2023)

The primary components of the experimental setup (Fig. 3.2) consist of: (i) a 48-ft-long almost fully eccentric annular section with an inner diameter of 2.375 inches and an outer diameter of 5.5 inches, along with a 2-inch pipe test section positioned in parallel with the annulus; (ii) a test fluid preparation and circulation tank, constructed from PVC, with a maximum capacity of 150 gallons; (iii) a steel solids injection tank with a volumetric capacity of 22 gallons and a pressure rating of 150 psi; (iv) a steel solids collection tank with a capacity of 15 gallons and a pressure rating of 150 psi; (v) centrifugal pumps for fluid circulation, with a maximum capacity of 500 gpm; (vi) two hydrocyclones, each with a capacity of 150 gpm, for separating solids from the returning

fluid; (vii) pipe rotating system with variable speed controller; viii) measuring instrumentation, including two Coriolis flowmeters (F1: low-range with a capacity of 230 gpm and F2: high-range with a capacity of 3000 gpm), as well as transmitters for measuring pressure gradient, static pressure, and temperature; and (ix) a Data Acquisition (DAQ) system designed for displaying and recording experimental parameters.

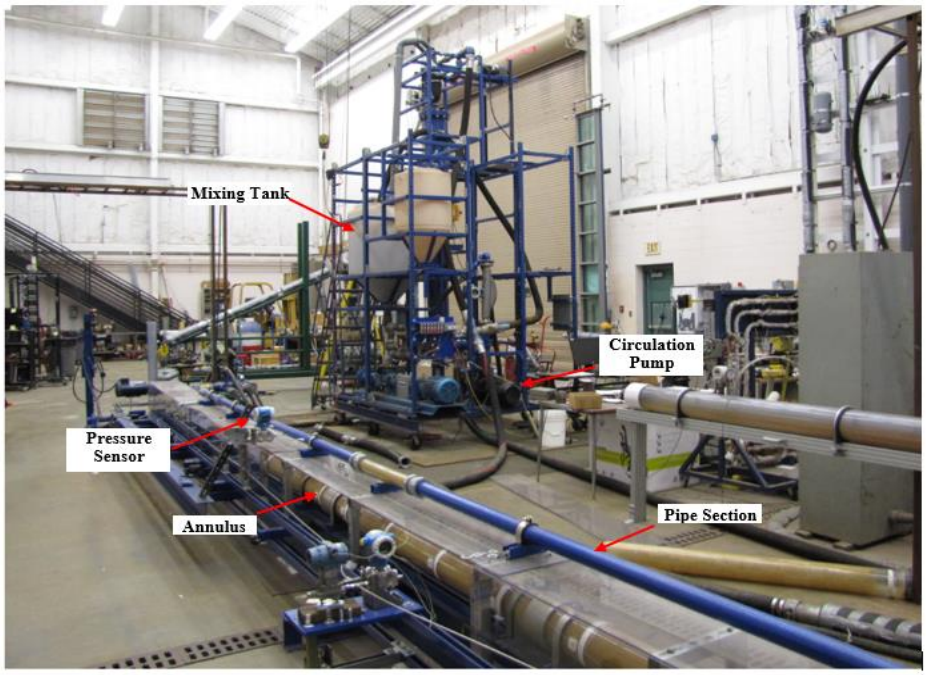


Figure 3. 2. A photo of the flow loop

Circulation pumps regulate the required flow rate through the use of Variable Speed Drives (VFDs). The pipe section functions as both a hydraulic test section and a bypass line, facilitating the removal of accumulated cuttings from the delivery and return lines. The return line from the test section is directed to the hydrocyclones, which are employed to separate cuttings from the test fluid. The removed cuttings are collected in

the cuttings collection tank, positioned beneath the hydrocyclones, and subsequently transferred to the injection tank via gravity-driven flow.

The annular test section (Fig. 3.3) is fully transparent, allowing for direct visualization of cleanout mechanisms and accurate recording of bed height measurements. Two 2-ft-long aluminum sections are installed within the annulus, matching the diameters of the transparent section. These aluminum sections facilitate connections to pressure measurement points, as well as drain and vent lines. Measuring tapes are affixed to the inner wall of the annulus to enable precise bed height measurements at 29 locations along the test section, with each measurement taken at intervals of approximately 1.5 feet.

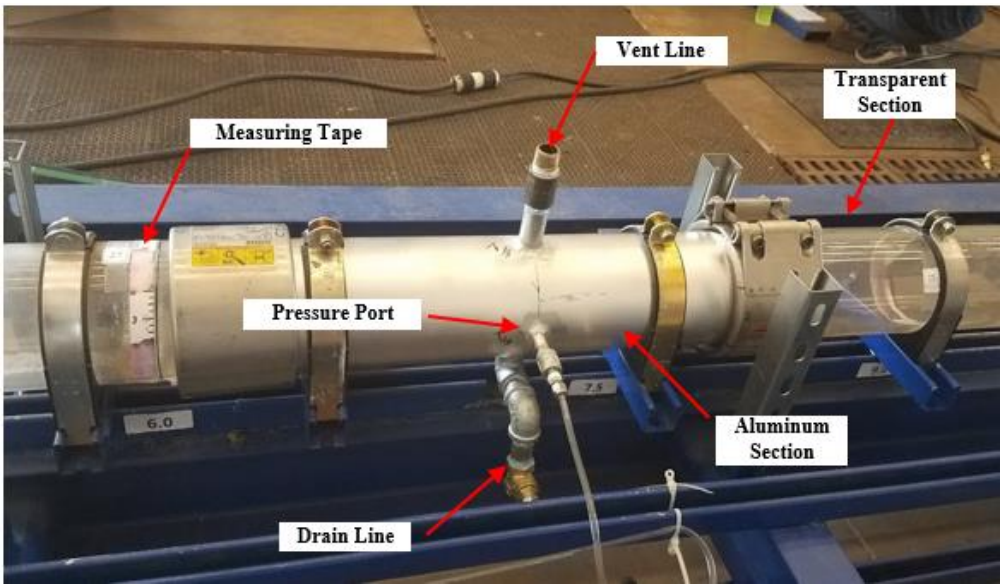


Figure 3. 3. Annular test section

A pipe rotation system (Fig. 3.4) equipped with a variable frequency drive (VFD) is installed to enable drillpipe rotation at controlled rotational speeds ranging from 0 to 180 rpm. This system comprises a drive motor with VFD, a speed reduction gear, rotary

bearings, and a shaft seal. The rotary bearing assemblies are designed, manufactured, and installed at both ends of the test section to facilitate the free rotation of the inner stainless-steel pipe, ensuring stable and efficient operations.

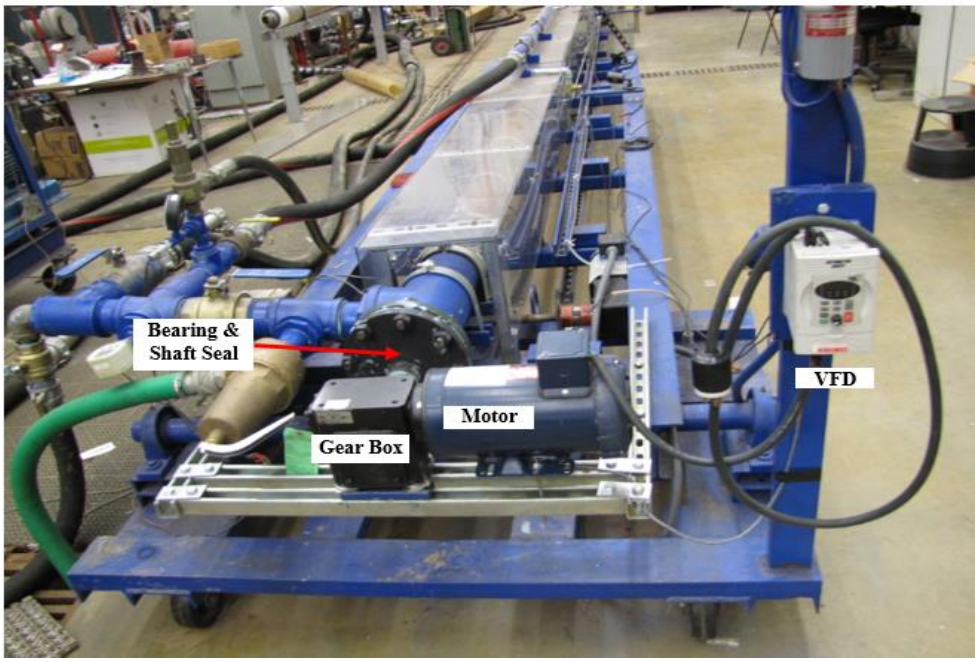


Figure 3. 4. Pipe rotation system

3.4 Test Fluids and Materials

The test fluids were prepared by dispersing technical-grade Xanthan gum (XG) and polyanionic cellulose (PAC) in tap water at varying concentrations, resulting in the formulation of thin and thick fluids (Table 3.1). The polymers, supplied in powder form, were thoroughly mixed to ensure uniform dispersion and subsequently allowed to hydrate for 24 hours. A commercial biocide was added to inhibit bacterial growth and prevent biological degradation of the fluids. Additionally, an antifoaming agent was incorporated to minimize foam formation in the storage tank and facilitate proper fluid mixing.

Specially processed monofilament synthetic fibers with an approximate diameter of 100 µm were utilized. Two distinct fiber types were employed: short fibers with length of 1/8 inch and long fibers measuring 1/4 inch.

The experiments were conducted using natural sand with a particle size distribution comparable to that of representative field wells, with a mean particle diameter of approximately 1246 µm. The particle size distribution of the sand is presented in Fig. 3.5. Measurements indicate that the sand had a density of 18.3 lbm/gal and an angle of repose of 35°, as reported by Garcia et al. (2022)

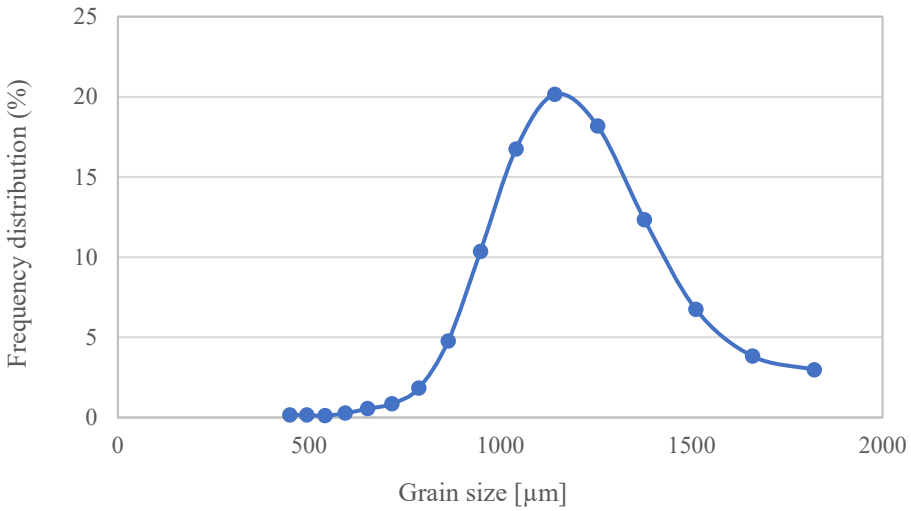


Figure 3. 5. Particle size distribution of sand (Garcia et al., 2024)

The rheological properties of the test fluids were measured using a 12-speed rotational viscometer (OFITE Model 900) both before and after fiber addition (Fig. 3.6). Given that fiber was introduced at a low concentration (0.04 wt%), its impact on fluid rheology was minimal. Both fiber types exhibited negligible influence on the rheological

behavior of the fluids. This observation indicates that under laminar flow conditions, the presence of fiber has an insignificant effect on flow hydraulics. Consequently, hydraulic parameters such as pressure loss, wall shear stress, and velocity distribution remain unaffected by fiber addition in laminar flow regimes.

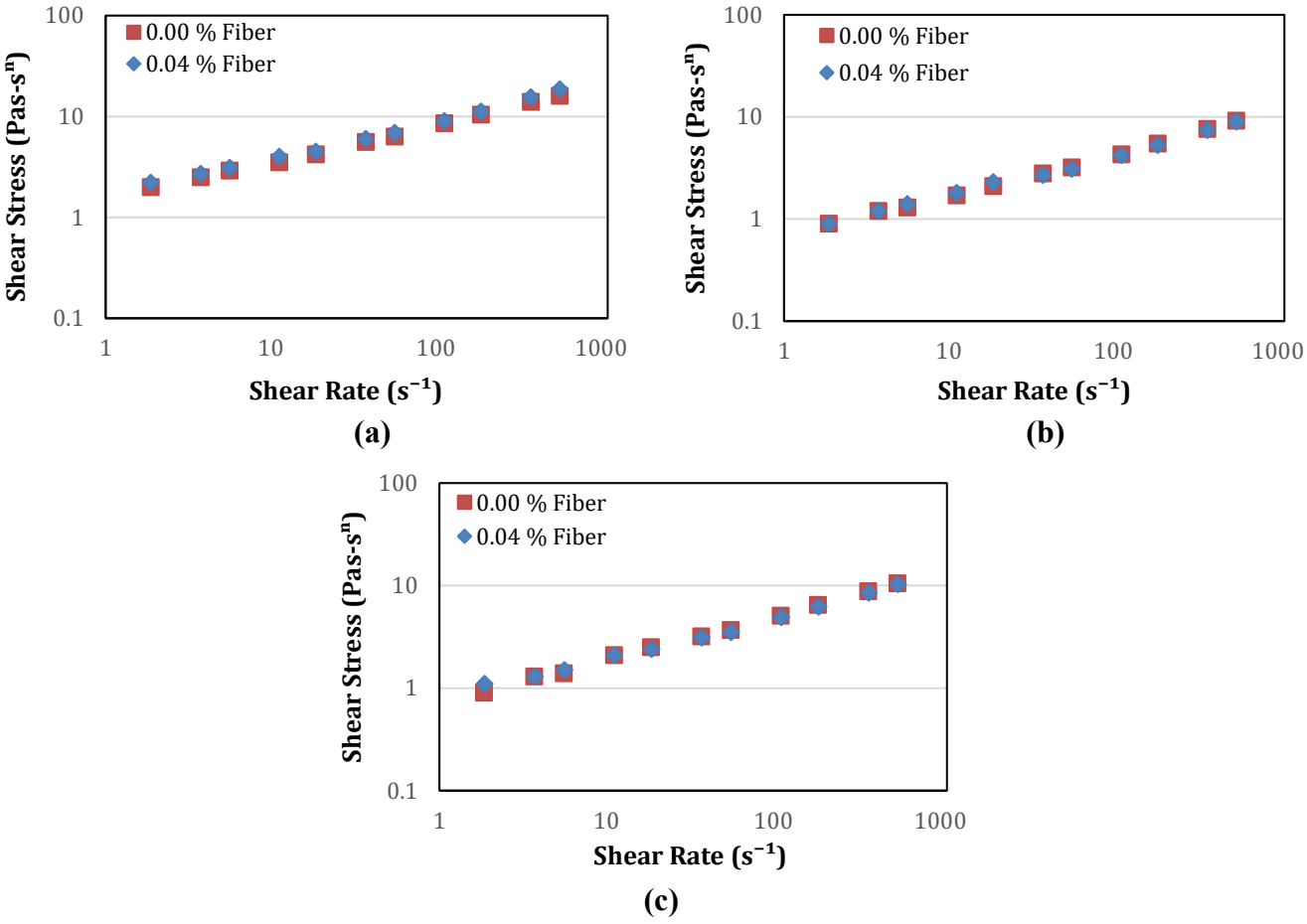


Figure 3. 6. Rheology of test fluids measured using a rotational viscometer with and without fiber: a) thick fluid (long fiber); b) thin fluid (long fiber); and c) thin fluid (short fiber) (Mendez et al., 2023)

Additionally, a pipe viscometer was employed to assess the effect of fiber on the hydraulics of test fluids under both laminar and turbulent flow conditions (Fig. 3.7).

Differential pressure measurements indicated similar values for fibrous and non-fibrous fluids at the same flow rates. In the case of thick fluid, fiber addition resulted in a slight reduction in pressure loss under turbulent flow conditions, suggesting that fibers contribute to turbulence suppression. However, for thin fluid, the presence of fiber had a negligible impact on pressure loss, regardless of the flow regime.

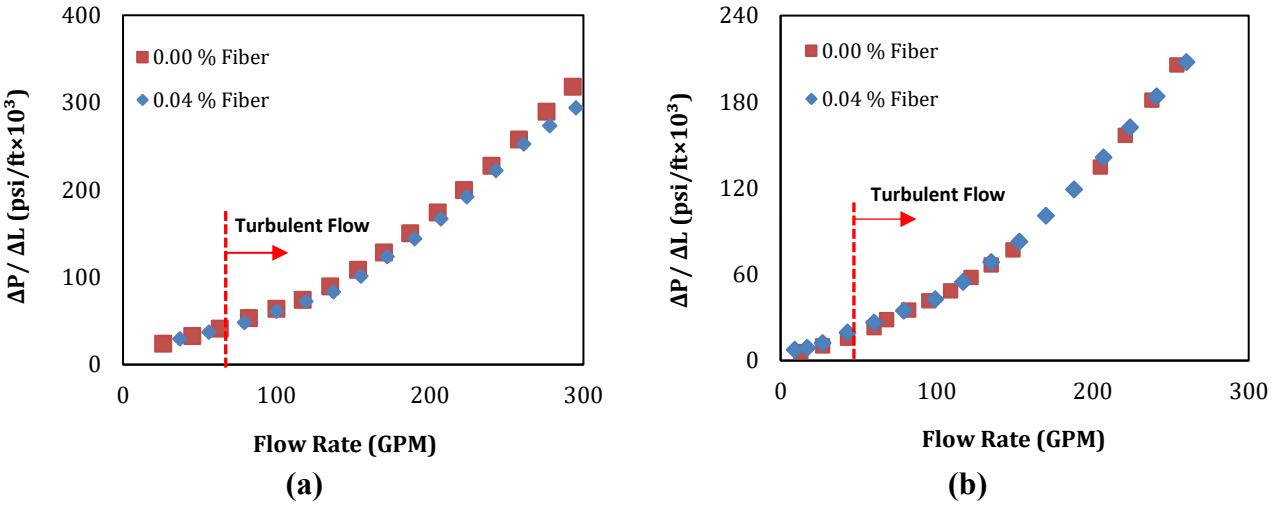


Figure 3. 7. Pressure loss versus flow rate in pipe viscometer for different fluids: a) thick fluid; and b) thin fluid (Mendez et al., 2023)

Table 3.1 presents the composition and rheological properties of the tested fluids. A regression analysis was performed using data obtained from the rotational viscometer (Fig. 3.6) to determine the rheological parameters of the test fluids. The data demonstrated a strong fit to the power-law rheology model. The correlation coefficient quantifies the relationship between the measured shear stress and shear rate based on the parameters n and K. Slight variations in the values of n and K were observed for the second thin fluid sample, which may be attributed to minor differences in fluid composition and/or

temperature difference during measurements. This variation could result in subtle changes in the fluid's flow behavior, leading to slight deviations in the rheological parameters n and K.

Table 3. 1. Rheological parameters of XG/PAC fluids (Mendez et al., 2023)

Composition			**Rheological Properties**		
Cleanout Fluids	Fluid Concentration (lb/bbl)	Fiber Concentraion (lb/bbl)	K (eq. cP)	n	R^2
Thick Fluid no Fiber	XG/PAC 0.87/0.87	0	1486	0.373	0.998
Thick Fluid with Long Fiber		0.14	1596	0.378	0.996
Thin Fluid no Fiber	XG/PAC 0.74/0.61	0	648	0.414	0.995
Thin Fluid with Long Fiber		0.14	678	0.403	0.991
Thin Fluid no Fiber (Repeat)	XG/PAC 0.74/0.61	0	704	0.427	0.999
Thin Fluid with Short Fiber		0.14	759	0.406	0.994

3.5 Testing Procedure

Following preliminary tests with water and polymeric fluids, a standardized testing procedure was established, comprising three primary steps: (i) fluid preparation, (ii) formation of a solids bed in the annulus, and (iii) bed erosion. Each step is described in detail below.

Step I: Fluid Preparation

The test fluid was prepared in the circulation tank by mixing the required quantities of water and viscosifying polymers using a high-speed agitator. Simultaneously, the fluid

was circulated through the flow loop to ensure uniform mixing. After 30 minutes of continuous agitation, mixing was discontinued, and the fluid was allowed to hydrate overnight. Following a 24-hour hydration period, the rheological properties of the fluid were measured using a rotational viscometer.

Step II: Formation of a Solids Bed in the Annulus

To establish a solids bed, the test fluid was first directed into the annular test section (Fig. 3.1) by closing the bypass valves (V4A and V4B) and opening the inlet and outlet valves of the annular section (V5A and V5B). The flow rate was maintained at 30 gpm. Solids injection commenced by opening the injection valve. As the mixture of test fluid and solids entered the annulus, solid particles settled due to the low fluid velocity, forming a deposit along the lower section of the annular test section. The returning fluid, containing non-deposited particles, was directed to the circulation tank via hydrocyclones, where solid particles were separated and collected in the solids collection tank. Circulation continued until a uniform and stable solids bed was formed. At this point, fluid circulation was halted, and the injection valve was closed.

Step III: Bed Erosion

The bed erosion process was conducted incrementally, beginning at the lowest flow rate established during preliminary tests (Fig. 3.8a). The fluid was circulated at a constant rate, allowing erosion to proceed until the bed height stabilized, indicating that equilibrium had been reached. Equilibrium was determined based on the stabilization of pressure loss across the annular test section (Fig. 3.8b). Bed height measurements were

recorded at multiple locations along the test section, including both the left and right sides. In the absence of pipe rotation, bed height measurements obtained from both sides of the test section were comparable. However, when tests were conducted with pipe rotation, significant differences in bed height were observed between the two sides. Following each measurement, the flow rate was incrementally increased and maintained until a new equilibrium condition was established. This stepwise increase in flow rate and subsequent equilibrium measurements continued until the solids bed was completely removed. Throughout the experiments, key parameters, including flow rate and pressure loss across the annular section, were continuously monitored and recorded using the data acquisition system. Upon completion of the test, the rheological properties of the test fluid were re-evaluated using a rotational viscometer.

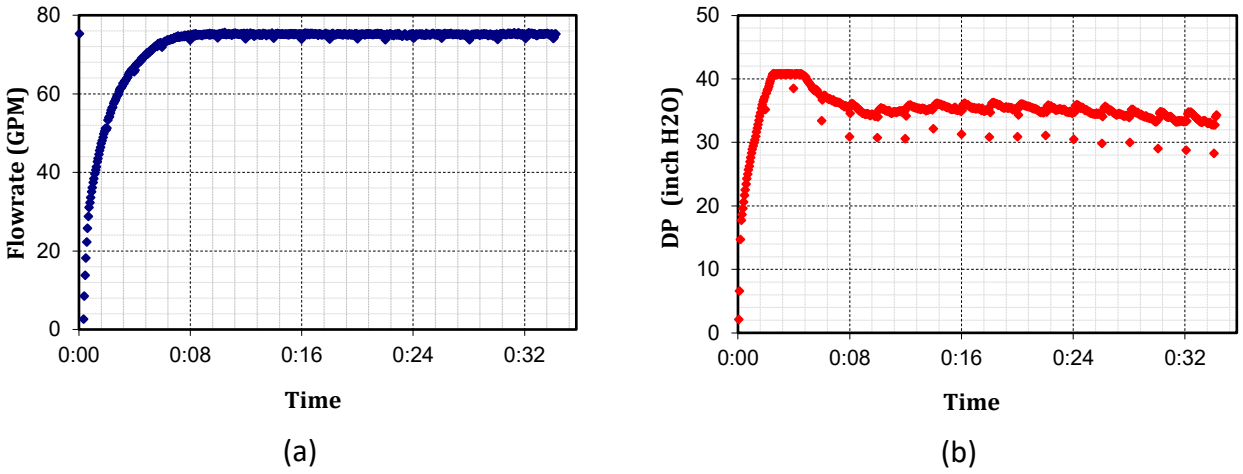


Figure 3. 8. Main test parameters during the erosion process: a) flowrate; and b) annular pressure loss (Mendez et al., 2023)

CHAPTER 4

Experimental Results and Discussions

This chapter presents a comprehensive analysis of the results obtained from hole-cleaning experiments. The tests were conducted in a horizontal orientation. The study first evaluates the role of fiber in enhancing hole cleanout by comparing the performance of fibrous fluids to non-fibrous fluids. The analysis focuses on pressure loss and equilibrium bed height across different flow rates. The accuracy of hydraulic models used to predict these parameters is assessed. Subsequently, the investigation examines the influence of wellbore solids bed irregularities on fluid flow and frictional pressure losses. These irregularities challenge conventional hydraulic models, which typically assume uniform bed conditions. The relationship between pressure loss and bed height variability is quantified using localized bed height measurements and statistical analysis. Finally, the impact of pipe rotation on hole cleaning is explored, analyzing how different fluid formulations and rotational speeds influence bed erosion and overall cleaning efficiency. These experiments provide critical insights for optimizing hole-cleaning operations.

4.1 Effects of Fibers

This section examines the effectiveness of fibers in enhancing hole cleanout operations in horizontal wells. The accuracy of hydraulic models is evaluated in predicting pressure loss during cleanout operations. Hole cleanout experiments were conducted to measure equilibrium bed height and pressure loss at various flow rates, both

with and without fiber. The impact of fiber on hole cleaning efficiency was assessed by comparing these experimental results. Additionally, the predictive capabilities of traditional and recent hydraulic models were analyzed by comparing their estimated frictional pressure losses with the measured values.

4.1.1 Hole Cleaning

A series of bed-erosion tests were conducted using various fluid formulations to evaluate the effects of fiber on hole cleaning. The test matrix is outlined in Table 4.1. For each experiment, the annular test section was initially filled with sand to a minimum level of 80% of the outer pipe diameter. This was to ensure complete coverage of the inner pipe. The tests were conducted at constant flow rates and continued for a sufficient duration to achieve equilibrium, defined by a stabilized pressure drop and a nearly constant average bed height. Equilibrium conditions were typically reached within 35 to 45 minutes. Upon completion of each test, bed height measurements were meticulously recorded along the annular test section.

The investigation was conducted in two phases. In the first phase, long fibers were tested with both thin and thick fluids. Results obtained from tests using thin fluids were previously published by Garcia et al. (2022). In this study, Garcia's results are integrated to facilitate a comparative analysis between thin and thick fluids, examining the impact of rheological differences on hole-cleaning performance.

Based on the performance improvements observed with fiber in thin fluids, the second phase explored whether the addition of short fibers to thin fluid could further

enhance cleaning efficiency. Tests were conducted in tandem, with each base fluid initially prepared and tested without fiber, followed by adding fiber to the same fluid for a repeat test. Consequently, the thin fluid was tested twice in the absence of fiber. While the tests followed identical procedures, minimal variations in the fluid's rheological properties were observed. To ensure an accurate comparison, the results of these experiments are presented separately.

Table 4. 1. Test Matrix - No Pipe Rotation (Mendez et al., 2023)

Number of Tests	30
Fluids	Thick Fluid, no fiber: 0.87 XG/0.87 PAC lb/bbl
	Thick Fluid, with long fiber: 0.87 XG/0.87 PAC lb/bbl, 0.04 wt% of long fiber
	Thin Fluid, no fiber 4: 0.74 XG/0.61 PAC lb/bbl (Garcia 2022)
	Thin Fluid, with long fiber: 0.74 XG/0.61 PAC lb/bbl, 0.04 wt% of long fiber (Garcia 2022)
	Thin Fluid, no fiber (Repeat): 0.74 XG/0.61 PAC lb/bbl
	Thin Fluid, with short fiber: 0.74 XG/0.61 PAC lb/bbl, 0.04 wt% of short fiber
Flow Rates	35, 65/75, 115,155 and 195 gpm
Deviation Angle	90° from vertical
Geometry	Outer casing: 5-1/2 in. (140 mm) OD, 5 in. (127 mm) ID; inner pipe: 2-3/8 in. (60 mm) OD

The quantitative evaluation of the cleanout process was conducted by analyzing the dimensionless equilibrium bed height and bed coverage as functions of flow rate. The dimensionless bed height is the ratio of the measured average cuttings bed height to the internal annulus diameter (H_{ave}/D_h). Bed coverage is expressed as the ratio of the bed cross-sectional area to the total cross-sectional area of the annulus. Figures 4.1 and 4.2 present the measured equilibrium bed height and bed coverage as functions of flow rate for different fluids, both with and without fiber.

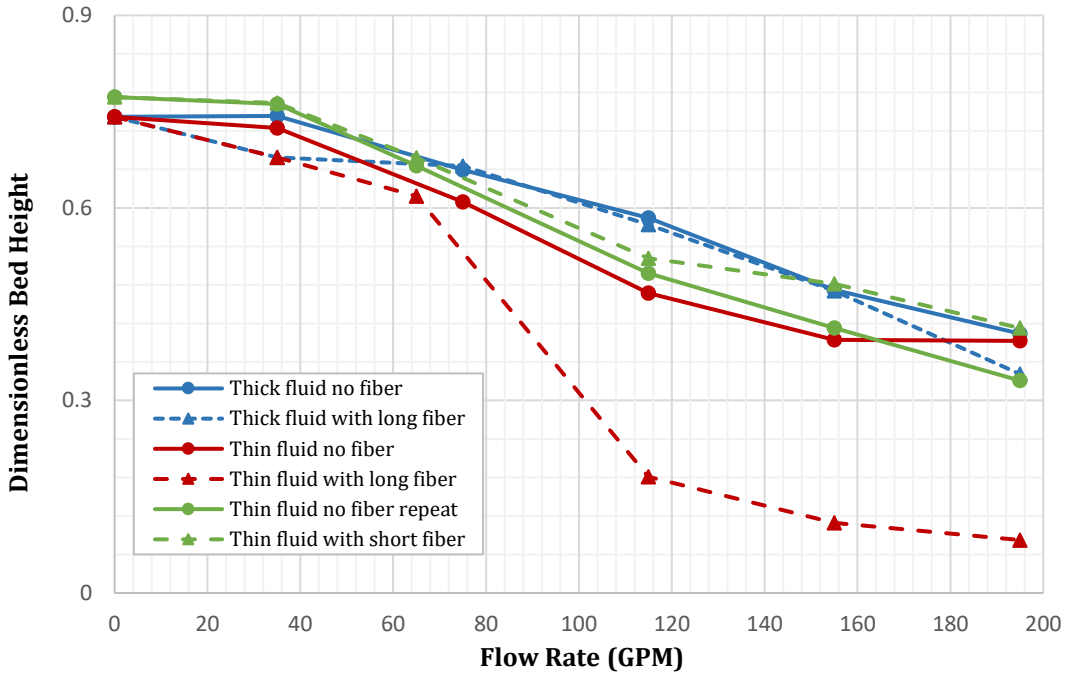


Figure 4. 1. Dimensionless bed height vs. flow rate (Mendez et al., 2023)

Thin fluid experiments without fiber were conducted twice; first to evaluate the performance of long fibers, and subsequently to assess the effectiveness of short fibers. As discussed in Section 3.4, although these fluids were formulated identically, slight variations were observed in their rheological properties. The hole-cleaning performances were generally comparable, except at the highest flow rate of 195 gpm. The mean bed height calculated from these repeated experiments was used to compare the performance of non-fibrous thin fluid with other test fluids. The repeated experiments were used to estimate the uncertainty in the dimensionless bed height measurement, yielding error bars of ±7.2% for each test. These error bars were not shown in Figure 4.1 due to the close proximity of the plotted lines but were included in the hole-cleaning experiments involving pipe rotation in the section 4.3

The uncertainties in measurements may be attributed to multiple factors, including minor variations in fluid rheology, slight deviations in the inner pipe position, and errors in measuring the average bed height. The latter is particularly sensitive to bed profile irregularities, which were more pronounced in experiments involving fiber. Bed height data were collected from 29 locations along the annular test section to minimize measurement errors associated with these irregularities. While increasing the number of measurement points could further enhance accuracy, it would also introduce additional complexity and effort in data collection.

In the absence of fiber, the thin fluid demonstrated superior hole-cleaning performance compared to the thick fluid (Figs. 4.1 and 4.2). The difference in performance was most pronounced within the flow rate range of 75 to 155 gpm, aligning with findings from previous studies (Leising and Walton, 1998; Zamora & Hanson, 1990). Variations in polymer concentration result in differences in the flow behavior, influencing the rheological properties and, consequently, the local fluid velocity and hydrodynamic forces acting on bed particles. Under identical flow rate and bed height situations, thinner fluids exhibit higher local fluid velocities near the bed (Pandya et al., 2020). The local fluid velocity profile is influenced not only by fluid rheology, but also by the prevailing flow regime and wellbore geometry. As a result, the lower-viscosity thin fluid provides more effective cuttings transport, leading to improved hole-cleaning performance relative to the thick fluid.

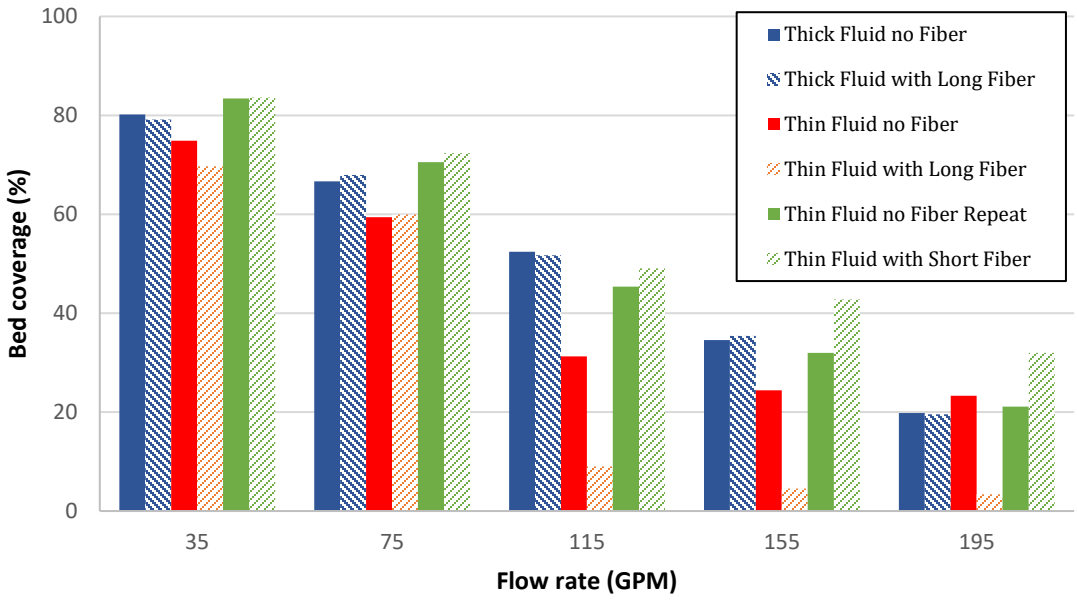


Figure 4. 2. Bed coverage at different flow rates with and without fiber (Mendez et al., 2023)

The effect of fiber was more pronounced in the thin fluid. At higher flow rates, when the equilibrium bed height was below 60% of the annular gap, the addition of long fibers significantly enhanced hole-cleaning performance. Notably, at a flow rate of 195 gpm, the annulus was nearly fully cleaned, with only 3% bed coverage when using the thin fluid with long fiber. However, some sand remained trapped beneath the inner pipe, since the annulus was not fully eccentric. This was caused by the presence of threaded pipe couplings, which created an approximately 0.3-inch gap between the inner pipe and the outer casing. Consequently, complete removal of the solid bed was not achieved. In eccentric wellbores, hole cleaning becomes particularly challenging when the cuttings bed is positioned below the top of the inner pipe, as stagnant flow zones with reduced local fluid velocity hinder effective solids transport.

Although previous studies (Elgaddafi et al., 2012; 2016) have demonstrated enhanced hydrodynamic forces with the addition of long fibers, this study did not indicate a significant impact of fiber on the hole-cleaning performance of the thick fluid. This is potentially due to the reduction in local fluid velocity and the formation of stagnant flow zones near bed particles, which may restrict the influence of fibers. At identical flow rates and bed heights, the thick fluid has a lower local fluid velocity near the bed compared to the thin fluid (Pandya et al., 2020). As a result, despite the presence of a fiber network, the local fluid velocity is insufficient to generate the necessary drag force to facilitate the removal of bed particles. Additionally, stagnant zones develop in eccentric annuli under both turbulent and laminar flow conditions. However, stagnant zones have significantly higher fluid velocities in turbulent flow than laminar flow. Our Results indicated that tests with thin fluids achieved higher Reynolds numbers than those with thick fluids, leading to enhanced hole-cleaning performances with the thin fluid.

The addition of long fibers enhanced the thin fluid's hole-cleaning performance, whereas short fibers did not yield a noticeable improvement. This limitation may be attributed to the absence of a well-developed fiber network in fluids containing short fibers. The formation of a fiber network is essential for generating a strong fiber-induced drag force, which plays a crucial role in cuttings transport (Elgaddafi et al., 2012). The ability of short fibers to generate significant fiber drag forces has not been extensively studied. No sedimentation experiments have been conducted to evaluate this effect. A reliable explanation for the reduced effectiveness of short fibers requires further investigation to determine their impact on cuttings transport and bed erosion mechanisms.

4.1.2 Hydraulics

Various simplified wellbore hydraulics models have been developed to predict pressure losses in horizontal wells, typically assuming concentric annular flow. However, the presence of a solids bed within the wellbore and the eccentric positioning of the drill pipe introduces significant variations in wall shear stress, increasing the complexity of the modeling process. In partially blocked annuli, the bed shear stress, critical for effective hole cleaning, differs significantly from the average wall shear stress (Reed & Pilehvari, 1993; Chen, 2005; Tang et al., 2016; Rojas et al., 2017). Consequently, the combined effects of drill pipe eccentricity and solids bed formation influence both pressure loss and hole-cleaning efficiency, necessitating more advanced modeling approaches.

Traditional wellbore hydraulic models (Whitaker, 1985; Chen, 2005) typically assume uniform bed shear stress (average shear stress) when calculating frictional pressure losses. However, more recent models (Tang et al., 2016; Rojas et al., 2017; Singh, 2019; Elgaddafi et al., 2021) have highlighted discrepancies between the bed shear stress and overall wall shear stress. These newer models incorporate empirical correlations, commonly derived from Computational Fluid Dynamics (CFD) simulations of power-law fluid flow within partially blocked annuli. They consider both laminar and turbulent flow conditions.

This study validates both traditional (Whitaker, 1985; Chen, 2005) and new (Elgaddafi et al., 2021) models using the obtained experimental data. Differential pressure measurements collected under equilibrium conditions are employed to assess the

models at various flow rates and for different fluids. Model inputs include the wellbore geometry, average bed height, fluid properties, and flow rate. Appendix A outlines the computation of geometric parameters, which are used to determine hydraulic diameter and calculate differential pressure. Reynolds number (Re) and average wall shear stress (τ_w) computations are explained in Appendix B for both model types. Regardless of flow regime, both approaches estimate the pressure gradient using the momentum balance relationship:

$$\frac{\Delta P}{\Delta L} = \frac{4\tau_w}{D_{hy}} \tag{4.1}$$

where $\frac{\Delta P}{\Delta L}$ is the pressure gradient, τ_w is the average wall shear stress, and D_{hy} is the hydraulic diameter, defined as the difference of the outer and the inner diameters. A detailed comparison of the traditional and the recent models is provided in Appendix B.

4.1.2.1 Tests without Solid Beds

The accuracy of the models was initially evaluated using data from hydraulic tests without a solids bed (H_{ave} = 0). Figures 4.3 and 4.4 present comparisons between the experimental measurements and model predictions across different test fluids. Cross-plot analyses validate the models' ability to replicate measurements at varying flow rates. The newly developed model demonstrates strong agreement with the experimental data, with a maximum deviation of approximately 21% for the thick fluid. In contrast, the traditional model exhibits error up to 90%.

During the thick fluid tests, flow conditions were predominantly laminar, as indicated by Reynolds numbers ranging from 22 to 2,588. Similarly, experiments

conducted with thinner fluids primarily exhibited laminar flow behavior, with Reynolds numbers between 59 and 3,444. However, a few tests transitioned into turbulent or transitional flow regimes. The newly developed model (Elgaddafi et al., 2021) demonstrated a high degree of accuracy under these conditions, with a maximum error of approximately 22% for the thin fluid. In contrast, the traditional/original models (Whitaker, 1985; Chen, 2005) exhibited significantly greater inaccuracies, with errors exceeding 100%. This overestimation of pressure loss is partially attributed to the conventional model's failure to account for drill pipe eccentricity, which reduces the pressure losses within the annulus.

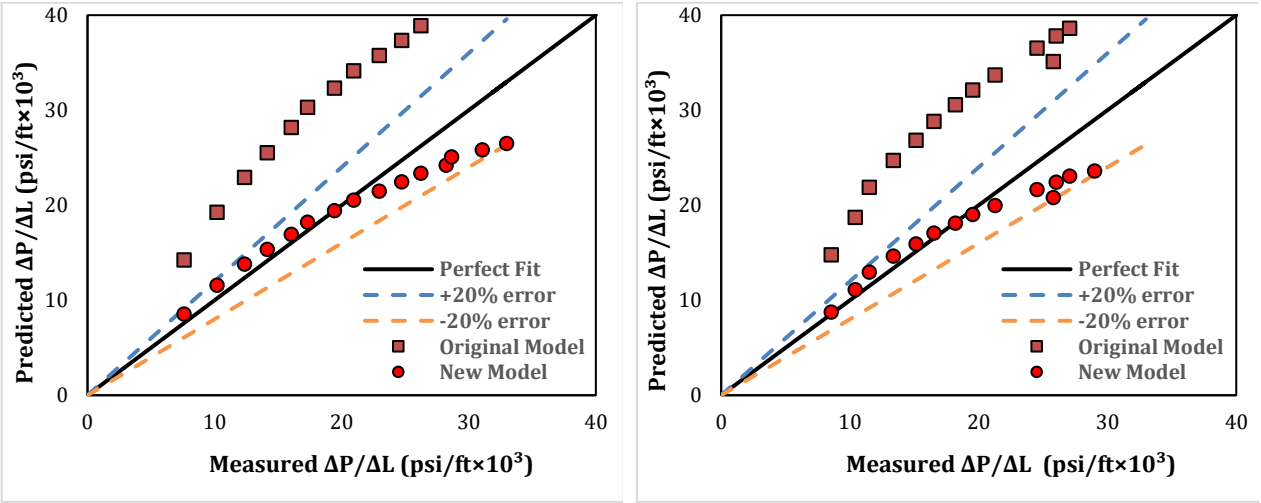
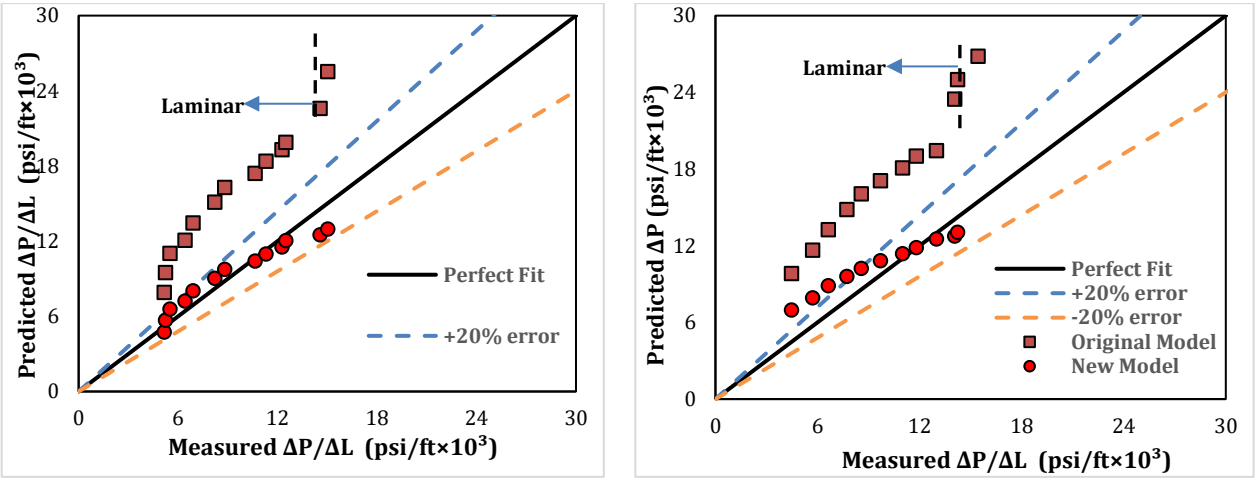


Figure 4. 3. Measured and predicted ΔP for hydraulic tests with thick fluid: a) without fiber; and b) with long fiber (Mendez et al., 2023)



(a) **(b)**

Figure 4. 4. Measured and predicted ΔP for hydraulic tests with thin fluid: a) without fiber; and b) with long fiber (Mendez et al., 2023)

4.1.2.2 Tests with a Stationary Bed

The hydraulic measurements obtained during the cleanout experiments are presented in Tables 4.2 to 4.7. These measurements were recorded once equilibrium flow conditions were established within the test section using differential pressure gauges, which had a systematic instrument uncertainty of ±1%. The experimental data were compared with the predictions of both the original and newly developed models. The calculated generalized Reynolds numbers (Whitaker, 1985; Chen, 2005) indicate the establishment of laminar flow conditions during the experiments, irrespective of polymer concentration or the presence of fiber.

Overall, the new model demonstrates better agreement with the experimental measurements with lower maximum errors compared to the original model. However, the accuracy of the new model is significantly reduced for fibrous fluids. This decrease in

accuracy may be attributed to the model's assumption of a uniform bed. Bed irregularities, such as dunes and ripples, are more pronounced in experiments involving fibrous fluids. Consequently, the deviation from the model's assumption may have contributed to the increased prediction errors during these tests.

Table 4. 2. Model validation for thick fluid without fiber (Mendez et al., 2023)

Test Results					Original model		New model	
Q (GPM)	H bed (in)	CV	Re_Gen	Experimental ΔP/ ΔL (psi/ft×10³)	Theoretical ΔP/ ΔL (psi/ft×10³)	Error (%)	Theoretical ΔP/ ΔL (psi/ft×10³)	Error (%)
35	4.34	0.014	35	58.1	92.8	60%	60.3	4%
75	3.88	0.031	148	40.1	60.8	52%	39.5	-1%
115	3.46	0.145	331	25.9	47.5	83%	30.8	19%
155	2.85	0.092	604	23.7	34.5	46%	22.4	-5%
195	2.47	0.113	926	20.3	30.9	52%	20	-1%

Table 4. 3. Model validation for thick fluid with long fiber (Mendez et al., 2023)

Test Results					Original model		New model	
Q (GPM)	H bed (in)	CV	Re_Gen	Experimental ΔP/ ΔL (psi/ft×10³)	Theoretical ΔP/ ΔL (psi/ft×10³)	Error (%)	Theoretical ΔP/ ΔL (psi/ft×10³)	Error (%)
35	3.98	0.118	41	57.5	52.2	-9%	37.3	-35%
75	3.91	0.039	146	46.5	63.3	36%	45.2	-3%
115	3.41	0.208	335	39.1	45.3	16%	32.4	-17%
155	2.84	0.271	605	40.3	34.3	-15%	24.5	-39%
195	2.13	0.360	955	42.9	27.6	-36%	22.1	-48%

Table 4. 4. Model validation for thin fluid without fiber (Mendez et al., 2023)

Test Results					Original model		New model	
Q (GPM)	H bed (in)	CV	Re_Gen	Experimental ΔP/ ΔL (psi/ft×10³)	Theoretical ΔP/ ΔL (psi/ft×10³)	Error (%)	Theoretical ΔP/ ΔL (psi/ft×10³)	Error (%)
35	4.24	0.106	78	24.2	36.3	50%	25.6	6%
75	3.60	0.044	334	15.2	21.8	43%	15.4	1%
115	2.82	0.150	781	12.1	14.5	20%	10.3	-15%
155	2.42	0.214	1334	7.5	13.3	77%	9.4	25%
195	2.41	0.111	1923	12.5	14.5	16%	10.3	-18%

Table 4. 5. Model validation for thin fluid with long fiber (Mendez et al., 2023)

Test Results					Original model		New model	
Q (GPM)	H bed (in)	CV	Re_Gen	Experimental ΔP/ ΔL (psi/ft×10³)	Theoretical ΔP/ ΔL (psi/ft×10³)	Error (%)	Theoretical ΔP/ ΔL (psi/ft×10³)	Error (%)
35	3.98	0.118	81	21.4	26.7	25%	18.9	-12%
65	3.65	0.063	241	20.0	23.5	18%	16.6	-17%
115	1.25	0.711	792	17.2	11.3	-34%	9	-48%
155	0.85	0.761	1254	14.9	13.4	-10%	10.2	-32%
195	0.70	0.882	1792	15.9	15.1	-5%	11.3	-29%

Table 4. 6. Model validation for thin fluid without fiber repeat (Mendez et al., 2023)

Test Results					Original model		New model	
Q (GPM)	H bed (in)	CV	Re_Gen	Experimental ΔP/ ΔL (psi/ft×10³)	Theoretical ΔP/ ΔL (psi/ft×10³)	Error (%)	Theoretical ΔP/ ΔL (psi/ft×10³)	Error (%)
35	4.440	0.016	60	31.5	64.8	106%	45.6	45%
65	3.910	0.050	203	25.0	36.6	46%	23.5	-6%
115	2.990	0.064	638	12.9	20.4	58%	13.1	2%
155	2.520	0.103	1065	14.8	20.0	34%	11.4	-23%
195	2.070	0.150	1629	14.6	17.8	22%	12.1	-17%

Table 4. 7. Model validation for thin fluid with short fiber (Mendez et al., 2023)

Test Results					Original model		New model	
Q (GPM)	H bed [in]	CV	Re_Gen	Experimental ΔP/ ΔL (psi/ft×10³)	Theoretical ΔP/ ΔL (psi/ft×10³)	Error (%)	Theoretical ΔP/ ΔL (psi/ft×10³)	Error (%)
35	4.450	0.025	62	35.1	66.4	89%	45.9	31%
65	3.980	0.047	215	29.3	36.6	25%	25.3	-14%
115	3.120	0.197	669	18.1	20.4	12%	14.1	-22%
155	2.900	0.221	1136	20.0	20.0	0%	13.8	-31%
195	2.520	0.244	1725	19.6	17.8	-9%	12.3	-37%

4.2 Effect of Bed Irregularities on Hydraulics

The results presented in Figure 4.5 compare the frictional pressure gradients obtained under equilibrium bed conditions with the predictions of both the original model (O-Model) and the new model (N-Model) for different fluid formulations. The data reveal notable deviations between experimental measurements and model predictions,

particularly in the presence of fiber. The addition of fiber results in a significant increase in frictional pressure gradient for both thin and thick fluids. This increase was observed despite minimal changes in rheological measurements obtained from rotational and pipe viscometers with fiber. Furthermore, bed thickness was significantly reduced with the incorporation of fiber, in tests involving thin fluids, even though a noticeable increase in pressure gradient was recorded.

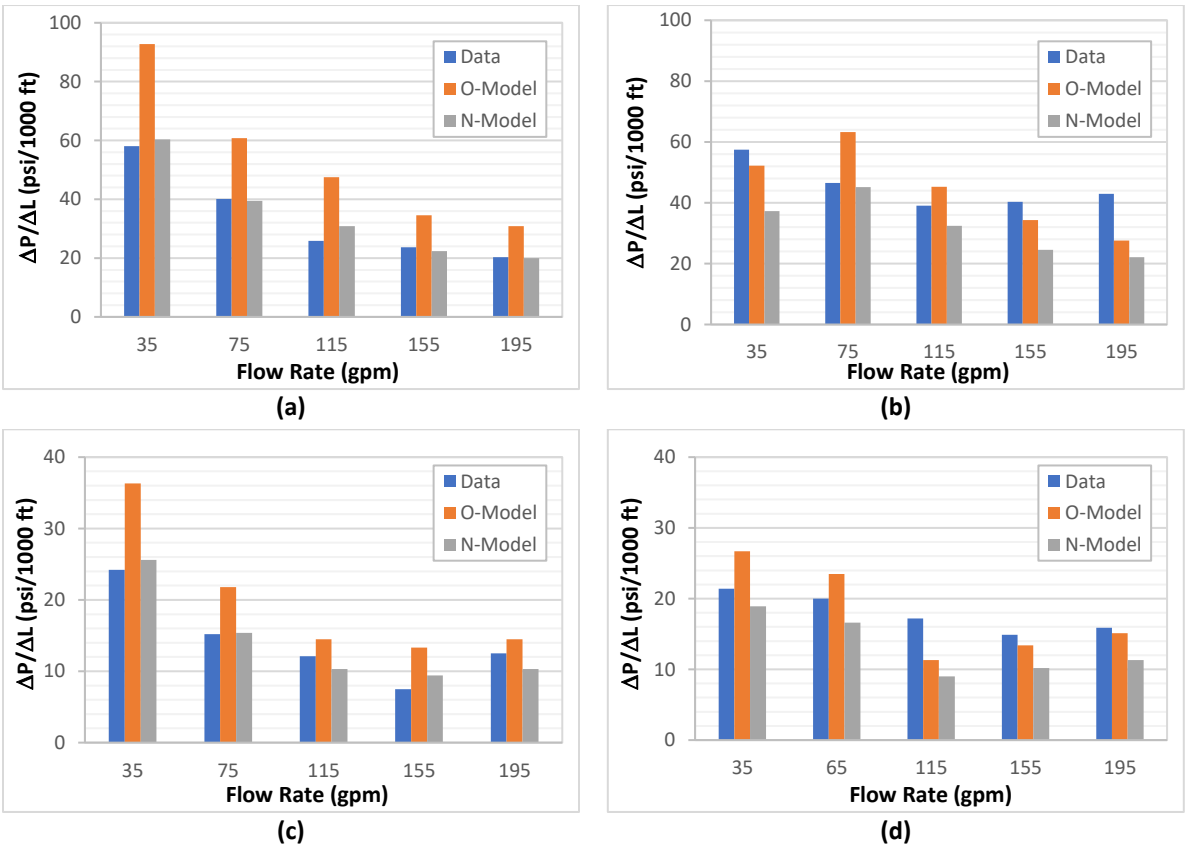


Figure 4. 5. Comparison of original and new model predictions with measurements: a) thick fluid, b) thick fluid with fiber, c) thin fluid, and d) thin fluid with fiber

A key observation was the formation of bed irregularities following fiber addition, which introduced variations in the bed profile. These irregularities contributed to

increased hydraulic resistance, leading to higher pressure losses. As a result, the measured frictional pressure gradients were consistently greater than those predicted by the new model for fibrous fluids. This discrepancy is attributed to the model's assumption of a uniform bed thickness, which does not account for the influence of bed irregularities on hydraulic resistance. Consequently, in most cases, the new model underpredicted pressure gradient by 10–50% compared to the measured values. The magnitude of these discrepancies is particularly pronounced in tests involving fibrous fluids, where bed non-uniformities played a more significant role in increasing the friction.

Localized bed height measurements from 29 stations along the test section were statistically analyzed to examine the relationship between the increased pressure losses and bed irregularities. The coefficient of bed height variation (CV) was defined as a quantitative metric to assess bed irregularities. CV is the ratio of the standard deviation to the mean of the measured bed height profile across the test section, expressed mathematically as:

$$\mathrm{CV} = \frac{\mathrm{H}_\sigma}{\mathrm{H}_{\mathrm{ave}}} \tag{4.2}$$

where $\mathrm{H}_{\mathrm{ave}}$ and H_σ are the mean and standard deviation of the bed height distribution. CV provides a measure of the extent to which the bed profile deviates from the uniform bed assumption used in hydraulic models. Figure 4.6 presents the bed profile for a test conducted with a non-fibrous thin fluid at a flow rate of 75 gpm. The bed appears relatively uniform, with only minor bed height variations observed near the inlet before reaching the differential pressure port. The port is positioned between bed height

measurement locations 4 and 27, with each consecutive measurement station spaced approximately 1.5 feet apart. Consequently, bed irregularities are minimal in this case.

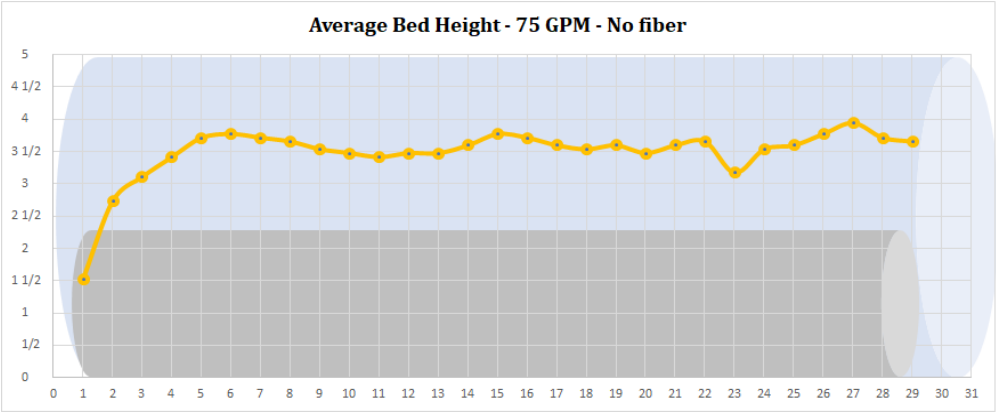


Figure 4. 6. Bed Height profile thin fluid no fiber at 75 GPM (Mendez et al., 2023)

Figure 4.7 presents the bed profile for a test conducted at a flow rate of 195 gpm with fiber. In this case, both the model prediction error and the coefficient of variation (CV) are high, indicating substantial deviations from the uniform bed assumption. The pronounced variation in bed height is primarily attributed to the formation of dunes, a phenomenon observed more frequently in experiments involving fibrous fluids. Detailed bed profiles for different fluids tested at various flow rates are provided in Appendix C.

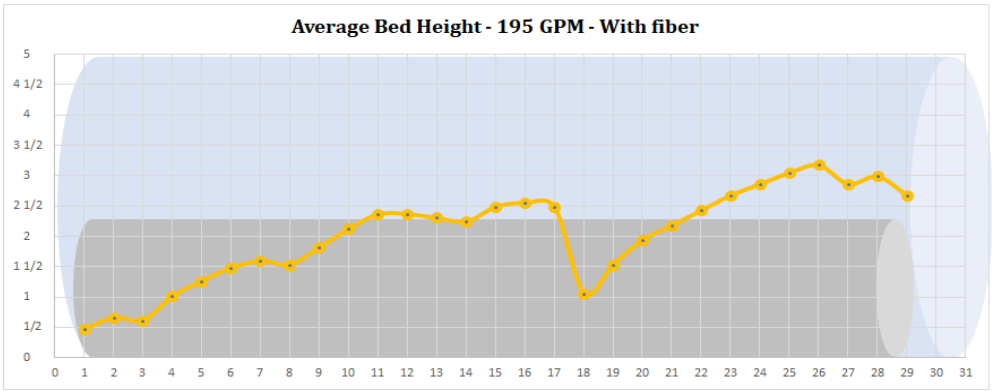


Figure 4. 7. Bed height profile thick fluid with fiber at 195 GPM (Mendez et al., 2023)

Overall, the bed profiles indicate the presence of dunes. This effect is more pronounced in experiments involving fibrous fluids. Figure 4.8 presents a scatter plot illustrating the model prediction error, defined in Equation (4.3), as a function of the coefficient of bed height variation (CV) for all measurements. Although the data points exhibit considerable scattering, a logarithmic relationship is observed between the prediction error and CV.

$$Error = \frac{\Delta P_p - \Delta P_m}{\Delta P_m} \tag{4.3}$$

where ΔP_m and ΔP_p represent the predicted and measured pressure losses, respectively. The observed scatter may be attributed to the non-uniform nature of bed irregularities, including variations in dune characteristics like shape, thickness, and length. These irregularities can develop distinct patterns or forms randomly, without a consistent structure, contributing to deviations in model predictions.

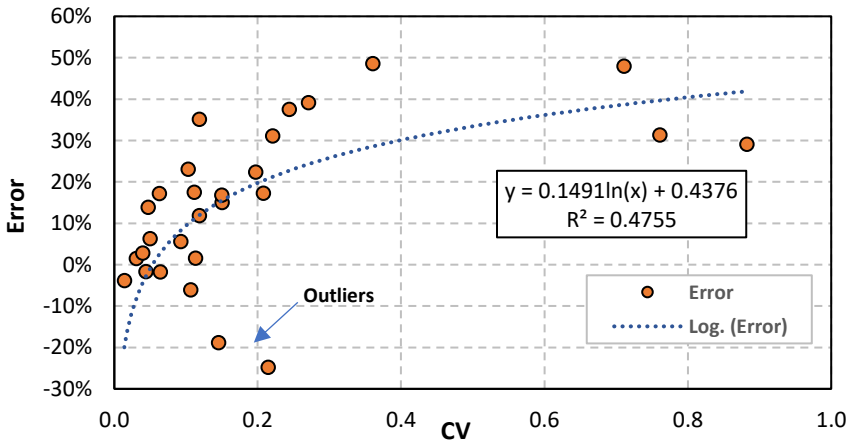


Figure 4. 8. Model prediction error vs. CV (Mendez et al., 2023)

The bed shear stress governs the local fluid velocity near the bed. It is regarded as the most critical factor for removing particles from the bed. A low bed shear stress promotes the development of irregular bed structures, such as dunes and ripples, which may form in the wellbore with or without a discernible pattern. Figure 4.9 illustrates the relationship between the coefficient of bed height variation (CV) and the Normalized Bed Shear Stress (NBSS) for all measurements. The NBSS is defined as the ratio of bed shear stress (τ_b) to average wall shear stress (τ_w):

$$NBSS = \frac{\tau_b}{\tau_w} \tag{4.4}$$

NBSS is calculated using the hydraulic models as presented in Appendix B, based on the measured average bed height under equilibrium conditions. An NBSS value below 1.0 indicates that the bed shear stress is lower than the average wall shear stress. The data show a strong correlation between CV and NBSS, confirming that dunes and ripples form when bed shear stress is significantly smaller than average wall shear stress. While most experiments were conducted at similar NBSS values (approximately 0.7), tests involving fibrous fluids exhibited higher CV values and lower NBSS values, particularly with the thin fluid.

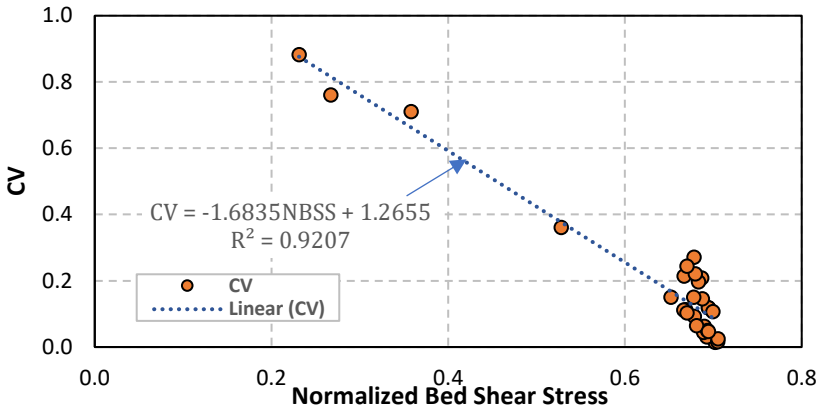


Figure 4. 9. CV versus normalized bed shear stress (Mendez et al., 2023)

4.3 Effect of Pipe Rotation

Additional bed erosion tests were conducted to evaluate the specific influence of pipe rotation on hole cleaning. These tests involved four fluid formulations and examined variations in both flow rate and pipe's rotation speed. The test matrix for this study is presented in Table 4.8. As in previous experiments, the annular test section was initially filled with sand to approximately 80% of its volume, ensuring full coverage of the inner pipe. The tests were conducted at constant flow rates and rotation speeds until an equilibrium bed height was established, as indicated by the stabilization of pressure drop. Bed height stabilization typically required 35 to 45 minutes. Once equilibrium was achieved, fluid circulation was stopped and bed height measurements were recorded at 29 locations along the annulus. Measurements were collected from both left and right sides of the outer pipe and averaged to determine the overall bed height. Results comprehensively assessed the combined effects of fluid properties and pipe rotation on hole-cleaning efficiency.

Table 4. 8. Test Matrix - Pipe Rotation (Garcia et al., 2024)

Number of Test	55
Fluids	Thick Fluid, density of 8.3 ppg, 0.87 XG/0.87 PAC lb/bbl
	Thick Fluid, density of 8.3 ppg, 0.87 XG/0.87 PAC lb/bbl, 0.04 wt% long fiber
	Thin Fluid with density of 8.3 ppg, 0.74 XG/0.61 PAC lb/bbl (Garcia 2022)
	Thin Fluid, density of 8.3 ppg,: 0.74 XG/0.61 PAC lb/bbl, 0.04 wt% long fiber (Garcia 2022)
Flow Rates	10, 20, 35, 55, 65, 75, 95, 115, 125, 135, 155, 165 and 195 gpm
Pipe rotation speed	0, 50, 100 and 150 rpm
Deviation Angle	90° from vertical
Geometry	Outer pipe: 5-1/2 in. (140 mm) OD, 5 in. (127 mm) ID; inner pipe: 2-3/8 in. (60 mm) OD

Figure 4.10 presents a comparative analysis of the hole-cleaning performances of thin and thick fluids without fibers under different pipe rotation conditions. The results demonstrate a clear enhancement in cleaning efficiency with pipe rotation for both fluid types. However, the thin fluid consistently performs better than the thick fluid, possibly due to the increased turbulence and higher local velocities near the bed. The viscous characteristics of a fluid play a critical role in determining local fluid velocity around deposited bed particles. Under turbulent flow conditions, the thin fluid generates higher local velocities near the bed than the thick fluid (Pandya et al., 2020), contributing to more effective cuttings transport and bed erosion. On the other hand, pipe rotation helps significantly enhance hole cleaning, particularly with the thin fluid. The bed is almost fully removed at the minimum tested flow rate with the thin fluid and pipe rotations of 100 and 150 rpm, due to the induced turbulence caused by the pipe rotation.

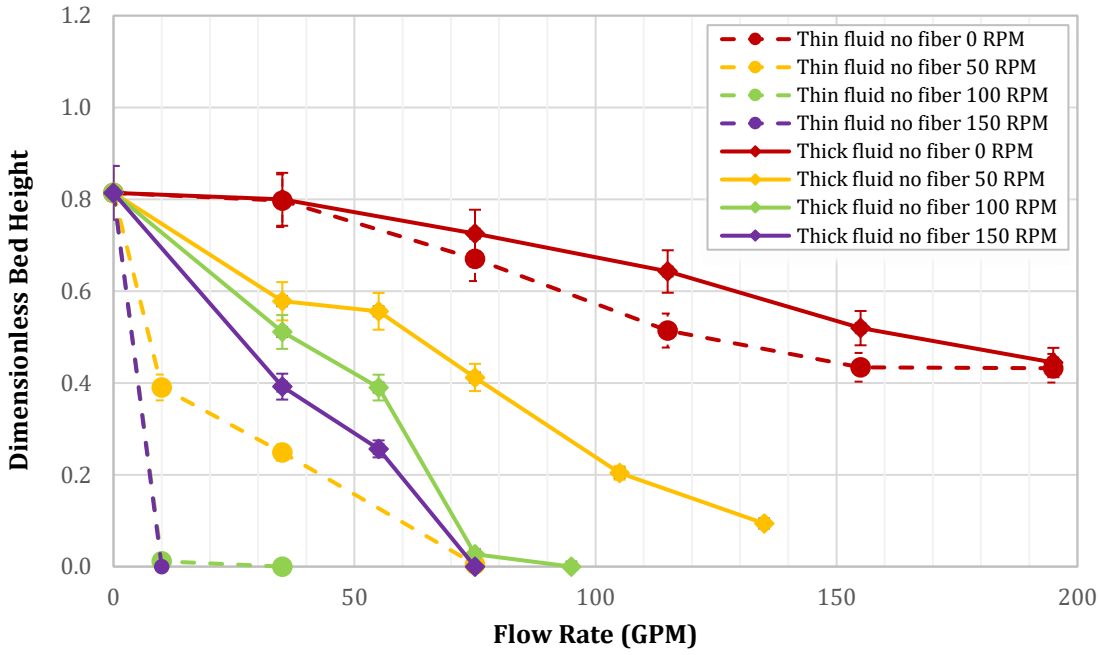


Figure 4. 10. Dimensionless bed height vs. flow rate (Thin and Thick fluid, no fiber) (Garcia et al., 2024)

The generalized Reynolds numbers presented in Tables 4.2 to 4.7 are below the conventional threshold for power-law fluid flow (Re_c = 3470-1370n). However, identifying the transition to turbulence in eccentric annuli with non-uniform cuttings beds remains complex. This transition is influenced by various factors, including flow geometry, pipe rotation speed, bed thickness, dune structure, surface roughness, and irregularities such as pipe skewness and wobbling. These factors can induce turbulence at Reynolds numbers lower than the conventional threshold (Kim & Hwang, 2003; Moradi & Tavoularis, 2019). As a result, the calculated Reynolds numbers cannot be directly compared to the standard critical value to classify the flow regime. It is therefore possible that the flow within the annulus is turbulent, even though the computed Reynolds numbers fell below the conventional threshold. This effect is particularly evident at higher

flow rates, where turbulence is more likely to develop. Under these conditions, the thin fluid consistently demonstrated enhanced cleaning performances, achieving greater efficiency in removing deposited solids.

Figure 4.11 depicts the relationship between dimensionless bed height and flow rate for the thin fluid, both with and without fiber, under varying drill-pipe rotation speeds. The results indicate that adding fiber and increasing pipe rotation significantly enhance hole-cleaning performance. Without pipe rotation, the presence of fiber in the thin fluid noticeably reduces the dimensionless bed height, particularly between 75 and 115 gpm. The introduction of pipe rotation further improves cleaning efficiency. Even at a low rotational speed of 50 rpm, nearly half of the bed is removed at a flow rate of 10 gpm. This improvement is attributed to both hydrodynamic and mechanical effects. Rotating the pipe induces helical flow, which prevents suspended particles from settling, and increases turbulence, dispersing particles within the fluid. Mechanically, the rotation agitates deposited cuttings, disrupts bed formation, and prevents compaction of the bed. At 100 rpm, the bed is fully cleaned at a flow rate of 35 gpm. At a rotational speed of 150 rpm, a flow rate of only 10 gpm is sufficient to clean the entire test section.

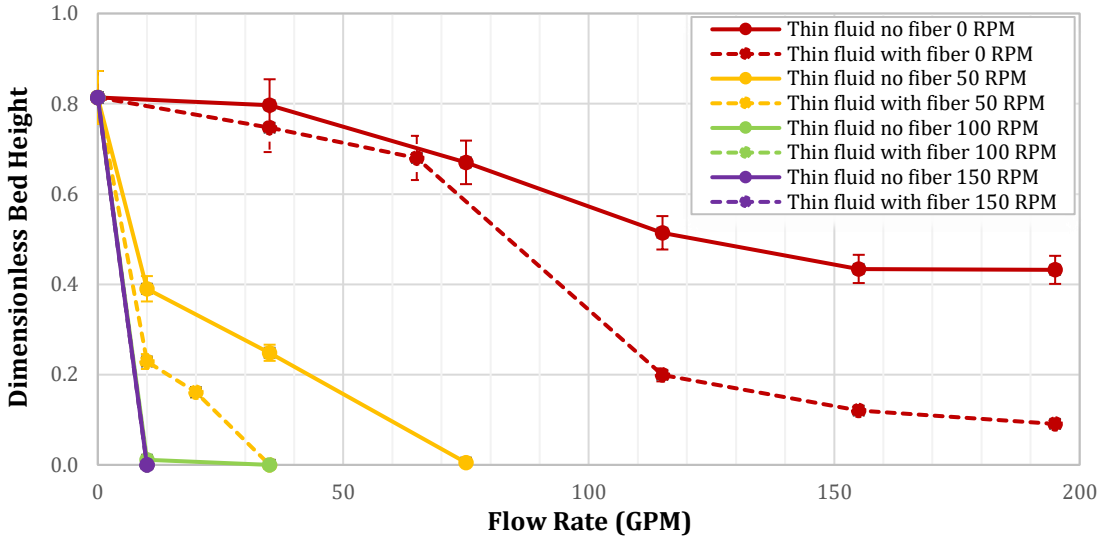


Figure 4. 11. Dimensionless bed height vs. flow rate (Thin fluid) (Garcia et al., 2024)

At higher rotational speeds (greater than 50 rpm), the effect of fiber on equilibrium bed height becomes negligible, indicated by the overlapping curves for cases with and without fiber. This suggests that the presence of fiber contributes to enhanced hole cleaning primarily at lower rotational speeds, where the turbulence generated by pipe rotation is insufficient to maintain particle suspension for extended durations.

Under low rotational speeds (50 rpm or less), the turbulence induced by the rotating pipe is not strong enough to prevent particle settling. This leads to re-deposition of cuttings that have been lifted by the agitation of inner pipe. In such scenarios, the addition of fiber improves hole cleaning efficiency by forming a network within the fluid, which mitigates sedimentation by increasing the drag forces on suspended particles. This fiber-induced drag enhances particle suspension, compensating for the reduced turbulence at lower rotational speeds. However, as rotational speed increases, the

mechanical agitation provided by pipe rotation alone becomes sufficient to prevent cuttings accumulation, diminishing the role of fiber in sustaining particle suspension. In conclusion, fiber addition is most effective in improving hole cleaning performance in horizontal wellbores when both rotational speed and fluid viscosity are low. In these conditions, fibers play a critical role in maintaining particle suspension and reducing bed formation.

Figure 4.12 presents dimensionless bed height measurements for thick fluid under various flow rates and inner pipe rotational speeds. While pipe rotation improves the hole-cleaning efficiency of the thick fluid, its effectiveness is less pronounced compared to that observed with the thin fluid. The most significant enhancement in cleaning performance occurs at lower rotational speeds (0 to 50 rpm), with the impact diminishing as rotational speed increases.

The incorporation of fiber provides a moderate improvement in the cleaning performance of the thick fluid with pipe rotation. At a rotational speed of 150 rpm, complete bed removal is achieved with fibrous fluid at a flow rate of 55 gpm. In contrast, without fiber, a higher flow rate of 75 gpm is required to achieve full cleaning at the same rotational speed. This represents a 27% reduction in the required flow rate with fiber. However, in the absence of pipe rotation, fiber addition has minimal influence on the cleaning efficiency of the thick fluid, as previously demonstrated in Figure 4.10.

A comparison between thin and thick fluids under identical test conditions (same rotational speed and flow rate) indicates that lower viscosity fluids exhibit superior cleaning performances in the horizontal configurations. This underscores the advantage

of reduced fluid viscosity for enhancing hole cleaning in horizontal well sections. However, higher viscosity or fiber addition may still be necessary to maintain effective cuttings transport in vertical wellbore sections.

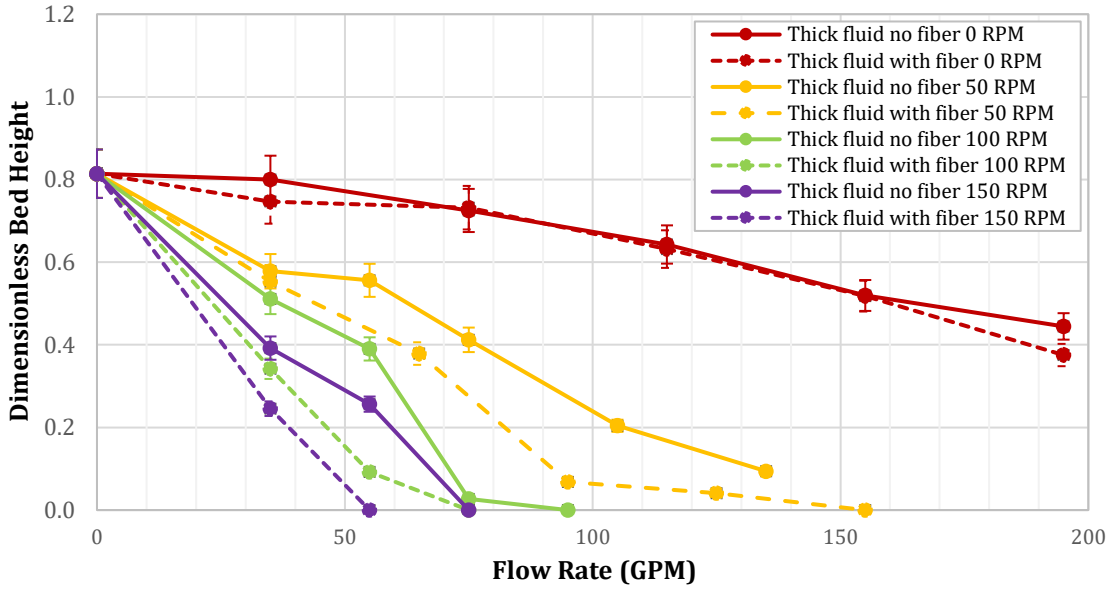


Figure 4. 12. Dimensionless bed height vs. flow rate (Thick fluid) (Garcia et al., 2024)

CHAPTER 5

Machine Learning Study

This chapter examines the predictive capabilities of various machine learning (ML) algorithms on hole-cleaning performance by analyzing data collected from multiple studies. The dataset includes a range of fluid types and flow loop configurations, providing a comprehensive representation of real-world conditions. The chapter begins with a theoretical overview of the employed ML methods, followed by a detailed discussion of the modeling and selection process. Model accuracy is enhanced by developing two dimensionless variables and integrating key parameters influencing hole-cleaning operations. The accuracy of the developed ML model is evaluated through validation procedures and sensitivity analysis. The chapter concludes with a comparative assessment between a mechanistic model and the chosen ML approach, demonstrating that the ML model yields more accurate predictions of hole-cleaning performance.

5.1 Theoretical Background

In this study, dimensionless bed height is predicted as a dependent variable, using various regression algorithms. The employed methodologies include linear regression, principal component analysis (PCA), multivariate adaptive regression splines (MARS), boosted decision trees (BDT), and deep learning (DL). This section provides a concise theoretical overview of the techniques applied, as outlined by Hastie et al. (2017), and introduces the mechanistic model used for validation.

5.1.1 Linear Regression

Linear regression is a fundamental modeling approach that provides a straightforward mathematical representation of relationships between variables. The model estimates the coefficients of a linear equation based on one or more independent variables, with the objective of minimizing the discrepancy between observed and predicted values. To achieve the optimal fit, the ordinary least squares (OLS) method is utilized to determine the best-fit line. Additionally, stepwise regression is implemented as an automated procedure to refine the model by systematically selecting the most significant predictors.

5.1.2 Multivariate Adaptive Regression Spline (MARS)

Multivariate Adaptive Regression Splines (MARS) is an advanced extension of stepwise linear regression, designed to effectively capture nonlinear relationships and manage high-dimensional data. The method constructs pairs of reflected basis functions, placing knots at observed data points to generate candidate functions. The modeling process consists of two phases: a forward pass, which iteratively introduces new function products to minimize training error, and a backward pass, which mitigates overfitting by removing less significant terms. MARS imposes constraints to enhance model efficiency, such as limiting the maximum interaction degree, to regulate the complexity and number of terms included in the final model.

5.1.3 Principal Component Analysis (PCA)

Principal Component Analysis (PCA) is a multivariate analytical technique widely employed for dimensionality reduction and exploratory data analysis. It facilitates the modeling of complex physical systems with multiple input variables by reducing the dataset's dimensional complexity. Through PCA, correlated variables are transformed into a new set of uncorrelated variables called principal components. In hole-cleaning experiments, PCA is a valuable tool for interpreting the relationships among different attributes, providing insights into their underlying patterns and interactions.

5.1.4 Decision Trees

The boosted decision tree (BDT) method partitions heterogeneous datasets into smaller, more homogeneous subsets based on specific predictor variables. The construction of a decision tree follows three fundamental steps: identifying optimal split points, determining whether nodes should be terminal or further divided, and assigning class labels to each node. Decision trees are particularly effective in modeling data with uncertain attribute significances and nonlinear relationships. In this study, both BDT and Random Forest (RF) algorithms are employed for tree-based model development.

5.1.5 Deep Learning (DL)

Deep learning algorithms, particularly artificial neural networks (ANNs), are designed to capture complex and implicit patterns within data. ANNs are structured with multiple layers, including input, hidden, and output layers, where each node contains input values, weights, biases, and an output. This computational process emulates the way

neurons interact in the human brain. Weights are assigned to input values, which are subsequently multiplied and summed, followed by the application of an activation function. If the resulting output exceeds the bias threshold, the node becomes active and transmits the data to the subsequent layer. Deep learning models, characterized by multiple hidden layers, require extended training times but offer highly adaptable nonlinear representations. Preventing overfitting is essential in the deep learning modeling process to ensure generalization and model reliability.

5.1.6 Mechanistic Model

Elgaddafi et al. (2021) developed a mechanistic model to predict bed heights in highly deviated wells under stationary drillpipe conditions. Bed shear stress correlations were included to enhance predictive accuracy. The model determines the critical transport velocity (CTV) while accounting for the influences of fiber drag force and fiber drag coefficient. The underlying assumptions include a flat and uniform solid bed, a highly eccentric pipe, and minimal particle collisions. In this study, this mechanistic model is employed to estimate bed heights under stationary pipe conditions, serving as an alternative for assessing the performances of the machine learning models.

5.2 Modelling

5.2.1 Data Characterization

Hole-cleaning measurements are gathered here to create a diverse dataset spanning a broad range of flow loops and testing conditions. The dataset facilitates a

comprehensive analysis and offers results that can support the design of future experiments. Initially, the dataset comprised 610 data points and 16 variables, aggregated from multiple published studies and experimental works conducted at different research facilities (Mendez et al. 2022; Garcia et al. 2022; George, 2012; Elgaddafi, 2011; Naik, 2015; Pandya, 2019; Adari, 1999; Sapru, 2001). The experiments were performed using flow loops with test section lengths ranging from 22 to 100 feet, hole diameters between 4 and 8 inches, and drill pipe diameters from 2 to 4.5 inches. These diverse experimental setups provide valuable insight into the physical mechanisms involved in hole cleaning, simulating a range of operational scenarios encountered in field applications.

The collected data include key parameters such as fluid rheology, cuttings size and density, flow rate, annular geometry, pipe rotation speed, and observed pressure gradient. These variables were used to explore how flow regime, fiber interaction, and mechanical agitation affect the efficiency of cuttings transport. A summary of the sources to the dataset is presented later in Table 5.4. Table 5.1 summarizes the selected input parameters, including their mean, minimum, maximum, median, Q1, Q3, the number of unique values, and standard deviation. Fluid rheology is characterized by the fluid consistency index (K) and the power-law exponent (n).

Table 5. 1. Data summary of some of the input parameters (Mendez et al., 2023)

Statistical Parameter	Wellbore Diameter (ID)	Horizontal Section (ft)	Cuttings Diameter (in)	Cuttings Density (ppg)	Flow Rate (gpm)
Number	610	610	610	610	610
Unique Data Number	3	6	7	7	40
Mean	5.08	38.85	0.067	20.11	104.73
Min	4	22	0.025	14.6	10
Q1	4	22	0.047	18.28	40
Median	4	22	0.049	20.86	70
Q3	5.5	48	0.078	21.69	118.75
Max	8	100	0.129	26.71	690
Standard Deviation	1.5	25.77	0.033	2.4	108

5.2.2 Data Preparation

The primary response variable examined in this study is the dimensionless bed height (DBH), defined as the ratio of bed height to wellbore diameter. This parameter provides a standardized measure for a comprehensive evaluation of hole cleaning performance. Figure 5.1 presents the cross-correlation plot, incorporating all key variables, where certain parameters exhibit notably high cross-correlation coefficients. Blue color blocks show direct relationships between the two parameters, while the red blocks show inverse relationships. The following key observations can be drawn from this plot:

- DBH demonstrates a strong correlation with cuttings properties, drillpipe rotational speed, and flow rate, all of which are critical factors influencing hole-cleaning efficiency in field operations.
- Fluid properties, represented by the parameters K and n, demonstrate a measurable influence on DBH.

- Wellbore diameter, inner pipe diameter, horizontal section length, and eccentricity exhibit strong intercorrelations, collectively characterizing wellbore geometry as reported in various studies.
- An inverse correlation between fiber concentration and DBH underscores the role of fibers in improving hole-cleaning efficiency by reducing bed height.

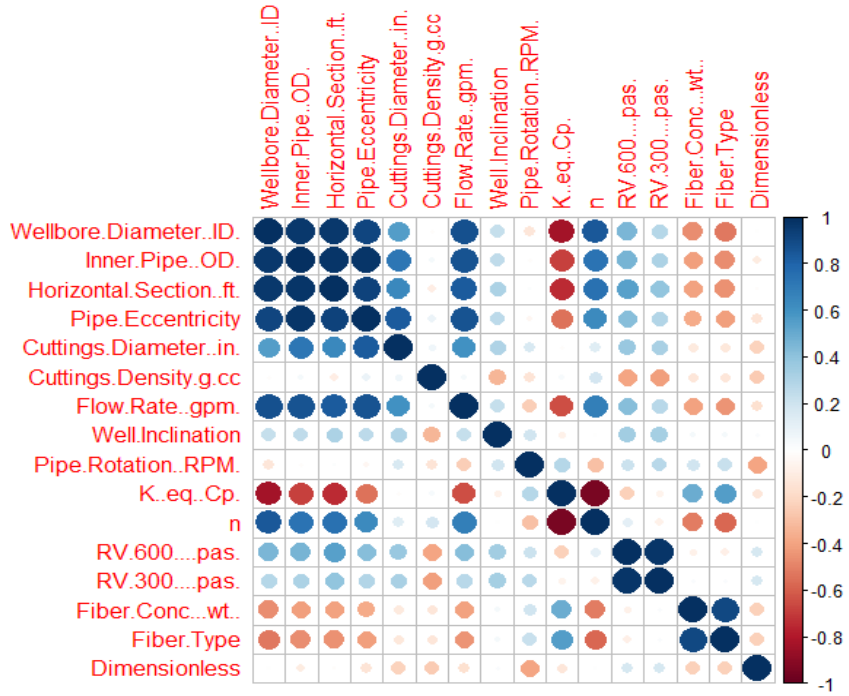


Figure 5. 1. Cross-correlation plot between all the tested variables (Mendez et al., 2023)

Figure 5.2 presents a comparison between the bed heights predicted by the BDT model and the measured training bed height. Differentiation techniques were applied to identify outliers and ensure data consistency. The dataset consists of information from eight sources, labeled 1 through 8. Cross-validation was conducted for the BDT modeling process, using a train control approach with five folds and a maximum tree depth of five

interactions. Multiple runs were performed to minimize the effects of algorithmic randomness. In addition, near-zero beds heights, likely recorded under non-equilibrium conditions, were excluded from the dataset. The trained model achieved an R-squared value of 0.9656, a root mean square error (RMSE) of 0.0396, and a mean absolute error (MAE) of 0.0296, indicating a high degree of predictive accuracy. Certain data points, particularly those from sources 1 to 3, exhibited notable prediction errors. However, most data points had errors below 25%, demonstrating overall model reliability and satisfactory predictive performance.

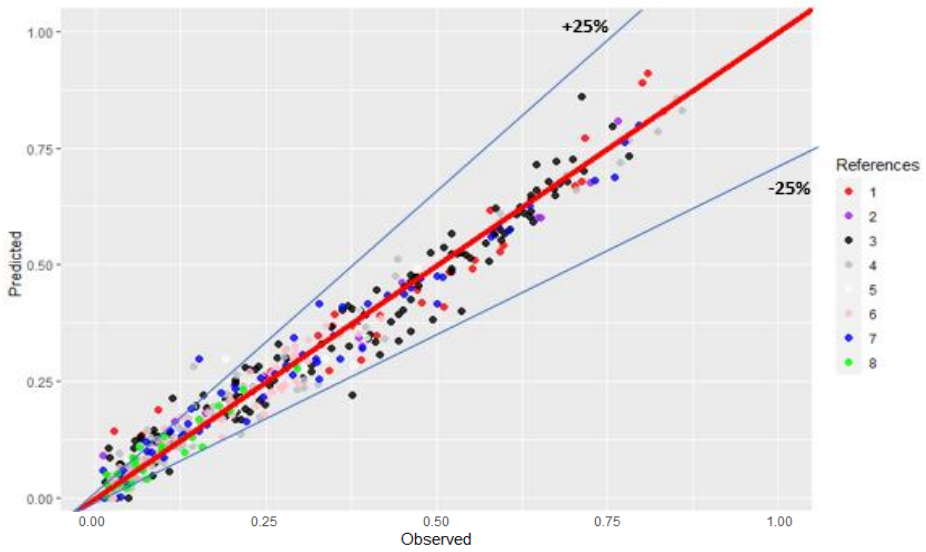


Figure 5. 2. Comparison of Measured vs. Predicted training data with BDT Model

Figure 5.3 illustrates the relative significance of various parameters in predicting the dimensionless bed height using the BDT algorithm. The results are consistent with established theoretical principles and practical applications in hole-cleaning operations.

A similar analysis was performed using the RF algorithm to assess the impacts of individual variables on dimensionless bed height predictions.

Both modeling approaches indicate that fiber type and pipe eccentricity have minimal effects on prediction outcomes. This is primarily attributed to the limited variability within the dataset. Among the 459 recorded observations, only five tests involve short fibers, one of the fiber types considered in the study. Additionally, eccentricity values predominantly range between 0.9 and 1, with only a few data points near 0.8, restricting the model's ability to comprehensively assess its impact. Due to the insufficient representation of these variables in the dataset, fiber type and eccentricity do not provide meaningful contributions to dimensionless bed height predictions. As a result, these parameters are excluded from further analysis.

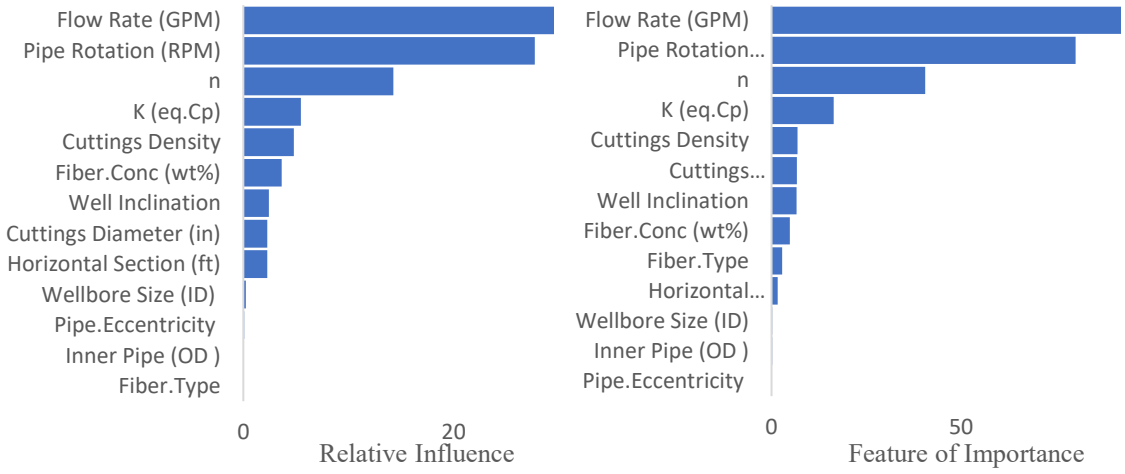


Figure 5. 3. BDT (left) and RF (right) charts for the most influential parameters in hole cleaning prediction (Mendez et al., 2023)

The analysis of variance supports prior findings that fiber type can be excluded as a variable. It also highlights other important factors, such as wellbore diameter and cutting density, as shown in Table 5.2. The F-value analysis is used to statistically assess the significance of input variables in predicting hole-cleaning performance. For a 99% confidence interval, the F-value threshold is 2.12, while for a 95% confidence interval, it is 1.71. Cutting density does not meet the significance criteria at the 95% confidence level, although the previously discussed ML techniques indicate it has a moderate influence. The significant parameters—those exceeding the F-value threshold—include flow rate, pipe rotation speed (RPM), fluid viscosity, cuttings diameter, and annular geometry. These variables have shown the greatest influence on model outputs such as pressure loss and bed height, highlighting their critical role in the hole-cleaning process for horizontal wells.

Table 5. 2. Analysis of Variance (Mendez et al., 2023)

Response: Dimensionless Bed Height					
	DF	**Sum Sq**	**F value**	**Pr (>F)**	**Remark**
Wellbore Diameter	1	0.05	2.23	1.36E-01	
Inner Pipe	1	0.41	18.35	2.25E-05	Significant
Horizontal Section	1	0.27	12.20	5.26E-04	Significant
Pipe Eccentricity	1	1.25	56.36	3.32E-13	Significant
Cuttings Diameter	1	1.57	70.74	5.58E-16	Significant
Cuttings Density	1	0.03	1.16	2.83E-01	
Flow Rate	1	0.63	28.47	1.52E-07	Significant
Well Inclination	1	0.06	2.89	8.97E-02	
Pipe Rotation	1	4.22	190.22	2.20E-16	Significant
K	1	1.03	46.41	3.13E-11	Significant
n	1	0.91	41.15	3.61E-10	Significant
Fiber Conc.	1	0.52	23.50	1.72E-06	
Fiber Type	1	0.00	0.01	9.08E-01	
Residuals	445	9.863			

DF: Degree of freedom; and Pr (>F) is the p value

The data is further examined using the PCA method, as shown in Figure 5.4, showing the variance distribution across variables and their principal components. A strong correlation is observed among horizontal length, inner pipe's outer diameter (OD), wellbore diameter, and pipe eccentricity, all of which are integral to wellbore geometry. Similarly, flow rate increases with test section length, attributed to larger wellbores requiring higher flow rates.

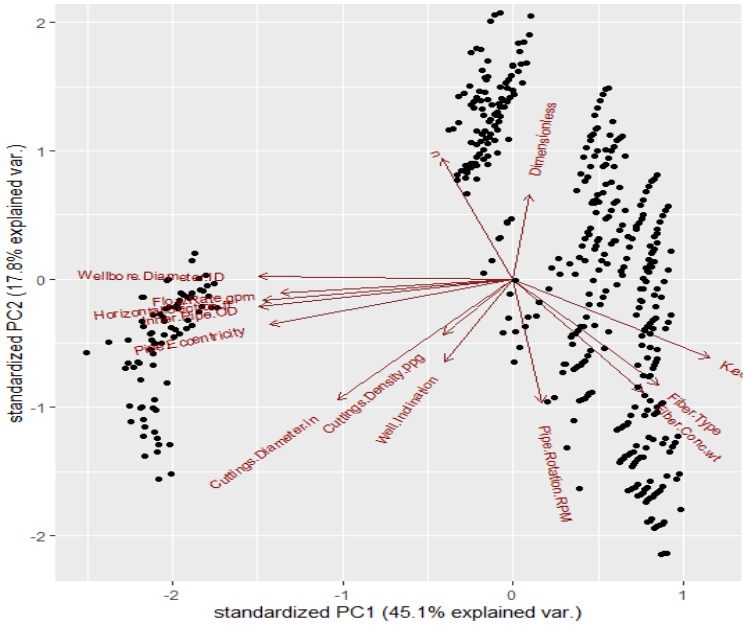


Figure 5. 4. PCA for the first two principal components and their relations with analyzed variables (Mendez et al., 2023)

5.2.3 Dimensional Model Evaluation

Principal component regression was performed to validate the model, using ten-fold cross-validation applied sequentially. The results align with the variability captured by each principal component. As indicated in Table 5.3, 11 principal components account for most of the variance.

Table 5. 3. Percentage of variance of principal component regression

Components	1	2	3	4	5	6	7	8	9	10	11	12	13
X	48.6	66.8	75.8	83.5	89.2	94.2	97.5	98.8	99.6	99.8	100	100	100
Dimensionless Bed Height	0.3	7.0	8.1	8.9	24.0	25.7	25.8	38.3	39.7	43.1	46.0	52.6	52.6

Based on the earlier considerations, fiber type and pipe eccentricity were excluded from the dataset. The model was enhanced by incorporating two dimensionless variables: Reynolds Number (N_{Re}) and square root of Taylor Number (Ta), which are defined in Appendix D. These variables were utilized in experimental and mechanistic models to improve precision and broaden applicability. Their inclusion allows for more generalized data training and enhances predictions for both experimental and field data. As shown in Figure 5.5, the training model achieved a higher R-squared value of 0.9764, along with lower RMSE (0.0329) and MAE (0.0248) values.

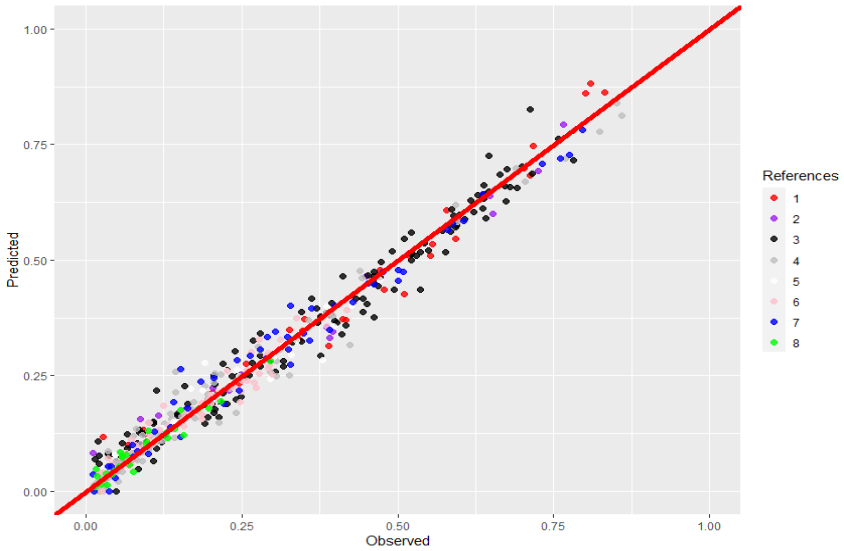


Figure 5. 5. Observed vs Predicted training data, after outlier removal and addition of dimensionless variables (Mendez et al., 2023)

5.3 Results and Discussion

5.3.1 Finalized Dataset

Table 5.4 presents the finalized dataset, comprising 458 data points and 12 input variables, with dimensionless bed height as the output variable. An additional 25 data points, representing a wide range of input variables and data sources, were reserved to evaluate the performance of the most accurate ML technique, as compared to a new mechanistic model.

Table 5. 4. Dataset summary

	(Mendez et al., 2022)	Garcia et al. 2022	George, 2012	Elgaddafi, 2011	Naik, 2015	Pandya, 2019	Adari, 1999	Sapru, 2001
Data Points	22	11	141	135	27	42	53	27
Geometry								
Wellbore Diameter, in	5	5	4	4	5	5	8	8
Inner Pipe OD, in	2.375	2.375	2	2	2.375	2.375	4	4.5
Horizontal Section, ft	48	48	22	22	34-54	34	80	100
Well inclination, deg	90	90	72-90	70-90	60-90	60-90	87-90	90
Operational parameters								
Flow Rate, gpm	35-125	10-75	10-80	20-85	80-120	80-120	150-690	200-350
Pipe Rotation, RPM	50-150	10-195	0-75	0-75	0	0	0	40-100
Fluid Properties								
K, centipoise	704-1596	678-696	2419-11606	4651	34-250	1-190	61.2-836	100-918
n	0.35-0.43	0.4-0.42	0.2-0.325	0.22	0.54-0.72	0.59-1	0.23-0.69	0.48-0.69
Fiber Conc., %wt	0-0.04	0-0.04	0-0.04	0-0.06	0	0	0	0
Fluid Type	WBM	WBM	WBM, SBM	WBM	WBM	WBM	WBM	WBM
Particle Properties								
Cuttings Diameter, in	0.049	0.049	0.047	0.079	0.025	0.025-0.03	0.125	0.13
Cuttings Density, ppg	18.32	18.32	18.32	21.7	14.6	20.9-26.7	21.36	22.03

5.3.2 Model Predictions

Cross-validation was performed using ten-fold and five-fold methods across all techniques, repeated multiple times to account for the stochastic nature of the algorithms, and the average results were compared. The deep learning (DL) model architecture included two hidden layers with 22 neurons in the first layer and 11 neurons in the second. The Rectified Linear Unit (ReLU) was used as the activation function. Keras library in Python was utilized to develop the model, which was trained over 50 epochs with a batch size of 5. The support vector machine (SVM) regression model applied a radial basis function kernel. The MARS model was designed with a maximum degree of 3 and up to 100 terms in the pruned model. The ordinary least squares (OLS) model utilized stepwise regression, dynamically adding or eliminating variables to achieve optimal results. The Random Forest (RF) model employed bagging and bootstrapping with replacement, using a maximum of 500 trees. Figure 5.6 shows the predictions of the models.

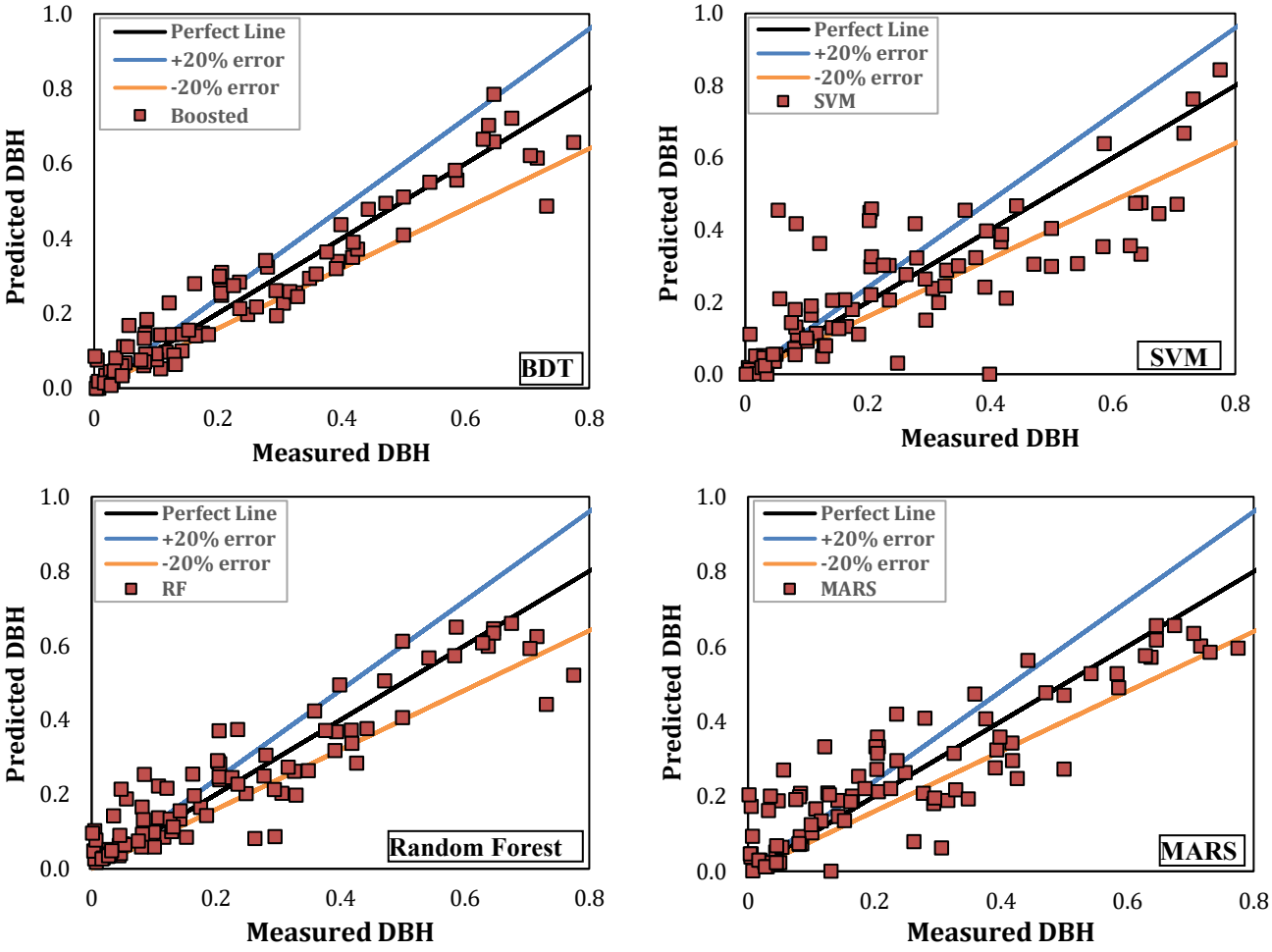


Figure 5. 6. Predictions of ML models for the Test Dataset (Mendez et al., 2023)

For model training and testing, 80% of the dataset was randomly selected, while predictions were generated for the remaining 20% (Fig. 5.6). The boosted decision tree (BDT) model proved to be the most accurate for predicting dimensionless bed height (DBH). It used Gaussian distributions with 201 trees, a shrinkage rate of 0.05, an interaction depth of 5, and a bagging fraction of 0.65. Hyperparameter tuning functions were used to identify optimal values for these parameters.

RMSE, MAE, and R-squared values were analyzed to determine the most suitable model, as presented in Table 5.5. Among the models, the BDT method demonstrated the best performance with the lowest RMSE and MAE and the highest R-squared value. Conversely, the OLS model showed the weakest performance, having the highest RMSE and MAE and the lowest R-squared value.

Table 5. 5. Perofrmances of ML models (Mendez et al., 2023)

Model	R-square	MAE	RMSE
BDT	0.92	0.046	0.060
RF	0.87	0.060	0.083
MARS	0.81	0.075	0.098
SVM	0.65	0.090	0.135
DL	0.35	0.140	0.180
OLS	0.25	0.149	0.180

5.4 Sensitivity Analysis

A sensitivity analysis was conducted using the BDT model to examine the effects of key variables on dimensionless bed height. As depicted in Figure 5.7, the effects of drill pipe rotational speed (RPM), flow rate, and fluid rheological parameters on dimensionless bed height align with the expected theoretical trends. Specifically, bed height decreases with an increase in both flow rate and drill pipe RPM, confirming their roles in enhancing cuttings transport efficiency. Similarly, when the flow behavior index (n) increases while the consistency index (K) remains constant, a reduction in bed height is observed. Conversely, an increase in K at a fixed n initially causes a slight rise in bed height, which then stabilizes at values exceeding 700 eq.cP. Overall, the BDT model

indicates that hole-cleaning efficiency improves with higher drill pipe RPMs, greater flow rates, and higher values of n, whereas increased K negatively impacts cleaning performance beyond a critical threshold. These findings validate the model's ability to capture hole-cleaning operations' underlying physics.

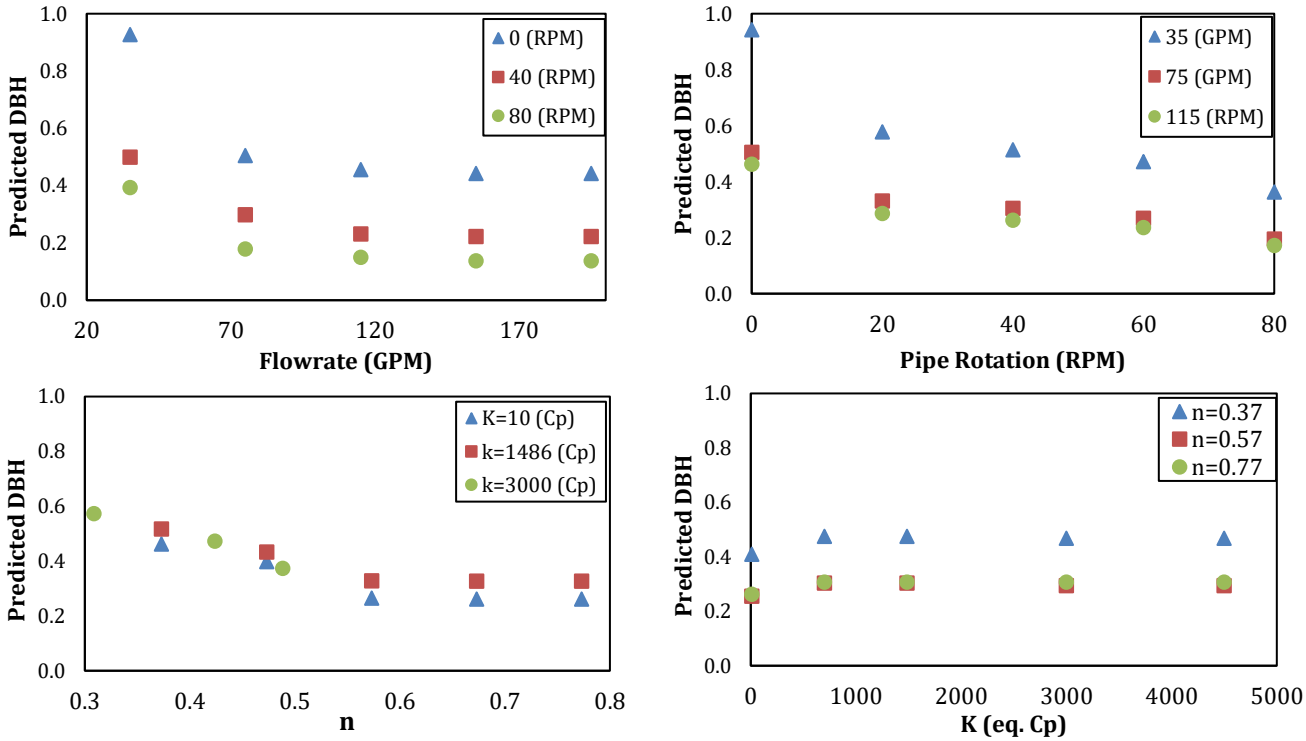


Figure 5. 7. Sensitivity analysis using BDT model. Flow Rate (Top right), Pipe Rotation (Top left), n (Bottom right), K (Bottom left). (Mendez et al., 2023)

5.5 Comparison of ML and Mechanistic Modeling

Elgaddafi et al. (2021) recently developed a mechanistic model to forecast bed height in hole-cleaning operations without pipe rotation. We selectively extracted a dataset comprising 25 data points from scenarios without inner pipe rotation to facilitate a comparative analysis between mechanistic and BDT models. These data points are

outlined in Table 5.6. They were obtained from multiple studies, encompassing a broad spectrum of wellbore inclinations, fluid properties, cuttings sizes, and cuttings densities. This diverse dataset provides a good foundation for evaluating the predictive capabilities of both modeling approaches across varying hole-cleaning conditions.

Table 5. 6. Dataset used for ML and mechanistic model comparison

	Mendez et al., 2022	Garcia et al., 2022	George, 2012	Pandya, 2019
Data Points	10	5	5	5
Geometry				
Wellbore Diameter, in	5	5	4	5
Inner Pipe OD, in	2.375	2.375	2	2.375
Horizontal Section, ft	48	48	22	34
Well inclination, deg	90	90	72	90
Operational Parameters				
Flow Rate, gpm	35-195	35-195	40-80	80-120
Pipe Rotation, RPM	0	0	0	0
Fluid Properties				
K, centipoise	1486-1596	648	2419	39-190
n	0.373-0.378	0.414	0.325	0.66-0.59
Fiber Conc., %wt	0-0.04	0	0	0
Fluid Type	WBM	WBM	SBM	WBM
Particle Properties				
Cuttings Diameter, in	0.049	0.049	0.047	0.031-0.025
Cuttings Density, ppg	18.318	18.318	18.318	26.7-20.9

As illustrated in Figure 5.8, the mechanistic model (Elgaddafi et al., 2021) cannot make accurate predictions, particularly with experimental data obtained from synthetic mud experiments. The model also shows substantial discrepancies with the fibrous fluid, and most of the predictions fall outside a 20% error margin. In contrast, most of the predictions made by the BDT model have a reasonable level of accuracy. Overall, the BDT model performs better than the mechanistic model in the evaluated fluid systems.

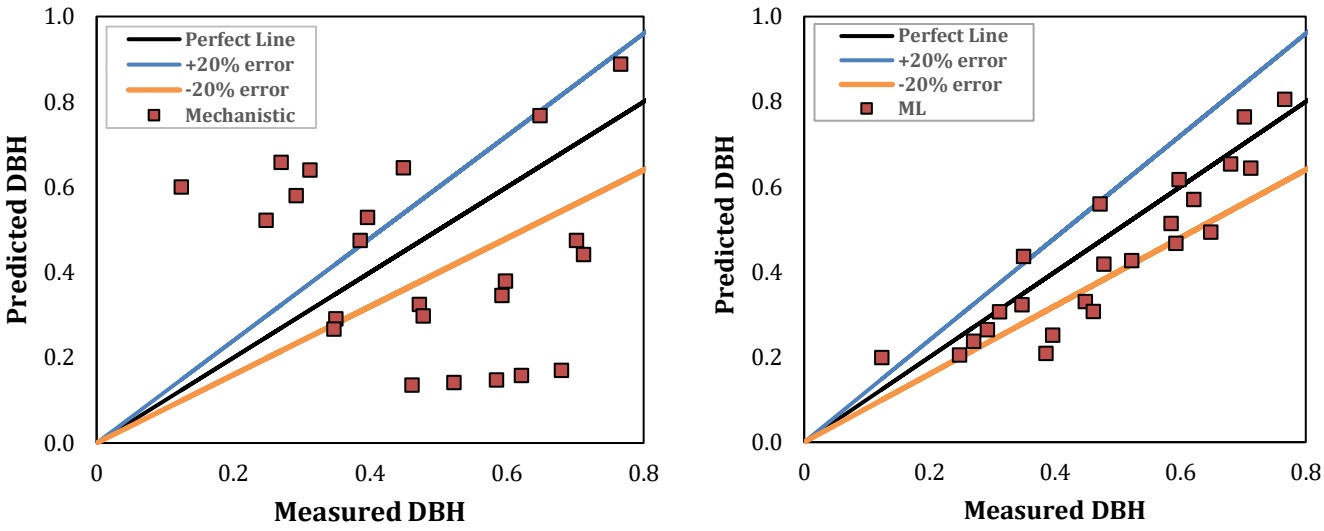


Figure 5. 8. Comparison of the predictions of mechanistic (left) and BDT (Right) models (Mendez et al., 2023)

CHAPTER 6

Conclusions and Recommendations

This study explores the impact of fibrous fluids, flow rate, and pipe rotation on hole-cleaning efficiency in horizontal wells. It evaluates the predictive capabilities of mechanistic and machine learning models. This chapter summarizes the study's key observations and results, and lists the conclusions drawn from both the experimental and modeling efforts. In addition, recommendations are made for future studies to increase our understanding of fiber-fluid interactions and enhance modeling techniques to better represent real-world drilling conditions. These insights aim to support the development of more effective data-driven strategies for wellbore cleaning in complex drilling environments.

6.1 Conclusions

This research investigates the effectiveness of fibrous fluids in enhancing hole cleaning in horizontal well configurations using both experimental and modeling approaches. The major conclusions drawn from the study are as follows:

- The addition of synthetic fibers to polymer-based drilling fluids significantly improves cuttings transport efficiency, particularly with low-viscosity fluids and at higher flow rates. Thin fluids with long fibers consistently achieve lower equilibrium bed heights and bed coverage compared to their non-fibrous counterparts.

- Long fibers outperform short fibers in enhancing hole cleaning. Fluids containing short fibers exhibit negligible improvement in bed erosion. This is likely due to their inability to form the necessary stable fiber network for generating fiber-induced drag forces.
- Fibers introduced at low concentrations (0.04 wt%) have minimal impact on the bulk rheological properties of the fluids, as confirmed by rotational and pipe viscometer tests. However, a slight reduction is observed in pressure loss for fibrous fluids under turbulent flow conditions, indicating minor turbulence suppression effects.
- Pipe rotation has a positive effect on hole cleaning performance with fiber-enhanced fluids. Rotation helps disrupt settled cuttings beds and enhance fluid-particle interactions, thereby improving the efficiency of bed erosion and particle suspension.
- Fibrous fluids tend to form more irregular cuttings beds, leading to higher frictional pressure losses than predicted by conventional models. These irregularities contribute to discrepancies between measured and predicted pressure drops.
- The newly developed mechanistic model, which accounts for bed and wall shear stress variations in partially blocked eccentric annuli, provides significantly improved pressure loss predictions compared to traditional models. However, this model's accuracy is reduced in the presence of fibrous fluids and irregular beds.
- The machine learning model demonstrates superior predictive accuracy compared to the mechanistic approach. Within its applicability domain, it offers a reliable and robust framework for evaluating and optimizing hole-cleaning performance.

6.2 Recommendations

Based on the findings of this study, the following recommendations are proposed for both practical applications and future research:

- Operators should consider using long synthetic fibers in low-viscosity polymer-based drilling fluids, particularly in horizontal and deviated sections of wellbores. Proper selection of fluid and fiber concentration can significantly enhance hole cleaning without adversely affecting hydraulic performance.
- Where feasible, pipe rotation should be incorporated into drilling operations as it provides mechanical agitation. Rotation complements the effects of fibrous fluids, especially under laminar flow regimes common in horizontal wells.
- Modeling approaches should account for bed irregularities, particularly in the presence of fiber. Empirical correction factors or enhanced mechanistic models incorporating bed variation help improve predictive reliability.
- Additional investigations into fiber type, shape, and flexibility could offer insights into the formation and effectiveness of fiber networks. Sedimentation and visualization studies can help explain the differences between long and short fibers.
- While laboratory results are promising, pilot-scale or field-level studies are necessary to validate the effectiveness of fibrous fluids in real drilling environments, at various pressures, temperatures, and wellbore geometries.
- Continued development of machine learning-based models is encouraged, especially those trained on large field-based datasets. These models can help in real-time

prediction of pressure losses, bed height, and cutting concentration, leading to improved operational decision-making.

- The incorporation of fiber can adversely affect the performance of downhole tools, such as measurement-while-drilling (MWD) systems. Further research is needed to develop strategies that mitigate these effects while preserving the benefits of improved hole-cleaning efficiency.

NOMENCLATURE

Symbols

D_{hy}	Hydraulic diameter
H_{ave}	Mean of the bed height distribution
H_{σ}	Standard deviation of the bed height distribution
n	Power law exponent
K	Fluid consistency index
OD	Outer diameter
n	Fluid behavior index / power law index
NRe	Reynolds Number
Ta	Taylor Number
R-square	Coefficient of determination

Greek Letters

ΔP_m	Measured pressure loss
ΔP_p	Predicted pressure loss
$\frac{\Delta P}{\Delta L}$	Pressure gradient
τ_b	Bed shear stress
τ_w	Overall wall shear stress

Acronyms

AI	Artificial Intelligence
ANOVA	Analysis of Variance
ANN	Artificial Neural Networks
BDT	Boosted Decision Tree
CFD	Computational Fluid Dynamics
CRISP-DM	Cross-Industry Standard Process for Data Mining
CT	Coiled Tubing
CTV	Critical Transport Velocity
CV	Coefficient of Variation
DBH	Dimensionless Bed Height
ECD	Equivalent Circulating Density
HEC	Hydroxyethylcellulose
LRMARS	Regression Spline
MAE	Mean Absolute Error
MARS	Multivariate Adaptive Regression Spline
ML	Machine Learning
NBSS	Normalized Bed Shear Stress
NPT	Nonproductive Time
OBM	Oil-Based Mud
PAC	Poly Anionic Cellulose
PCA	Principal Component Analysis

ReLU	Rectified Linear Unit
RF	Random Forest
RMSE	Root Mean Square Error
ROP	Rate of penetration
SBM	Synthetic-based muds
SVM	Support Vector Machine
SPP	Surface Pumping Pressure
VFD	Variable Speed (Frequency) Drive
XG	Xanthan Gum

REFERENCES

Adari, R. B. (1999). *Development of Correlations Relating Bed Erosion to Flowing Time for Near Horizontal Wells*. The University of Tulsa.

Ahmed, R. M., Skalle, P., Johansen, S. T., Svein, J., & Saasen, A. (2001). Mechanistic model for cuttings removal from solid bed in inclined channels. *Journal of Petroleum Science and Engineering*, *30*, 129–141.

Ahmed, R. M., & Takach, N. E. (2009). Fiber sweeps for hole cleaning. *SPE Drilling and Completion*, *24*(4), 564–573. https://doi.org/10.2118/113746-PA

Ahmed, R. M., Takach, N. E., & Savitri, M. (2009). Experimental study on fiber sweeps in horizontal and highly deviated configurations. *SPE Production and Operations Symposium, Proceedings*, 631–637. https://doi.org/10.2118/120644-ms

Ahmed, R., Skalle, P., & Johansen, S. T. (2003). A mechanistic model to determine the critical flow velocity required to initiate the movement of spherical bed particles in inclined channels. *Chemical Engineering Science*, *58*(10), 2153–2163. https://doi.org/10.1016/S0009-2509(03)00061-7

Ahmed, R., Skalle, P., & Saasen, A. (2005). Application of a three-layer modeling approach for solids transport in horizontal and inclined channels. *Chemical Engineering Science*, *60*(10), 2557–2570. https://doi.org/10.1016/j.ces.2004.12.011

Ahmed, R, Saasen, A., & Skalle, P. (2004). Application of the minimum transport velocity model for drag-reducing polymers. *Journal of Petroleum Science and Engineering*, *44*, 303–316. https://doi.org/10.1016/j.petrol.2004.03.002

Ahmed, Ramadan, Enfis, M., Miftah-El-Kheir, H., Laget, M., & Saasen, A. (2010). The effect of drillstring rotation on equivalent circulation density: Modeling and analysis of field measurements. *Proceedings - SPE Annual Technical Conference and Exhibition*, *7*, 5375–5385. https://doi.org/10.2118/135587-ms

Ahmed, Ramadan, & Miska, S. (2008). IADC / SPE 112604 Experimental Study and Modeling of Yield Power-Law Fluid Flow in Annuli with Drillpipe Rotation. *IADC/SPE Drlling Conference*, (March). Orlando.

Akhshik, S., Behzad, M., & Rajabi, M. (2015). CFD-DEM approach to investigate the effect of drill pipe rotation on cuttings transport behavior. *Journal of Petroleum Science and Engineering*, *127*, 229–244. https://doi.org/10.1016/j.petrol.2015.01.017

Al, K., Salaheldin, A., Abdulwahab, E., Emad, A., & Abdulazeez, R. (2019). Cutting concentration prediction in horizontal and deviated wells using artificial intelligence techniques. *Journal of Petroleum Exploration and Production Technology*, *9*(4), 2769–2779. https://doi.org/10.1007/s13202-019-0672-3

Alkinani, H. H., Al-hameedi, A. T. T., Dunn-norman, S., Al-alwani, M. A., & Lian, D. (2019). *Application of Descriptive Data Analytics : How to Properly Select the Best Ranges of Viscosity and Flow Rate for Optimal Hole Cleaning ?*

Azouz, I., Shirazi, S. A., Pilehvari, A., & Azar, J. J. (1993). Numerical simulation of laminar flow of yield-power-law fluids in conduits of arbitrary cross-section. *Journal of Fluids Engineering, Transactions of the ASME*, *115*(4), 710–716.

https://doi.org/10.1115/1.2910203

Brown, N. ., Bern, P. ., & Weaver, A. (1989). Cleaning Deviated Holes: New Experimental and Theoretical Studies. *SPE/IADC Drilling Conference*. New Orleans, Louisiana.

Chen, Z. (2005). *Cuttings transport with foam in horizontal concentric annulus under elevated pressure and temperature conditions*. The University of Tulsa.

Cho, H., Shah, S. N., & Osisanya, S. O. (2000). A three-segment hydraulic model for cuttings transport in horizontal and deviated wells. *SPE International Horizontal Well Technology Conference Proceedings*, 1–16. https://doi.org/10.2523/65488-ms

Clark, R. K., & Bickham, K. L. (1994). Mechanistic model for cuttings transport. *Proceedings - SPE Annual Technical Conference and Exhibition*, *Delta*, 139–153. https://doi.org/10.2523/28306-ms

Colebrook, C. F., Blench, T., Chatley, H., Essex, E. H., Finniecome, J. R., Lacey, G., … Macdonald, G. G. (1939). Turbulent Flow in Pipes, With Particular Reference To the Transition Region Between the Smooth and Rough Pipe Laws. (Includes Plates). *Journal of the Institution of Civil Engineers*, *12*(8), 393–422. https://doi.org/10.1680/ijoti.1939.14509

Dodge, D. W., & Metzner, A. B. (1959). Turbulent Flow of Non-Newtonian Systems. *A.I.CH.E*, *5*(2), 189–204.

Duan, M., Miska, S., Yu, M., Takach, N., Ahmed, R., & Zettner, C. (2008). Transport of

small cuttings in extended-reach drilling. *SPE Drilling and Completion*, *23*(3), 258–265. https://doi.org/10.2118/104192-pa

Duan, M., Miska, S., Yu, M., Takach, N., Ahmed, R., & Zettner, C. (2009). Critical conditions for effective sand-sized-solids transport in horizontal and high-angle wells. *SPE Drilling and Completion*, *24*(2), 229–238. https://doi.org/10.2118/106707-PA

Elgaddafi, R. (2011). *Hole Cleaning Performance of Water-Based Fiber-Containing Sweep Fluids*. The University of Oklahoma.

Elgaddafi, R., & Ahmed, R. (2020). Fibrous cleanout fluids in horizontal and inclined wells. *Society of Petroleum Engineers - SPE/ICoTA Well Intervention Conference and Exhibition 2020, CTWI 2020*. https://doi.org/10.2118/199868-MS

Elgaddafi, R., Ahmed, R., George, M., & Growcock, F. (2012). Settling behavior of spherical particles in fiber-containing drilling fluids. *Journal of Petroleum Science and Engineering*, *84–85*, 20–28. https://doi.org/10.1016/j.petrol.2012.01.020

Elgaddafi, R., Ahmed, R., & Growcock, F. (2016). Settling behavior of particles in fiber-containing Herschel Bulkley fluid. *Powder Technology*, *301*, 782–793. https://doi.org/https://doi.org/10.1016/j.powtec.2016.07.006

Elgaddafi, R., Ahmed, R., Karami, H., Nasser, M., & Hussein, I. (2021). Mechanistic modeling of wellbore cleanout in horizontal and inclined wells. *SPE/ICoTA Well Intervention Conference and Exhibition 2021, CTWI 2021*, (February), 22–25. https://doi.org/10.2118/204442-MS

Enfis, M., Ahmed, R., & S, O. (2013). New Hydraulic Model for Flow of Herschel-Buckley Fluid in Pipes and Annuli. *Canadian Energy Technology & Innovation*, *1*, 41–47.

Garcia, S., Mendez, M., Ahmed, R., Karami, H., Nasser, M., & Hussein, I. A. (2024). Effects of Pipe Rotation on the Performance of Fibrous Water-Based Polymeric Fluids in Horizontal Well Cleanout. *SPE Journal*, *29*(2), 764–779. https://doi.org/10.2118/210347-PA

George, M. (2012). *Flow Behavior and Hole Cleaning Efficiency of Synthetic-Based Fiber-Containing Drilling Fluids*. The University of Oklahoma.

George, M., Ahmed, R., & Growcock, F. (2011). Rheological Properties of Fiber-Containing Drilling Sweeps at Ambient and Elevated Temperatures. *Paper AADE-11-NTCE-35, Presented at the 2011 AADE National Technical Conference and Exhibition, Houston, April 12–14*, (December 2015).

George, M., Elgaddafi, R., Ahmed, R., & Growcock, F. (2014). Performance of fiber-containing synthetic-based sweep fluids. *Journal of Petroleum Science and Engineering*, *119*(July), 185–195. https://doi.org/10.1016/j.petrol.2014.05.009

Guo, X., & Li, W. (2017). Numerical Simulation on Cuttings Transport with Drillpipe Rotation in Extended Reach Well. *IOP Conference Series: Materials Science and Engineering*, *250*(1). https://doi.org/10.1088/1757-899X/250/1/012033

Hastie, T., Tibshirani, R., & Friedman, J. (2017). *The Elements of Statistical Learning* (Second). https://doi.org/10.1007/b94608

Kenny, P., Sunde, E., & Hemphill, T. (1996). Hole cleaning modelling: What's `n' got to do with it? *Proceedings of the IADC/SPE Drilling Conference*, 479–492. https://doi.org/10.2523/35099-ms

Kerunwa, A., Obibuike, J. U., Duru, U. I., & Ekwueme, S. T. (2021). The Effects of Fluid Rheology and Drillstring Eccentricity on Drilling Hydraulics. *Open Journal of Yangtze Oil and Gas*, *06*(04), 129–145. https://doi.org/10.4236/ojogas.2021.64012

Khaled, M. S., Khan, M. S., Ferroudji, H., Barooah, A., Rahman, M. A., Hassan, I., & Hasan, A. R. (2021). Dimensionless data-driven model for optimizing hole cleaning efficiency in daily drilling operations. *Journal of Natural Gas Science and Engineering*, *96*(July), 104315. https://doi.org/10.1016/j.jngse.2021.104315

Kim, Y.-J., & Hwang, Y.-K. (2003). Experimental study on the vortex flow in a concentric annulus with a rotating inner cylinder. *Journal of Mechanical Science and Technology*, *17*, 562–570. https://doi.org/10.1007/BF02984457

Kozicki, W., Chou, C. H., & Tiu, C. (1966). Non-Newtonian flow in ducts of arbitrary cross-sectional shape. *Chemical Engineering Science*, *21*(8), 665–679. https://doi.org/10.1016/0009-2509(66)80016-7

Larsen, T. I., Pilehvari, A. A., & Azar, J. J. (1997). Development of a new cuttings-transport model for high-angle wellbores including horizontal wells. *SPE Drilling and Completion*, *12*(2), 129–134. https://doi.org/10.2118/25872-pa

Leising, L. J., & Walton, I. C. (1998). Cuttings transport problems and solutions in coiled tubing drilling. *Proceedings of the IADC/SPE Asia Pacific Drilling Technology*

Conference, APDT, 85–100. https://doi.org/10.2523/39300-ms

Leising, Larry J, & Newman, K. R. (1993). Coiled-Tubing Drilling. *SPE Annual Technical Conference and Exhibition*, (December), 227–232.

Li, J., & Luft, B. (2014). Overview of solids transport studies and applications in oil and gas industry - Experimental work. *Society of Petroleum Engineers - SPE Russian Oil and Gas Exploration and Production Technical Conference and Exhibition 2014, RO and G 2014 - Sustaining and Optimising Production: Challenging the Limits with Technology*, *2*, 1365–1401. https://doi.org/10.2118/171285-ms

Li, J, Walker, S., & Aitken, B. (2002). Remove Sand From Deviated Wellbores With a Solids Transport Simulator and a Coiled Tubing Cleanout Tool. *SPE Annual Technical Conference and Exhibition*, (September). San Antonio, TX.

Li, J, Wilde, G., & Crabtree, A. (2005). Do Complex Super-Gel Liquids Perform Better Than Simple Linear Liquids i n Hole Cleaning With Coiled Tubing ? *SPE/ICoTA Coiled Tubing Conference and Exhibition*, (April). Woodlands, Tx.

Li, Jeff, & Walker, S. (2001). Sensitivity Analysis of Hole Cleaning Parameters in Directional Wells. *SPE Journal*, (December 2001), 356–363.

Mahmoud, H., Hamza, A., Nasser, M. S., Hussein, I. A., Ahmed, R., & Karami, H. (2020). Hole cleaning and drilling fluid sweeps in horizontal and deviated wells: Comprehensive review. *Journal of Petroleum Science and Engineering*, *186*(November 2019), 106748. https://doi.org/10.1016/j.petrol.2019.106748

Masuda, Y., Doan, Q., Oguztoreli, M., Naganawa, S., Yonezawa, T., Kbayashi, A., & Kamp, A. (2000). Critical Cuttings Transport Velocity in Inclined Annulus: Experimental Studies and Numerical Simulation. *SPE/PS-CIM International Conference on Horizontal Well Technology*. https://doi.org/10.2523/65502-ms

Mendez, M., Ahmed, R., Karami, H., Nasser, M., Hussein, I. A., Garcia, S. P., & Gonzalez, A. (2023). Applications of Machine Learning Methods to Predict Hole Cleaning in Horizontal and Highly Deviated Wells. *SPE Drilling & Completion*, (December 2023), 21–22.

Mendez, M., Garcia, S., Ahmed, R., Karami, H., Nasser, M., & Hussein, I. (2022). Effect of Fluid Rheology on the Performance of Fibrous Fluid in Horizontal Well Cleanout. *Society of Petroleum Engineers - SPE/ICoTA Well Intervention Conference and Exhibition, CTWI 2022*, (February), 22–23. https://doi.org/10.2118/209018-MS

Mendez, M., Garcia, S. P., Ahmed, R., Karami, H., Nasser, M., & Hussein, I. A. (2023). Effect of Fluid Viscosity and Fiber Length on the Performance of Fibrous Fluid in Horizontal Well Cleanout. *SPE Drilling & Completion*, (March 2023), 52–72.

Moradi, H. V., & Tavoularis, S. (2019). Flow instability in weakly eccentric annuli. *Physics of Fluids*, (April). https://doi.org/10.1063/1.5088992

Naik, S. (2015). *Effect of Fluid Rheology and Flow Rate on Wellbore Cleanout Process in Horizontal and Directional WellS* (University of Oklahoma). https://doi.org/10.1145/3132847.3132886

Ozbayoglu, E., Ozbayoglu, M., Ozdilli, B. G., & Erge, O. (2021). *Optimization of Flow*

Rate and Pipe Rotation Speed Considering Effective Cuttings Transport Using Data-Driven Models.

Pandya, S. (2019). *Wellbore Cleanout in Inclined and Horizontal Wellbores-The Effects of Fluid Rheology, Inclination, and Solids Density*. The Univeristy of Oklahoma.

Pandya, S., Ahmed, R., & Shah, S. (2019). Experimental study on wellbore cleanout in horizontal wells. *Journal of Petroleum Science and Engineering*, *177*(September 2018), 466–478. https://doi.org/10.1016/j.petrol.2019.02.069

Pandya, S., Ahmed, R., & Shah, S. (2020). Wellbore cleanout in inclined and horizontal wellbores: The effects of flow rate, fluid rheology, and solids density. *SPE Drilling and Completion*, *35*(1), 48–68. https://doi.org/10.2118/194240-PA

Rasi, M. (1994). Hole Cleaning in Large, High-Angle Wellbores. *Drilling Conference - Proceedings*, (1), 299–310. https://doi.org/10.2118/27464-ms

Reed, T. D., & Pilehvari, A. A. (1993). New model for laminar, transitional, and turbulent flow of drilling muds. *Production Operations Symposium*, 469–482. https://doi.org/10.2523/25456-ms

Rojas, S., Ahmed, R., Elgadda, R., & George, M. (2017). Flow of power-law fluid in a partially blocked eccentric annulus. *Journal of Petroleum Science and Engineering*, *157*(July), 617–630. https://doi.org/10.1016/j.petrol.2017.07.060

Sanchez, R. A., Azar, J. J., & Bassal, A. A. (1999). Effect of Drillpipe Rotation on Hole Cleaning During Directional-Well Drilling. *SPE Journal*, (June), 101–108.

Sapru, A. (2001). *Study of Effect of Drill Pipe Rotation on Cuttings Bed Erosion in Horizontal Wells*. The University of Tulsa.

Singh, R. (2019). *CFD Analysis of Power-Law Fluid in a Partially Blocked Eccentric Annulus Under Turbulent Flow Conditions* (Vol. 8). University of Oklahoma.

Tang, M., Ahmed, R., & He, S. (2016). Modeling of yield-power-law fluid flow in a partially blocked concentric annulus. *Journal of Natural Gas Science and Engineering*, *35*, 555–566. https://doi.org/10.1016/j.jngse.2016.09.001

Whitaker, A. (1985). *Theory and Applications of Drilling Fluid Hydraulics*. Retrieved from https://books.google.com/books?id=IsqWAAAACAAJ

Xu, H., & Aidun, C. K. (2004). Characteristics of fiber suspension flow in a rectangular channel. *International Journal of Multiphase Flow*, *31*(3), 318–336. https://doi.org/10.1016/j.ijmultiphaseflow.2004.12.003

Zamora, M., & Hanson, P. (1990). Selected Studies in High-Angle Hole Cleaning. *Proceedings Indonesia Petroleum Association*, (October 1990).

Zhang, F., Miska, S., Yu, M., Ozbayoglu, E., & Takach, N. (2015). Pressure Profile in Annulus: Solids Play a Significant Role. *Journal of Energy Resources Technology, Transactions of the ASME*, *137*. https://doi.org/10.1115/1.4030845]

Appendix A

Geometric Calculation

According to Elgaddafi et al. (2021), the following equations can be developed to describe different wellbore geometry parameters considering a uniform cuttings bed height, h, in the annulus (Fig. A.1).

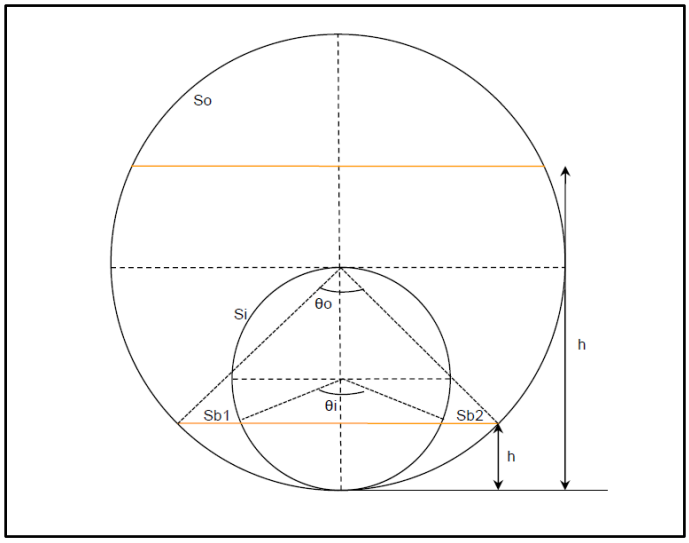


Figure A.1. Standard geometry configuration for eccentric annulus (Elgaddafi et al., 2021)

The following two equations are used to determine the wetted perimeter (S) and flow area (A_f) for any configuration:

$$S = S_i + S_o + S_b \tag{A.1}$$

$$A_f = A_o - A_i \tag{A.2}$$

For h < D_i: The following expressions can be derived from the flow geometry to determine various geometric parameters. R_i and R_o are the radii of the inner and outer pipes, respectively. H_{bed} is the bed height.

$$\theta_o = 2 \times \cos^{-1}\left(\frac{R_o - H_{bed}}{R_o}\right) \quad \text{(A.3)}$$

$$\theta_i = 2 \times \cos^{-1}\left(\frac{R_i - H_{bed}}{R_i}\right) \quad \text{(A.4)}$$

$$S_o = \theta_o * R_o \quad \text{(A.5)}$$

$$S_i = \theta_i * R_i \quad \text{(A.6)}$$

$$S_b = \left(2 * \sqrt{R_o^2 - (R_o - H_{bed})^2}\right) - \left(2 * \sqrt{R_i^2 - (R_i - H_{bed})^2}\right) \quad \text{(A.7)}$$

$$A_o = R_o^2\left(\frac{\theta_o}{2}\right) + (R_o - H_{bed})\sqrt{R_o^2 - (R_o - H_{bed})^2} \quad \text{(A.8)}$$

$$A_i = R_i^2\left(\frac{\theta_i}{2}\right) + (R_i - H_{bed})\sqrt{R_i^2 - (R_i - H_{bed})^2} \quad \text{(A.9)}$$

$$A_f = Ao - A_i \quad \text{(A.10)}$$

For h > D_i: The following expressions can be derived from geometry.

$$\theta_o = 2 \times \cos^{-1}\left(\frac{R_o - H_{bed}}{R_o}\right) \quad \text{(A.11)}$$

$$S_o = \theta_o * R_o \quad \text{(A.12)}$$

$$S_i = 0 \quad \text{(A.13)}$$

$$S_b = 2 * \sqrt{R_o^2 - (R_o - H_{bed})^2} \quad \text{(A.14)}$$

$$A_o = R_o^2\left(\frac{\theta_o}{2}\right) + (R_o - H_{bed})\sqrt{R_o^2 - (R_o - H_{bed})^2} \quad \text{(A.15)}$$

$$A_i = 0 \quad \text{(A.16)}$$

$$A_f = Ao - A_i \tag{A.17}$$

After the formation of a stationary solids bed, the hydraulic diameter is computed as:

$$D_{hy} = \frac{4A_f}{S_o + S_i + S_b} \tag{A.18}$$

where A_f is the flow's cross-sectional area, S_o, S_i, and S_b are the wetted perimeters of the wellbore, drill pipe, and cuttings bed.

Appendix B

Hydraulic Models

In this section, two applied approaches for predicting the average bed shear stress are discussed.

B.1 Traditional (Original) Hydraulic Model

In most of the existing wellbore hydraulic models, the average bed shear stress is determined directly from the overall wall shear stress, which is calculated as:

$$\tau_w = f\frac{\rho_f U^2}{2} \tag{B.1}$$

where f is Fanning friction factor. U and ρ_f are the mean fluid velocity and its density. For laminar flow ($Re_{gn} < 2100$), the Fanning friction factor is expressed as:

$$f = \frac{16}{Re_{gn}} \tag{B.2}$$

where Re_{gn} is a general Reynolds number given by (Whitaker, 1985; Chen, 2005):

$$Re_{gn} = \frac{8U^2\rho_f}{K\left(\frac{8U}{D_{eff}}\right)^n} \tag{B.3}$$

The effective diameter is defined as: $D_{eff} = d_h/G$, where d_h is the hydraulic diameter calculated using Eqn. (A.18), and G is a parameter with no dimensions:

$$G = \frac{(3-Z)n+1}{(4-Z)n}\left(1+\frac{Z}{2}\right) \tag{B.4}$$

Where Z is a dimensionless parameter that is defined as:

$$Z = 1-(1-k^Y)^{1/Y} \qquad \text{where } Y = 0.37n^{-0.14} \tag{B.5}$$

where k is the diameter ratio ($k = D_P/D_h$). For turbulent flow, many implicit correlations (Dodge & Metzner, 1959; Colebrook et al., 1939) were developed to compute friction factors for Newtonian and non-Newtonian fluids. Enfis (2013) proposed an explicit correlation for power-law fluids, which is given by:

$$f = 0.0918 * n^{-0.364} * Re_{gn}^{(0.12Ln(n)-0.27)} \quad \text{(B.6)}$$

B.2 New Hydraulic Model

Several CFD studies (Rojas et al., 2017; Singh, 2019; Tang et al., 2016) have been performed to examine the impact of stationary bed development on the annular flow of power-law fluids. Based on the CFD results, new correlations are developed to calculate the average bed shear stress.

For Fully Buried Pipe: When the flow is laminar and the inner pipe diameter is fully buried ($H_{bed} > D_p$), the normalized bed shear stress (i.e. the ratio of average bed shear stress to the overall shear stress) is determined as (Tang et al., 2016):

$$\frac{\tau_b}{\tau_w} = a_1 + b_1\left(\frac{H_{bed}-H}{2r_h}\right) + c_1\left(\frac{H_{bed}-H}{2r_h}\right)^2 + d_1\left(\frac{H_{bed}-H}{2r_h}\right)^3 \quad \text{(B.7)}$$

where τ_w is the overall wall shear stress. The empirical coefficients a_1 to d_1 are functions of diameter ratio as described in Table B.1. H_{bed} is the bed thickness in the annulus. H is the annular clearance ($r_h - r_p$) where r_h and r_p are the radii of the hole and drill pipe, respectively. In Eqn. B.8, the overall wall shear stress is calculated as:

$$\tau_w = K\left(\frac{8U}{D^*_{eff}}\right)^n \quad \text{(B.8a)}$$

where the modified effective diameter (D^*_{eff})is obtained as follows:

$$D^*_{eff} = 4A_f/(S_i + S_p + S_h) \qquad 0 \le H_{bed} \le 0.5x \tag{B.8b}$$

$$D^*_{eff} = S_i.H_{bed} + I_n \qquad 0.5x \le H_{bed} \le 1.5x \tag{B.8c}$$

$$D^*_{eff} = 1.07 \times 4A_f/(S_i + S_p + S_h), \quad 1.5x \le H_{bed} \le D_h \tag{B.8d}$$

where A_f, S_i, S_p, and S_h are computed from Appendix A. x is the hydraulic radius of a concentric annulus with no cuttings bed. It is computed as $x = 0.5(D_h - D_p)$. S_i and I_n are empirical coefficients determined by the following correlations (Tang et al. 2016):

$$S_i = [1.07D_{hy}(1.5x) - D_{hy}(0.5x)]/x \tag{B.10}$$

$$I_n = D_{hy}(0.5x) - 0.5x.S_l \tag{B.11}$$

Table B. 1. Empirical coefficients values used in Eqn. (B.7)

Empirical coefficient	Value
a1	$0.85998 - 0.75366k + 0.40328k^2$
b1	$0.12922 + 1.6713k - 1.71512k^2$
c1	$-0.27887 - 4.01044k + 4.81040k^2$
d1	$2.20354 - 3.43634k + 1.20312k^2$

In the case of turbulent flow, the existing model is used, utilizing friction pressure loss for average bed shear stress calculation. At $H_{bed} > D_p$, average bed shear stress computed from friction pressure loss is the closest prediction to the actual bed shear stress.

For Partially Buried Pipe: When the bed height is less than the inner pipe diameter ($H_{bed} \leq D_p$), the normalized bed shear stress is determined once the expected flow regime is known. For laminar flows ($Re_k < 2100$), the normalized bed shear stress can be calculated using the following equation (Rojas et al., 2017):

$$\left(\frac{\tau_b}{\tau_w}\right)^n = A_1 H_b^{4.511} + B_1 H_b^{2.51} + C_1 H_b^{0.51} + D_1 n k^{0.51} + E_1 (n H_b)^{1.431} + F_1 n + G_1 \quad \text{(B.12)}$$

Similarly, the normalized bed shear stress can be computed for turbulent flow using the equation given below (Singh 2019):

$$\left(\frac{\tau_b}{\tau_w}\right)^n = A_2 H_b^{4.5} + B_2 H_b^{2.5} + C_2 H_b^{0.51} + D_2 n k^{0.51} + E_2 (n H_b)^{1.4} + F_2 n + G_2 \quad \text{(B.13)}$$

To determine the flow regime, a generalized Kozicki Reynolds number is used (Kozicki et al. 1966):

$$Re_k = \frac{D_{hy}^n U^{2-n} \rho_f}{8^{n-1} K \left(\frac{a}{n} + b\right)^n} \quad \text{(B.14)}$$

The hydraulic diameter is calculated using Eqn. (A.18). The constants *a* and *b* are determined from the dimensionless bed height as:

$$a = \lambda_0 H_b^3 + \lambda_1 H_b^2 + \lambda_2 H_b + \lambda_3 \quad \text{(B.15a)}$$

$$b = b_0 H_b^3 + b_1 H_b^2 + b_2 H_b + b_3 \quad \text{(B.15b)}$$

where λ_0, λ_1, λ_2, λ_3, b_0, b_1, b_2, and b_3 are dimensionless coefficients computed according to the correlations presented in Table B.2.

Table B. 2. Empirical coefficient used in Eqn. (B.15) (Rojas et al. 2017)

$\lambda_0 = -6.2328k^2 + 4.1994k - 0.845$	$b_0 = -0.964k^2 + 5.425k - 1.321700$
$\lambda_1 = 9.152k^2 - 6.7796k + 1.10960$	$b_1 = -0.1792k^2 - 8.1756k + 2.0884$
$\lambda_2 = -3.236k^2 + 2.7778k - 0.0881$	$b_2 = 0.836k^2 + 3.4122k - 0.932500$
$\lambda_3 = 0.284k^2 - 0.4266k + 0.06684$	$b_3 = 0.2456k^2 - 0.2934k + 0.87610$

In Eqns. B.12 and B.13, τ_w is the overall wall shear stress, A1 – G1 and A2 – G2 are empirical coefficients for laminar and turbulent bed shear stress correlations. They are presented in **Table B.3**. H_b is dimensionless bed height (H_{bed}/D_P) and *k* is the diameter ratio (D_p/D_h). In this approach, predicting τ_b requires the calculation of the overall wall shear stress using Eqn. B.1. The Fanning friction factor is calculated from geometric parameters as (Rojas et al. 2017):

$$f = \frac{\left(\frac{a}{n}+b\right)^n \left(2^{3n+1}\right)}{Re} \tag{B.16}$$

where *Re* is the Reynolds number computed as:

$$Re = \frac{\rho_f U^{2-n} D_{hy}^n}{K} \tag{B.17}$$

For turbulent flow, the Fanning friction factor is calculated from the explicit correlation, Eqn. B.6. In Eqn. B.16, the values of parameters *a* and *b* are computed using Eqn. B.15. Figure B.1 shows a block diagram that describes the numerical procedure developed to calculate the overall and bed shear stresses.

Table B. 3. Empirical coefficients used in Eqns. (B.12) and (B.13)

Empirical coefficient	Value	Empirical coefficient	Value
A_1	0.4668	A_2	0.4930
B_1	-0.7470	B_2	-0.7909
C_1	0.8957	C_2	0.8590
D_1	-0.5166	D_2	-0.5004
E_1	0.6366	E_2	0.4878
F_1	-0.4077	F_2	-0.2851
G_1	0.5250	G_2	0.5559

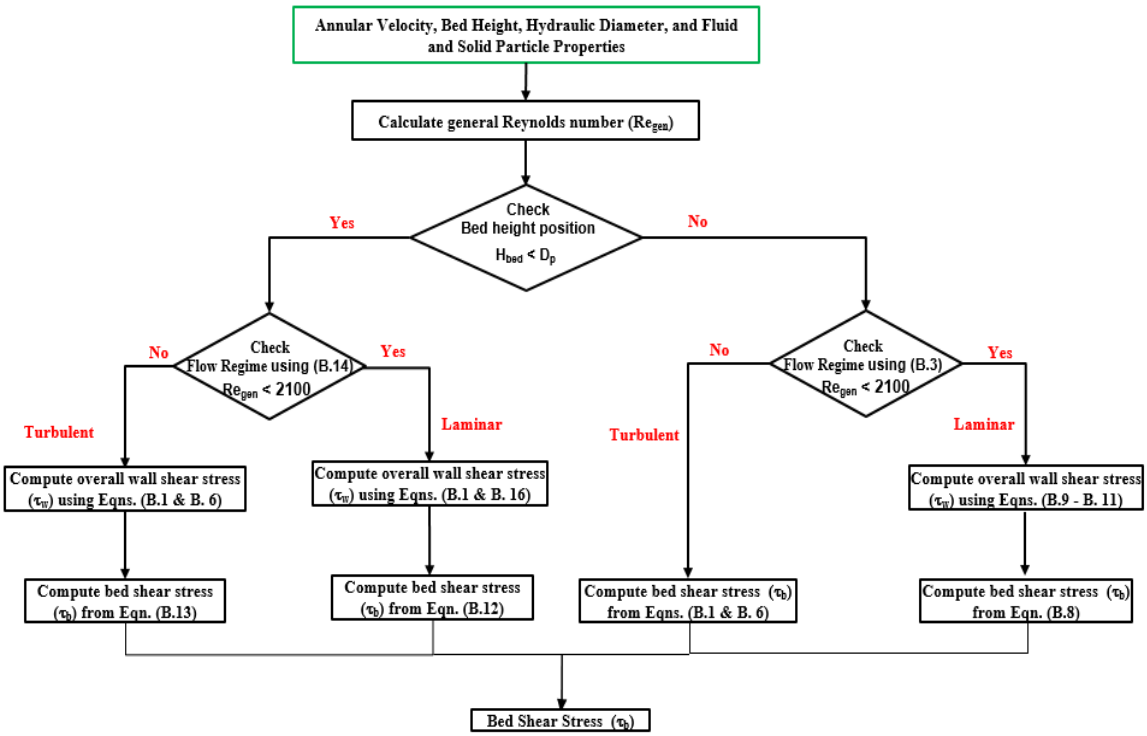


Figure B. 1. Block diagram showing the numerical procedure for determining the bed shear stress

Appendix C

Bed Profiles

Figures C.1 to C.6 present the bed profiles observed in the test section with various fluids at different flow rates. Bed profiles are only shown for a few selected flow rates to avoid excessive overlapping of data points.

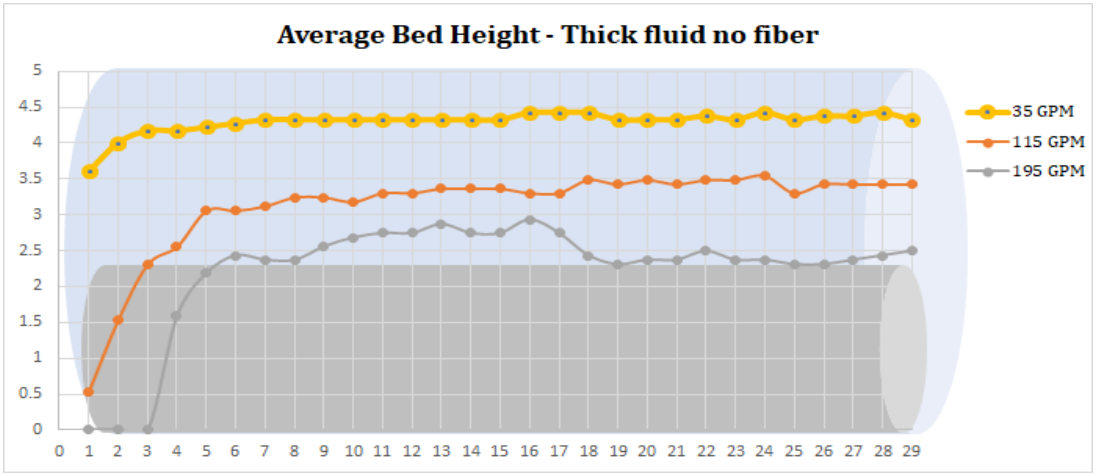


Figure C.1. Bed Height profile of thick fluid no fiber at 35, 115 and 195 GPM

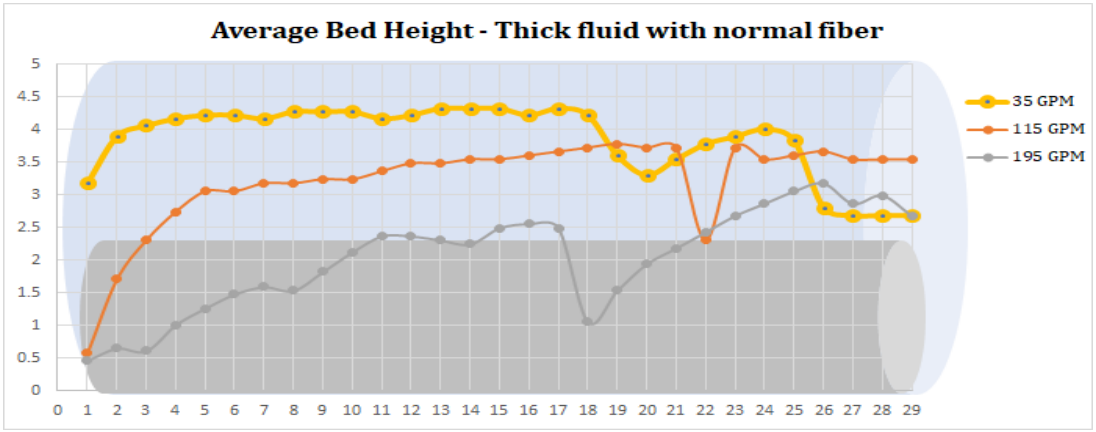


Figure C.2. Bed Height profile of thick fluid with long fiber at 35, 115 and 195 GPM

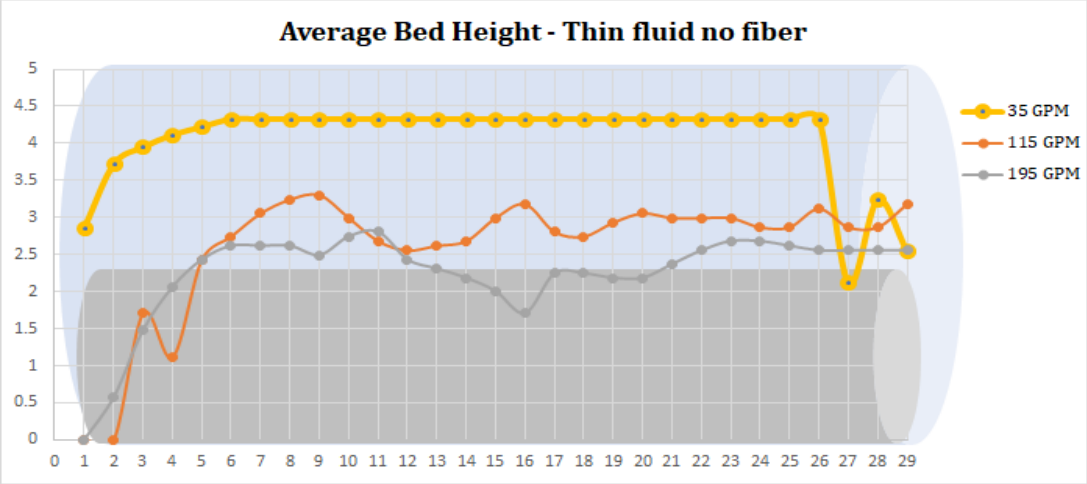


Figure C.3. Bed height profile of thin fluid no fiber at 35, 115 and 195 GPM

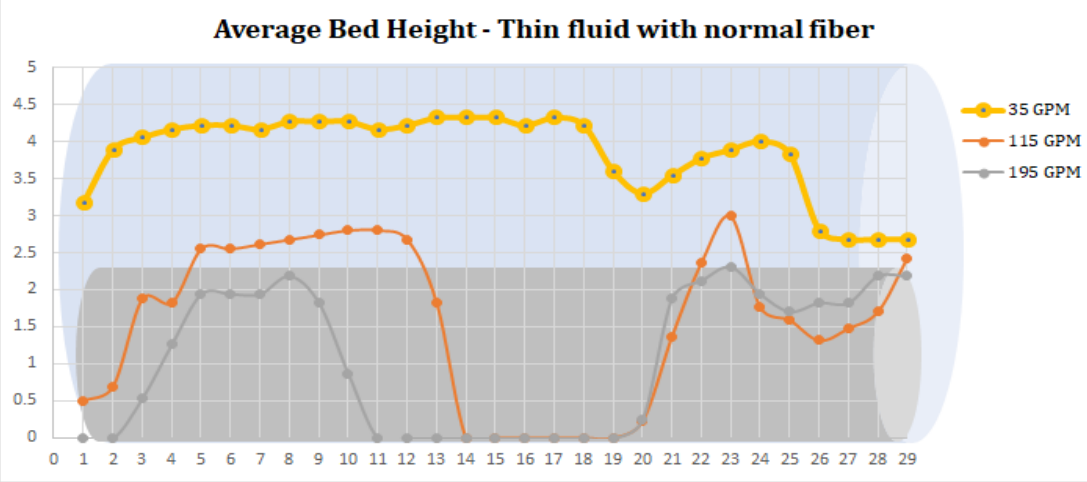


Figure C.4. Bed height profile of thin fluid with short fiber at 35, 115 and 195 GPM

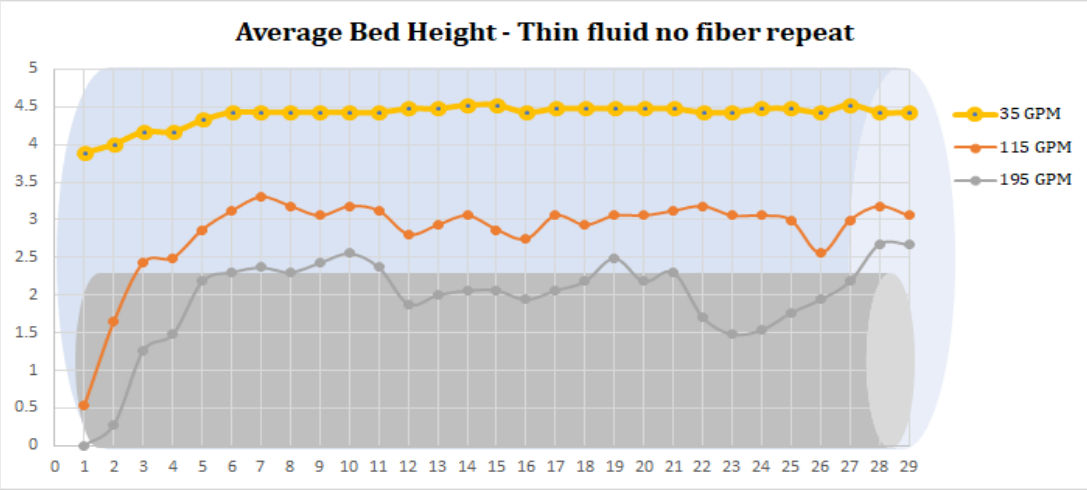


Figure C.5. Bed height profile of thin fluid no fiber repeat at 35, 115 and 195 GPM

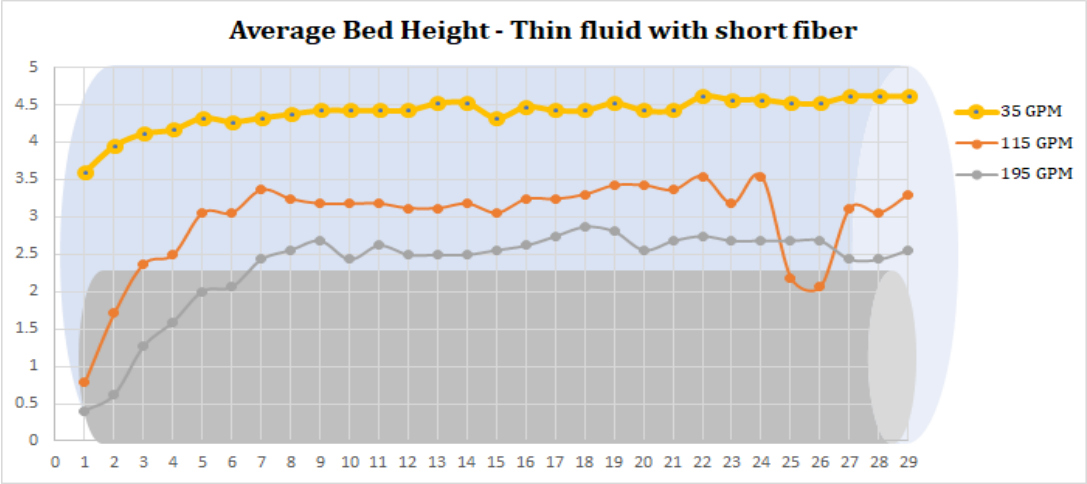


Figure C.6. Bed height profile of thin fluid with short fiber at 35, 115 and 195 GPM

Appendix D

Dimensionless Variables

Two dimensionless variables are used in the modeling process for this work. These numbers will be presented in this section.

Reynolds Number

$$N_{Re} = 109000 \frac{\rho v^{2-n}}{K} \left[\frac{0.0208\,(d_2 - d_1)}{2+1/n}\right]^n \tag{D.1}$$

Taylor Number

$$T_a = \frac{D_i\,(D_o - D_i)\text{^}3}{16} \left(\frac{\rho\omega}{\mu_{app}}\right)^2 \tag{D.2}$$

$$\mu_{app} = K\dot{\gamma}_{\theta-z}^{n-1} \tag{D.3}$$

$$\dot{\gamma}_{\theta-z} = \sqrt{\dot{\gamma}_\theta^2 + \dot{\gamma}_z^2} \tag{D.4}$$

$$\dot{\gamma}_z = \frac{1+2n}{3n} \frac{12U}{D_o - D_i} \tag{D.5}$$

$$\dot{\gamma}_\theta = \frac{\omega D_i}{D_o - D_i} \tag{D.6}$$